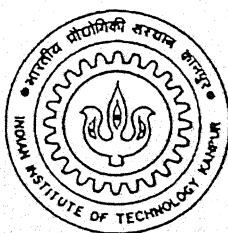


SPATIAL MODAL ANALYSIS IN BEAMS

by
VAZE A. V.



TH
ME/1998/M
V4775

to the
DEPARTMENT OF MECHANICAL ENGINEERING
INDIAN INSTITUTE OF TECHNOLOGY KANPUR

July, 1998

**SPATIAL MODAL ANALYSIS
IN BEAMS**

by
VAZE A. V.

**DEPARMENT OF MECHANICAL ENGINEERING
INDIAN INSTITUTE OF TECHNOLOGY, KANPUR
JULY, 1998**

22 SEP 1998 / ME
CENTRAL LIBRARY
I. I. T., KANPUR

Vol. No. A 126252

Entered In System.

ME-1998-M-VAZ-SPA



A126252

Name of the student: Vaze A. V.

Roll. no. 9620532.

Degree for which submitted: M.Tech.

Department: Mechanical

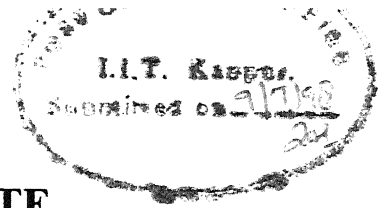
Thesis title: Spatial Modal Analysis In Beams

Supervisor's Name: Dr. N. S. Vyas

Month and Year of submission: July 7th 1998

ABSTRACT


Spatial Modal Testing is a parameter estimation approach which involves obtaining spatial information of a structure's dynamics at a large number of points at a specified frequency. This is in contrast to the classical Modal Testing procedures which offer few spatial degrees of freedom and many frequency based degrees of freedom. Spatial Modal Analysis is a relatively new development and previous attempts have been restricted to approximation of a single normal mode function of a beam. The present study extends the basic concepts for development of a more general procedure for estimation of modal parameters of two modes adjacent to a test excitation frequency. This is done through estimation of a modal participation factor. Steady state spatial data of beam excited at an arbitrary frequency and location are obtained and recursive form of Forsythe polynomials are employed to approximate the deflected beam shape. Least square technique is used to curve fit the measured responses and obtain the coefficients of Forsythe polynomials. Orthogonality properties of the normal mode functions are further employed to decompose the Forsythe polynomial representation into the individual mode shapes of the beam contributing to the response. Spatial modal frequencies and damping factors are consequently obtained. The procedure is numerically illustrated for a variety of boundary conditions of the beam. The effect of measurement inaccuracies and other errors are also numerically illustrated. Experimental investigations are also carried out to verify the developed procedure.



CERTIFICATE

It is certified that the work contained in the thesis entitled 'Spatial Modal Analysis in Beams', by Vaze A. V. has been carried out under my supervision and that this work has not been submitted elsewhere for a degree.

July 7th, 1998


Nalinaksh S Vyas
Associate Professor
Department of Mechanical Engineering
Indian Institute of Technology
Kanpur 208016

ACKNOWLEDGEMENTS

It gives me a great pleasure to express my sincere gratitude to Dr. Nalinaksh S. Vyas , my thesis supervisor, for his inspiring guidance and constant encouragement throughout the course of this work. I must thank him for suggesting me a very interesting problem in the area of modal analysis and building the confidence in me in pursuing the work.

I am highly thankful to Mr. A. A. Khan and Mr. A. Chatterjee for their close association and valuable suggestions. Thanks are due to Mr. M. M. Singh for his service available whenever needed, due to Ms. Lalita S. for her help and cooperation throughout the course, and Mr. S. Parida for his help in conducting the experiments. Lastly, I would like to thank one and all who were in a way or other associated with me.

Vaze A. V.

Indian Institute of Technology, Kanpur
July, 1998

ABSTRACT

Spatial Modal Testing is a parameter estimation approach which involves obtaining spatial information of a structure's dynamics at a large number of points at a specified frequency. This is in contrast to the classical Modal Testing procedures which offer few spatial degrees of freedom and many frequency based degrees of freedom. Spatial Modal Analysis is a relatively new development and previous attempts have been restricted to approximation of a single normal mode function of a beam. The present study extends the basic concepts for development of a more general procedure for estimation of modal parameters of two modes adjacent to a test excitation frequency. This is done through estimation of a modal participation factor. Steady state spatial data of beam excited at an arbitrary frequency and location are obtained and recursive form of Forsythe polynomials are employed to approximate the deflected beam shape. Least square technique is used to curve fit the measured responses and obtain the coefficients of Forsythe polynomials. Orthogonality properties of the normal mode functions are further employed to decompose the Forsythe polynomial representation into the individual mode shapes of the beam contributing to the response. Spatial modal frequencies and damping factors are consequently obtained. The procedure is numerically illustrated for a variety of boundary conditions of the beam. The effect of measurement inaccuracies and other errors are also numerically illustrated. Experimental investigations are also carried out to verify the developed procedure.

CONTENTS

NOMENCLATURE	i
LIST OF FIGURES	ii
LIST OF TABLES	iv
1. INTRODUCTION	1
2. ESTIMATION PROCEDURE FORMULATION	4
2.1 Forsythe polynomials	4
2.2 Mode shape estimation	5
2.3 Estimation of natural frequencies and damping ratios	8
2.4 Remarks	9
3. NUMERICAL SIMULATION	10
3.1 Non-dimensional parameters	10
3.2 Case studies	12
3.3 Influence of the number of measurement stations	25
3.4 Effect of measurement errors	25
3.5 Influence of error in the point of force application	26
3.6 Remarks	43
4. EXPERIMENTAL INVESTIGATIONS	44
5. CONCLUSIONS	65
REFERENCES	66

NOMENCLATURE

$y(x)$	Displacement response
ρ	Force density
E	Modulus of elasticity
A	Area of cross section
I	Area moment of inertia
F	Magnitude of applied force
x_μ	Measurement station
ω	Excitation frequency
ω_j	j th natural frequency of the beam
$\psi_j(x_\mu)$	j th mode shape at station x_μ
ξ_j	j th damping ratio
$Y_r(x_\mu)$	Real component of response amplitude approximated
$Y_i(x_\mu)$	Imaginary component of response amplitude approximated
$\nu_r(x_\mu)$	Real component of response amplitude experimentally measured at station x_μ
$\nu_i(x_\mu)$	Imaginary component of response amplitude experimentally measured at station x_μ
$p_k(x_\mu)$	Forsythe polynomial at station x_μ
$\varepsilon_r(x_\mu)$	Least square error (real)
$\varepsilon_i(x_\mu)$	Least square error(imaginary)
S_{jk}	Constants in Forsythe polynomials
χ_j	j th spatial frequency
κ	Nondimensional parameter ($EI / \rho g A l^3$)
r_j	j th natural frequency ratio (ω / ω_j)
$H(x)$	Nondimensionalised response
$H_r(x_\mu)$	Nondimensionalised real component of response amplitude approximated
$H_i(x_\mu)$	Nondimensionalised imaginary component of response amplitude approximated
$q_r(x_\mu)$	Nondimensionalised real component of response amplitude experimentally measured at station x_μ
$q_i(x_\mu)$	Nondimensionalised imaginary component of response amplitude experimentally measured at station x_μ
$\bar{\varepsilon}_r(x_\mu)$	Nondimensionalised least square error (real)
$\bar{\varepsilon}_i(x_\mu)$	Nondimensionalised least square error(imaginary)

LIST OF FIGURES

Figure	Description	Page
3.1(a)-(b)	Simulated in phase and out of phase response amplitude for simply supported configuration ($\kappa=0.1$)	15
3.2(a)-(b)	Estimated and exact mode shapes for simply supported configuration ($\kappa=0.1$)	16
3.3(a)-(b)	Simulated in phase and out of phase response amplitude for simply supported configuration($\kappa=1.0$)	17
3.4(a)-(b)	Estimated and exact mode shapes for simply supported configuration ($\kappa=1.0$)	18
3.5(a)-(b)	Simulated in phase and out of phase response amplitude for simply supported configuration($\kappa=10.0$)	19
3.6(a)-(b)	Estimated and exact mode shapes for simply supported configuration ($\kappa=10.0$)	20
3.7(a)-(b)	Simulated in phase and out of phase response amplitude for cantilever configuration($\kappa=1.0$)	21
3.8(a)-(b)	Estimated and exact mode shapes for cantilever configuration ($\kappa=1.0$)	22
3.9(a)-(b)	Simulated in phase and out of phase response amplitude for fixed-fixed configuration($\kappa=1.0$)	23
3.10(a)-(b)	Estimated and exact mode shapes for fixed-fixed configuration ($\kappa=1.0$)	24
3.11(a)-(b)	Estimated and exact mode shapes for simply supported configuration with influence of number of stations ($\kappa=1.0$)	27
3.12(a)-(b)	Errors for simply supported configuration with influence of number of stations ($\kappa=1.0$)	28
3.13(a)-(b)	Estimated and exact mode shapes for cantilever configuration with influence of number of stations ($\kappa=1.0$)	29
3.14(a)-(b)	Errors for cantilever configuration with influence of number of stations ($\kappa=1.0$)	30
3.15(a)-(b)	Estimated and exact mode shapes for fixed-fixed configuration with influence of number of stations ($\kappa=1.0$)	31
3.16(a)-(b)	Errors for fixed-fixed configuration with influence of number of stations ($\kappa=1.0$)	32
3.17(a)-(b)	Simulated in phase and out of phase response amplitude for simply supported configuration with measurement error ($\kappa=1.0$)	33
3.18(a)-(b)	Estimated and exact mode shapes for simply supported configuration with measurement error($\kappa=1.0$)	34
3.19(a)-(b)	Simulated in phase and out of phase response amplitude for cantilever configuration with measurement error ($\kappa=1.0$)	35
3.20(a)-(b)	Estimated and exact mode shapes for cantilever configuration with measurement error($\kappa=1.0$)	36
3.21(a)-(b)	Simulated in phase and out of phase response amplitude for fixed-fixed configuration with measurement error ($\kappa=1.0$)	37
3.22(a)-(b)	Estimated and exact mode shapes for fixed-fixed configuration with measurement error($\kappa=1.0$)	38

3.23(a)-(b)	In phase and out of phase response amplitude for simply supported configuration with error in force application ($\kappa=1.0$)	39
3.24(a)-(b)	Estimated and exact mode shapes for simply supported configuration with error in force application ($\kappa=1.0$)	40
3.25(a)-(b)	In phase and out of phase response amplitude for fixed-fixed configuration with error in force application ($\kappa=1.0$)	41
3.26(a)-(b)	Estimated and exact mode shapes for fixed-fixed configuration with error in force application ($\kappa=1.0$)	42
4.1	Experimental setup overall view	45
4.2	Experimental setup	45
4.3	Details of instrumentation	46
4.4(a)-(b)	Response amplitude and phase angle for simply supported beam with 10 number of stations	48
4.5(a)-(b)	In phase and out of phase response amplitude for simply supported beam with 10 number of stations	49
4.6(a)-(b)	Estimated and exact mode shapes for simply supported beam with 10 number of stations	50
4.7(a)-(b)	Errors in mode shapes for simply supported beam with 10 number of stations	51
4.8(a)-(b)	Response amplitude and phase angle for simply supported beam with 20 number of stations	52
4.9(a)-(b)	In phase and out of phase response amplitude for simply supported beam with 20 number of stations	53
4.10(a)-(b)	Estimated and exact mode shapes for simply supported beam with 20 number of stations	54
4.11(a)-(b)	Errors in mode shapes for simply supported beam with 20 number of stations	55
4.12(a)-(b)	Response amplitude and phase angle for fixed-fixed beam with 10 number of stations	56
4.13(a)-(b)	In phase and out of phase response amplitude for fixed-fixed beam with 10 number of stations	57
4.14(a)-(b)	Estimated and exact mode shapes for fixed-fixed beam with 10 number of stations	58
4.15(a)-(b)	Errors in mode shapes for fixed-fixed beam with 10 number of stations	59
4.16(a)-(b)	Response amplitude and phase angle for fixed-fixed beam with 20 number of stations	60
4.17(a)-(b)	In phase and out of phase response amplitude for fixed-fixed beam with 20 number of stations	61
4.18(a)-(b)	Estimated and exact mode shapes for fixed-fixed beam with 20 number of stations	62
4.19(a)-(b)	Errors in mode shapes for fixed-fixed beam with 20 number of stations	63

LIST OF TABLES

Table	Description	Page
3.1	Exact and estimated natural frequencies and damping ratios of simply supported beam	13
3.2	Exact and estimated natural frequencies and damping ratios of cantilever beam	14
3.3	Exact and estimated natural frequencies and damping ratios of fixed-fixed beam	14
3.4	Exact and estimated natural frequencies and damping ratios with measurement errors	16
4.1	Exact and estimated natural frequencies of simply supported beam with experimental data	47
4.2	Exact and estimated natural frequencies of fixed -fixed beam with experimental data	64

CHAPTER 1

INTRODUCTION

Modal Testing encompasses the processes involved in testing components or structures with the objective of obtaining a mathematical description of their dynamic or vibration behaviour. The form of the mathematical description or model varies considerably from one application to the next. It can be an estimate of natural frequency and damping factor in one case and a full mass-spring-dashpot model for the next. One of the earlier developments in the area was by Kennedy and Pancu (1947) who evolved descriptions like 'Resonance Testing' and Mechanical Impedance' for applications involving natural frequency and damping determination of aircraft structures. This activity paved the way for more precise measurements and thus more powerful applications. Bishop and Gladwell (1963) described the state of the theory of resonance testing which, at that time, was considerably in advance of its practical implementation. By 1970 there had been major advances in transducers, electronics and digital analyzers and the techniques of modal testing were firmly established. Reference can be made to papers by Allemang (1984) and Mitchell (1984) for bibliographies of studies pertaining to basic modal testing methods. The text by Ewins (1984) is widely referred to as a treatise encompassing most of the aspects of classical modal testing.

The most common modal testing applications involve - estimation of natural frequencies and description of mode shapes, using just sufficient detail and accuracy to permit their identification and correlation with those from a theoretical model. In a classical approach this is done through obtaining frequency response function (FRF) estimates from time dependent forces and responses spatially distributed about the structure. The denominator of the frequency response function comprises of the spatially invariant natural frequency and damping parameters, while the numerator contains the spatial information on the mode shape of the structure.

The above classical procedure offers few spatial degrees of freedom and many frequency based degrees of freedom. For example, a typical test may have, say a hundred measurement locations on a structure, each with several thousand spectral lines of frequency information. The alternative to this approach is to obtain spatial information at many more points on the structure than the number of spectral lines. This is recently becoming realized through developments in Laser Doppler data acquisition techniques. The scanning laser is able to acquire velocity information at a number of spatial locations on the structure with sufficient density, accuracy and speed to offer the possibility of extraction of modal parameters from spatially intensive arrays as opposed to the classical frequency intensive format. The need for exploring the spatial data intensive procedure arises from the problems faced in validating analytical structural models. These models, typically finite elements models, are characterized by a large number of spatial degrees of freedom to compare with common experimental modal models.

Attempts towards spatial modal analysis of beams have been made recently by Archibald and Wicks (1991), Archibald (1992), and by West et al (1993). Standard autoregressive models as in Pisarenko Harmonic Decomposition (Pisarenko, 1973) and Oversize Total Least Squares have been used to approximate a normal mode function of the beam and are shown to yield unbiased results in the presence of measurement noise. West et al (1994) have also, alternatively employed the recursive form of Forsythe polynomials to approximate a normal mode function. The orthogonality property of Forsythe polynomials yields easier least square formulation and removes the ill conditioning problem while extracting the Forsythe coefficients from measured data.

The above attempts have, however, been restricted to approximation of a single normal mode function of a beam by a polynomial function. The steady state vibration amplitude is obtained at various points along the length of a beam for an excitation frequency very close to one of its natural frequencies. The excitation frequency being very close to a natural frequency, it has been assumed that contribution from adjacent modes is negligible and the deformed beam shape resembles the corresponding normal function of the beam. This may, however, not be always possible, for firstly, it requires an *a-priori* knowledge of the natural frequencies of the beam and secondly, it may not

always be possible to place the excitation force accurately enough on the structure, so as to constrain the response to a particular mode.

A general procedure for estimation of modal participation, as well as the calculation of natural frequencies and damping ratios, from steady state spatial data of beam excited at an arbitrary frequency and location, is described here. Recursive form of Forsythe polynomials is first employed to approximate the deflected beam shape. Least square technique is used to curve fit the measured responses and obtain the coefficients of Forsythe polynomials. Orthogonality properties of the normal mode functions is further employed to decompose the Forsythe polynomial representation into the individual mode shapes of the beam contributing to the response. The individual mode shapes estimates are further processed to fit the governing fourth order spatial equation of beams to obtain the spatial modal frequency. Standard relations give the modal damping ratios and natural frequencies from estimated spatial frequencies.

Chapter 2 describes the spatial modal analysis algorithm. The computer simulated studies are described in Chapter 3 and the experimental investigations are discussed in Chapter 4. Chapter 5 gives the conclusions of the present study and outlines the scope for future work.

CHAPTER 2

ESTIMATION PROCEDURE FORMULATION

The procedure, developed for estimation of modal participation from steady state spatial data of beam, is discussed in this chapter. The beam is excited at an arbitrary frequency and the contribution, of the two natural modes of the beam, lying on either side of the excitation frequency, to the beam response is estimated. Estimates are also obtained for the mode shapes and natural frequencies of these adjacent modes. The beam response is obtained at a number of spatial points along its length, in terms of the in-phase and out-of-phase vibration amplitudes. Recursive form of Forsythe polynomials is first employed to approximate the deflected beam shape. Least square technique is used to curve fit the measured responses and obtain the coefficients of Forsythe polynomials. Orthogonality properties of the normal mode functions is further employed to decompose the Forsythe polynomial representation into the individual mode shapes of the beam contributing to the response. The individual mode shapes estimates are further processed to fit the governing fourth order spatial equation of beams to obtain the spatial modal frequency. Standard relations give the modal damping ratios and natural frequencies from estimated spatial frequencies.

2.1 Forsythe Polynomials

In view of the orthogonality property of the natural mode shapes of the beam, orthogonal polynomials are most suited to approximate them. West et al (1993) used recursive form of Forsythe polynomials to approximate the fundamental beam mode for easier formulation and removal of ill-conditioning. Based on the results of the above mentioned work the present study also employs Forsythe Polynomials for extraction of mode shapes from measured spatial data. Forsythe polynomials are defined as (Forsythe, 1957)

$$p_0(x) = 1$$

$$p_1(x) = xp_0(x) - \alpha_1 p_0(x) \quad (2.1)$$

$$p_{i+1}(x) = xp_i(x) - \alpha_{i+1} p_i(x) - \beta_i p_{i-1}(x)$$

with

$$\alpha_{i+1} = \sum_{\mu=1}^N x_{\mu} [p_i(x_{\mu})]^2 / \sum_{\mu=1}^N [p_i(x_{\mu})]^2 \quad (2.2)$$

$$\beta_i = \sum_{\mu=1}^N x_{\mu} p_i(x_{\mu}) p_{i-1}(x_{\mu}) / \sum_{\mu=1}^N [p_i(x_{\mu})]^2 \quad (2.3)$$

2.2 Mode Shape Estimation

The steady state response of an Euler beam excited at a point $x = a$ along its length by a force $F_0 e^{i\omega t}$ can be written in standard form as

$$y(x) = \sum_{j=1}^{\infty} [F \psi_j(a) \psi_j(x) (\omega_j^2 - \omega^2) / \{(\omega_j^2 - \omega^2)^2 + 4\xi_j^2 \omega^2\} - i2F \psi_j(x) \psi_j(a) \xi_j \omega_j \omega / \{(\omega_j^2 - \omega^2)^2 + 4\xi_j^2 \omega^2\}] e^{i\omega t} \quad (2.4)$$

where

$$F = F_0 / \rho A l$$

and ω_j is the j th natural frequency, $\psi_j(x)$ is the j th mode shape and ξ_j is the equivalent j th modal damping ratio.

Employing the Forsythe polynomials, the j th mode shape of the beam is expressed as,

$$\psi_j(x) = \sum_{k=0}^h S_{jk} p_k(x) \quad (2.5)$$

where

$$S_{jk} \quad j = 1, 2, 3, \dots; \quad k = 1, 2, 3, \dots, h$$

are constants to be estimated from the measured data.

Defining

$$A_j = F \psi_j(a) (\omega_j^2 - \omega^2) / \{(\omega_j^2 - \omega^2)^2 + 4\xi_j^2 \omega^2\} \quad (2.6)$$

$$B_j = 2F \psi_j(a) \omega_j \omega \xi_j / \{(\omega_j^2 - \omega^2)^2 + 4\xi_j^2 \omega^2\} \quad (2.7)$$

the displacement response of the beam, equation (2.4), can be rewritten as

$$y(x) = \sum_{j=1}^{\infty} [A_j \psi_j(x) - iB_j \psi_j(x)] e^{i\omega x} \quad (2.8)$$

Substitution of equation (2.8) in (2.11) gives

$$y(x) = \sum_{j=1}^{\infty} \left[(A_j - iB_j) \sum_{k=1}^h \{S_{jk} p_k(x)\} \right] e^{i\omega x} \quad (2.9)$$

Considering that only two natural modes (with natural frequencies ω_m and ω_{m+1}) of the beam, lying on either side of the excitation frequency ω (i.e. $\omega_m < \omega < \omega_{m+1}$), predominantly contribute to the response (ignoring the contribution of the natural modes lying farther away from the excitation frequency), the beam response of equation (2.9), reduces to the approximation

$$y(x) = [(A_m - iB_m) \sum_{k=1}^h \{S_{mk} p_k(x)\} + (A_{m+1} - iB_{m+1}) \sum_{k=1}^h \{S_{m+1,k} p_k(x)\}] e^{i\omega x} \quad (2.10)$$

The magnitudes of the real and imaginary components of the response then, are,

$$\begin{aligned} Y_r(x) &= A_m \sum_{k=1}^h S_{mk} p_k(x) + A_{m+1} \sum_{k=1}^h S_{m+1,k} p_k(x) \\ Y_i(x) &= B_m \sum_{k=1}^h S_{mk} p_k(x) + B_{m+1} \sum_{k=1}^h S_{m+1,k} p_k(x) \end{aligned} \quad (2.11)$$

If the experimental measurements are made at stations x_μ , ($\mu = 1, N$) along the length of the beam, the real and imaginary components of the response, approximated through equation (2.10) should be

$$\begin{aligned} Y_r(x_\mu) &= A_m \sum_{k=1}^h S_{mk} p_k(x_\mu) + A_{m+1} \sum_{k=1}^h S_{m+1,k} p_k(x_\mu) \\ Y_i(x_\mu) &= B_m \sum_{k=1}^h S_{mk} p_k(x_\mu) + B_{m+1} \sum_{k=1}^h S_{m+1,k} p_k(x_\mu) \end{aligned} \quad (2.12)$$

However, if $\nu_r(x_\mu)$ and $\nu_i(x_\mu)$ are the real and imaginary components of the response amplitude actually measured, experimentally, the least square error between the measured amplitudes and their Forsythe approximations of equation (2.12) are

$$\begin{aligned} \varepsilon_r &= \sum_{\mu=1}^N [Y_r(x_\mu) - \nu_r(x_\mu)]^2 \\ \varepsilon_i &= \sum_{\mu=1}^N [Y_i(x_\mu) - \nu_i(x_\mu)]^2 \end{aligned} \quad (2.13)$$

Minimizing the errors with respect to S_{mk} and $S_{m+1,k}$ ($k = 1, 2, \dots, h$) and noting the orthogonality property of the Forsythe polynomials

$$\sum_{\mu=1}^N p_i(x_\mu) p_j(x_\mu) = 0 \quad i \neq j \quad (2.14)$$

the following set of equations are obtained

$$\begin{aligned} A_m S_{mk} + A_{m+1} S_{m+1,k} &= c_k \\ B_m S_{mk} + B_{m+1} S_{m+1,k} &= d_k \quad k = 1, 2, \dots, h \end{aligned} \quad (2.15)$$

with

$$\begin{aligned} c_k &= \sum_{\mu=1}^N v_r(x_\mu) p_k(x_\mu) / \sum_{\mu=1}^N [p_k(x_\mu)]^2 \\ d_k &= \sum_{\mu=1}^N v_i(x_\mu) p_k(x_\mu) / \sum_{\mu=1}^N [p_k(x_\mu)]^2 \end{aligned} \quad (2.16)$$

The constants S_{mk} and $S_{m+1,k}$ can be written from (2.14) and (2.15) as,

$$\begin{aligned} S_{mk} &= (c_k B_{m+1} / A_{m+1} - d_k) / [(B_{m+1} / A_{m+1} - B_m / A_m) A_m] \\ S_{m+1,k} &= (c_k B_m / A_m - d_k) / [(B_{m+1} / A_{m+1} - B_m / A_m)(-A_{m+1})] \end{aligned} \quad (2.17)$$

The orthogonality properties of the mode shapes of a beam of constant properties over its span ($x=0$ to $x=L$) require that

$$\int_0^L \psi_i(x) \psi_j(x) dx = 0 \quad i \neq j \quad (2.18)$$

$$\int_0^L \psi''_i(x) \psi''_j(x) dx = 0 \quad i \neq j \quad (2.19)$$

In terms of the Forsythe approximation the above modal orthogonality implies,

$$\begin{aligned} \sum_{\mu=1}^N \sum_{k=0}^h S_{ik} p_k(x_\mu) \sum_{k=0}^h S_{jk} p_k(x_\mu) &= 0 \quad i \neq j \\ \sum_{\mu=1}^N \sum_{k=0}^h S_{ik} p''_k(x_\mu) \sum_{k=0}^h S_{jk} p''_k(x_\mu) &= 0 \quad i \neq j \end{aligned} \quad (2.20)$$

Substitution in the above, from equations (2.17) for modes m and $m+1$ and noting the relations (2.18) and (2.19), one obtains

$$\sum_{\mu=1}^N \sum_{k=0}^h (c_k B_{m+1} / A_{m+1} - d_k)(c_k B_m / A_m - d_k) p_k^2(x_\mu) = 0 \quad (2.21)$$

$$\sum_{\mu=1}^N \sum_{k=0}^h (c_k B_{m+1} / A_{m+1} - d_k) p_k''(x_\mu) \sum_{k=0}^h (c_k B_m / A_m - d_k) p_k''(x_\mu) = 0 \quad (2.22)$$

Using the values of c_k, d_k (computed from experimental data, equation (2.16)) equations (2.21) and (2.22) can be readily solved for the ratios B_m / A_m and B_{m+1} / A_{m+1} . These ratios are further substituted in equations (2.17) to obtain the constants S_{mk} and $S_{m+1,k}$ as multiples of A_m and A_{m+1} respectively.

Usage of S_{mk} and $S_{m+1,k}$, thus determined, in equation (2.17), give the approximations for the m th and $(m+1)$ th mode shapes, $\psi_m(x)$ and $\psi_{m+1}(x)$, respectively.

2.3 Estimation Of Natural Frequencies And Damping Ratios

The mode shapes of a beam, irrespective of its boundary conditions, are governed by the differential equation,

$$\psi_m''''(x) = \chi_m^4 \psi_m(x) \quad (2.23)$$

where ψ_m'''' denotes differentiation with respect to x and the spatial frequency χ_m is related to the natural frequency ω_m of the beam as,

$$\chi_m^4 = \omega_m^2 (\rho A / EI) \quad (2.24)$$

(ρ, A, E, I being the mass density, area of cross section, modulus of elasticity and area moment of inertia of beam).

The spatial frequency can be obtained from (2.23) as,

$$\chi_m^4 = \left[\sum_{k=0}^h S_{mk} p_k''''(x_\mu) / \sum_{k=0}^h S_{mk} p_k(x_\mu) \right] / N \quad (2.25)$$

and the natural frequency ω_m can be readily calculated from equation (2.24).

From equations (2.6) and (2.7) the ratios B_m / A_m can be expressed as

$$B_m / A_m = 2\xi_m \omega_m \omega / (\omega_m^2 - \omega^2) \quad (2.26)$$

Employing the computed values of ω_m and that of B_m / A_m (from equations 2.21 and 2.22) the equivalent modal damping ratios ξ_m can be calculated.

2.4 Remarks

The procedure involves the approximation of incorporating the participation of only two beam modes in the vibration response. Successive modal properties of the beam can be estimated by successive application of the procedure with the beam excited at different frequencies. Damping is taken to be equivalent viscous in nature, in the present analysis. The procedure and the errors incurred are numerically illustrated in the next chapter.

CHAPTER 3

NUMERICAL SIMULATION

The procedure developed for estimation of modal participation, mode shapes, natural frequencies and damping ratios, in the previous chapter is illustrated here through numerical simulation. The numerical simulation is carried out for different values of nondimensionalised beam parameters and boundary configurations. The effect of possible measurement noise is illustrated in all these cases. In addition, the influence of the number of response measurement stations on the accuracy of the estimates is illustrated. The influence of an error in excitation force location is also investigated.

3.1 Non-Dimensional Parameters

The response of the beam, subjected to an excitation, as described in the previous chapter, is simulated through a computer program employing standard response formulae (Timoshenko, 1928). The estimation procedure developed is then applied to this simulated response for extraction of the modal parameters. Noting equation (2.4), the geometric and material properties of the beam are incorporated by defining the nondimensional parameter

$$\kappa = [EI / \rho g A l^3]^{(1/2)} \quad (3.1)$$

(g , the gravitational acceleration is taken as 9.81 m/s). The response is simulated and subsequent estimation procedure is illustrated for $\kappa = 0.1, 1.0$ and 10.0 , for simply supported, clamped-clamped and clamped-free boundary configurations.

The nondimensional response

$$H(x) = \sum_{j=1}^{\infty} [\bar{A}_j \psi_j(x) - \bar{B}_j \psi_j(x)] e^{i\alpha x} \quad (3.2)$$

with

$$r_j = \omega / \omega_j$$

$$\bar{A}_j = \psi_j(a)(1 - r_j^2) / ((1 - r_j^2)^2 + 4\xi_j^2 r_j^2)$$

$$\bar{B}_j = \psi_j(a)(2r_j) / ((1 - r_j^2)^2 + 4\xi_j^2 r_j^2) \quad (3.3)$$

$$H(x) = y(x) / y_{st}$$

$$y_{st} = F / \rho A l \omega_1^2$$

is numerically simulated through the computer.

The numerically simulated response is fed as input to the modal estimation algorithm, based on the procedure described in the previous chapter.

The estimation process has also been nondimensionalised. Referring to equations (2.4)-(2.9) and taking the response to be constituted primarily of the m th and $(m+1)$ th beam modes, which lie on either side of the excitation frequency, ω , the magnitudes of the real and imaginary components of the response the nondimensionalised Forsythe approximation of the response are

$$\begin{aligned} H_r(x) &= \bar{A}_m \sum_{k=1}^h S_{mk} p_k(x) + \bar{A}_{m+1} \sum_{k=1}^h S_{m+1,k} p_k(x) \\ H_i(x) &= \bar{B}_m \sum_{k=1}^h S_{mk} p_k(x) + \bar{B}_{m+1} \sum_{k=1}^h S_{m+1,k} p_k(x) \end{aligned} \quad (3.4)$$

Defining, the real and imaginary components of the measured response in nondimensional terms as

$$\begin{aligned} q_r(x) &= v_r(x) \omega_1^2 / (F / \rho A l) \\ q_i(x) &= v_i(x) \omega_1^2 / (F / \rho A l) \end{aligned} \quad (3.5)$$

the nondimensionalised least square errors are

$$\begin{aligned} \bar{\varepsilon}_r &= \sum_{\mu=1}^N [H_r(x) - q_r(x)]^2 \\ \bar{\varepsilon}_i &= \sum_{\mu=1}^N [H_i(x) - q_i(x)]^2 \end{aligned} \quad (3.6)$$

The nondimensionalised errors are now minimized with respect to S_{mk} and $S_{m+1,k}$ ($k=1,2,\dots,h$) for estimation of constants S_{mk} and $S_{m+1,k}$ and subsequently the m th and $(m+1)$ th modal parameters, as described in the previous chapter.

3.2 Case Studies

Three boundary condition configurations are chosen for study - (i) Simply-Supported (ii) Clamped-Free and (iii) Clamped-Clamped. The estimation, using the computer simulated response is carried out for three values of the nondimensional beam parameter, κ . The three values chosen for the parameter κ are 0.1, 1.0 and 10.0. The procedure is illustrated in all these cases for participation of the first two beam modes (i.e. $m = 1$, in equation (3.4)). The damping ratios, ξ_1 and ξ_2 are chosen as 0.02 for illustration. The nondimensional input force amplitude, $F / \rho g A l$ is kept as 100 in all the cases. The excitation frequency ω , in all the cases is chosen as be as the mean of the first and second natural frequencies ($\omega = (\omega_1 + \omega_2) / 2$), so that participation of the two modes is duly accounted for.

Simply -supported :

Figures 3.1 (a) and (b) show the in-phase and out-of-phase components of the computer simulated spatial response $H(x)$, using equation (3.2), for a simply-supported configuration with $\kappa = 0.1$, the excitation being given at its mid-point. The response is plotted as a function of the nondimensional distance, x/l , along the beam. The response of the beam is constituted of contributions of natural modes having mode shapes, which are symmetric with respect to the mid-point (the excitation being provided at the centre of the beam). The response therefore consists of contributions from modes 1, 3, 5,..... The estimation procedure is applied by picking up this spatial response at hundred number of points along the beam (the influence of the number of these measurement points is discussed in a later section. As stated in the earlier chapter, only the modes lying adjacent to the excitation frequency get estimated (mode 1 and mode 3, in this case). Figs. 3.2 (a) and (b) show the estimated first and third mode shapes, along with the exact mode shape of the beam. The estimated natural frequencies and damping ratios are given in Table 3.1. Figures 3.3 (a)-(b) and 3.4 (a)-(b), similarly show the simulated response input and the estimated modes shapes, respectively for a value of the nondimensional beam parameter $\kappa = 1.0$, while Figs 3.5

(a)-(b) and 3.6 (a)-(b) give the corresponding curves for $\kappa=10.0$. The natural frequency and damping estimates are listed in Table 3.1, along with their exact values.

Table 3.1 **Exact and Estimated Natural Frequencies and Damping Ratios**
for Simply Supported Configuration

κ	Mode	Natural Frequencies			Damping Ratios		
		Exact	Estimated	Error	Exact	Estimated	Error
0.1	1	3.091	3.042	1.58	0.02	0.01970	1.95
	3	27.821	27.329	1.76	0.02	0.01961	1.50
1.0	1	30.910	30.424	1.58	0.02	0.01970	1.95
	3	278.211	273.292	1.76	0.02	0.01961	1.50
10.0	1	309.100	304.245	1.58	0.02	0.01970	1.95
	3	2782.110	2732.921	1.76	0.02	0.01961	1.50

The procedure developed can be seen to give good estimates of the mode shapes and natural frequency and damping ratios. Also, as can be seen from the Figs. 3.2, 3.4 and 3.6 and Table 3.1, the accuracy of the procedure is practically the same for the three values of the nondimensional parameter κ . The error in the natural frequency and damping estimates is of the order of 2%.

Cantilever:

Figs. 3.7 (a) and (b) show the in-phase and out-of-phase steady state response amplitudes of a cantilever with nondimensional parameter $\kappa=1.0$, excited at its free end. Though the response comprises of all possible cantilever modes, estimation is carried out for modes 1 and 2 only, the excitation frequency lying in-between the two, their contribution is taken to be most significant. Figs. 3.8 (a) and (b) depict the estimated and exact mode shapes. The corresponding natural frequencies and damping ratios are given in Table 3.2. The estimation is carried out for other values of the nondimensional beam parameter κ , as in the case of the simply-supported configuration. The results are reported here for only one value of κ ($=1.0$), since the results are not seen to differ with change in this parameter.

**Table 3.2 Exact and Estimated Natural Frequencies and Damping Ratios
for Cantilever Configuration**

κ	Mode	Natural Frequencies			Damping Ratios		
		Exact	Estimated	Error	Exact	Estimated	Error
1.0	1	11.012	11.278	2.75	0.02	0.01945	2.75
	2	69.014	70.844	3.70	0.02	0.02074	3.70

Fixed-Fixed beam:

The excitation is provided at the mid-point of the beam. The modes contributing to the response are 1, 3, 5, 7,.... Figs. 3.9 (a) and (b) give the in-phase and out-of-phase components of the computer simulated spatial response $H(x)$, for $\kappa = 1.0$. As in the simply-supported and cantilever cases, κ is not found to be a parameter significant to the estimation procedure and results are reported only for a case with $\kappa=1.0$. Excitation frequency being chosen to lie between modes 1 and 3, estimation gets carried out for these two modes only. Figs. 3.10 (a) and (b) show the estimated mode shapes 1 and 3, while the natural frequencies and damping ratios, consequently computed are listed in Table 3.3.

**Table 3.3 Exact and Estimated Natural Frequencies and Damping Ratios
for Fixed-Fixed Configuration**

κ	Mode	Natural Frequencies			Damping Ratios		
		Exact	Estimated	Error	Exact	Estimated	Error
1.0	1	70.075	68.241	2.61	0.02	0.02065	3.25
	3	378.679	369.236	2.49	0.02	0.01925	3.75

The procedure can be seen to give fairly accurate results, the error being of the order of 2-3 %. It can also be seen that, ignoring the participation of modes lying far from the excitation frequency does not entail much error.

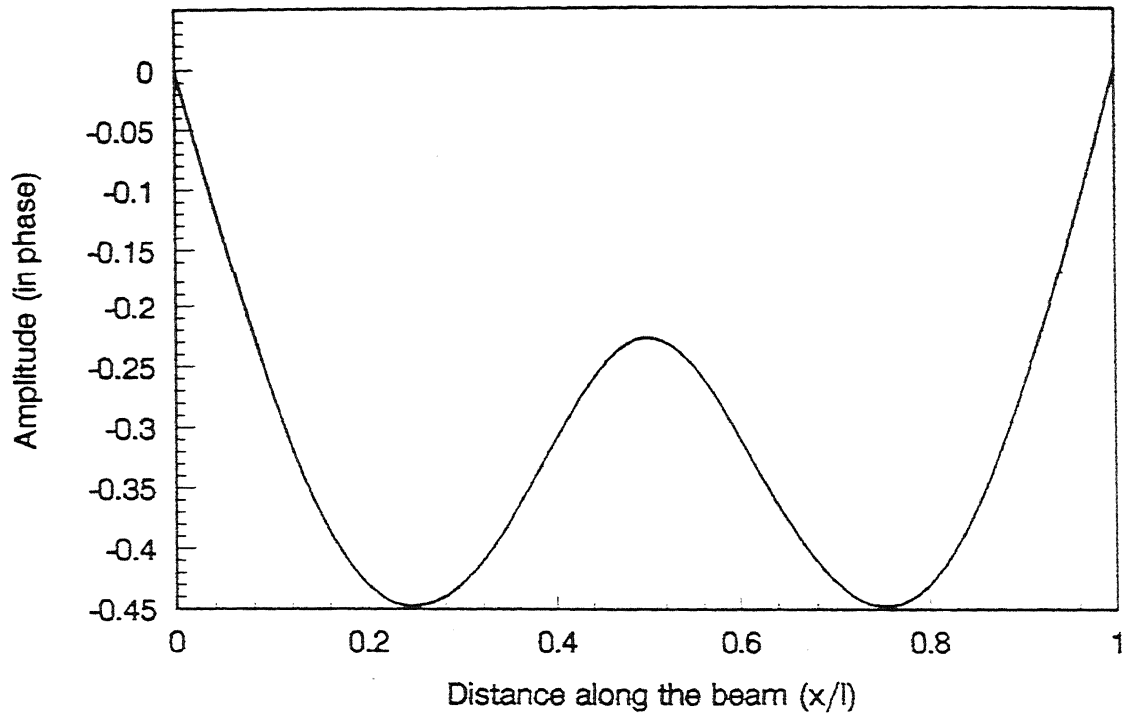


Fig. 3.1 (a) Simulated in phase response amplitude of simply supported beam ($\kappa=0.1$)

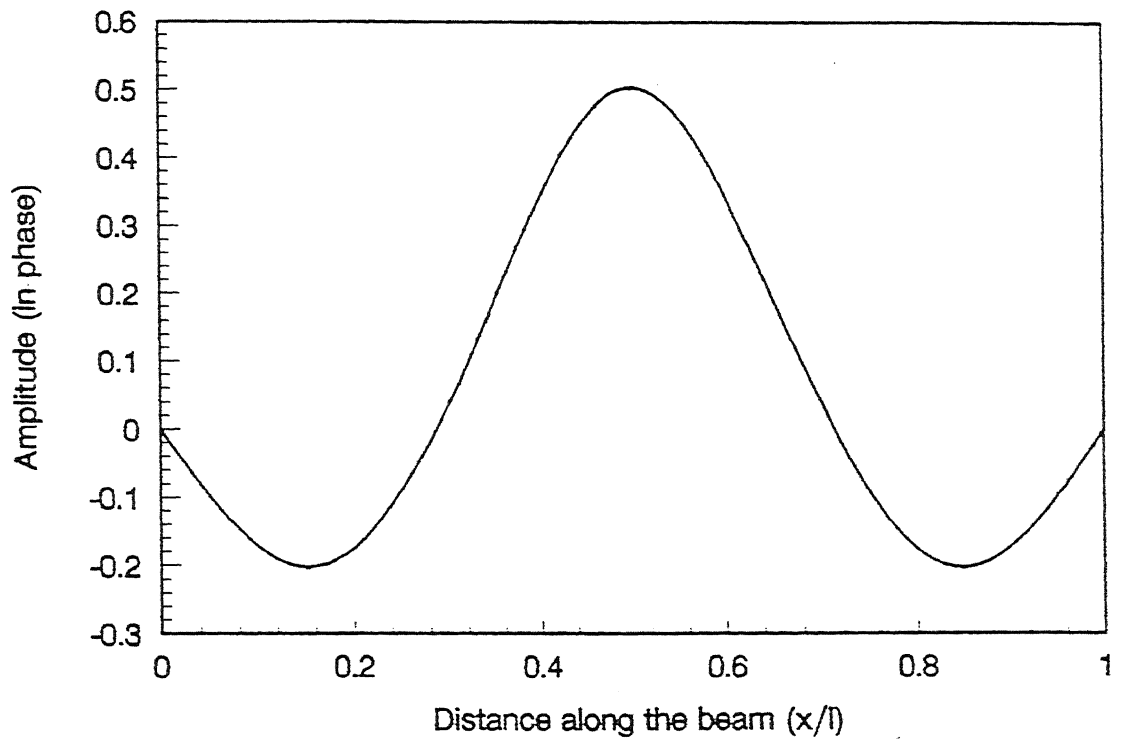
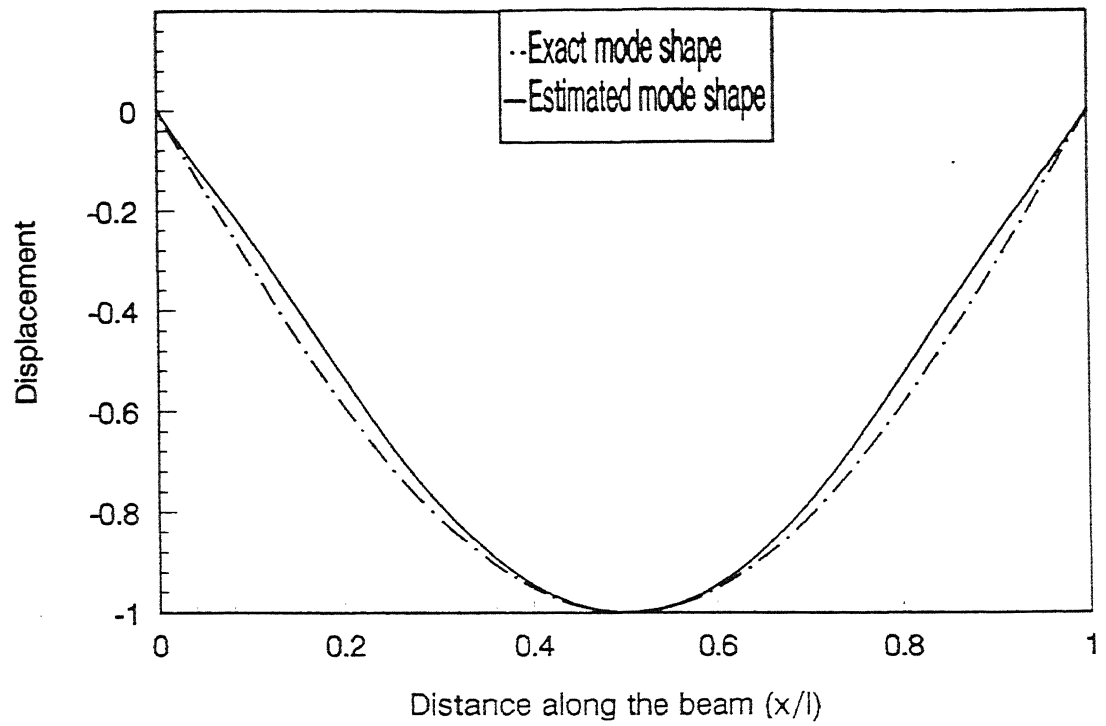
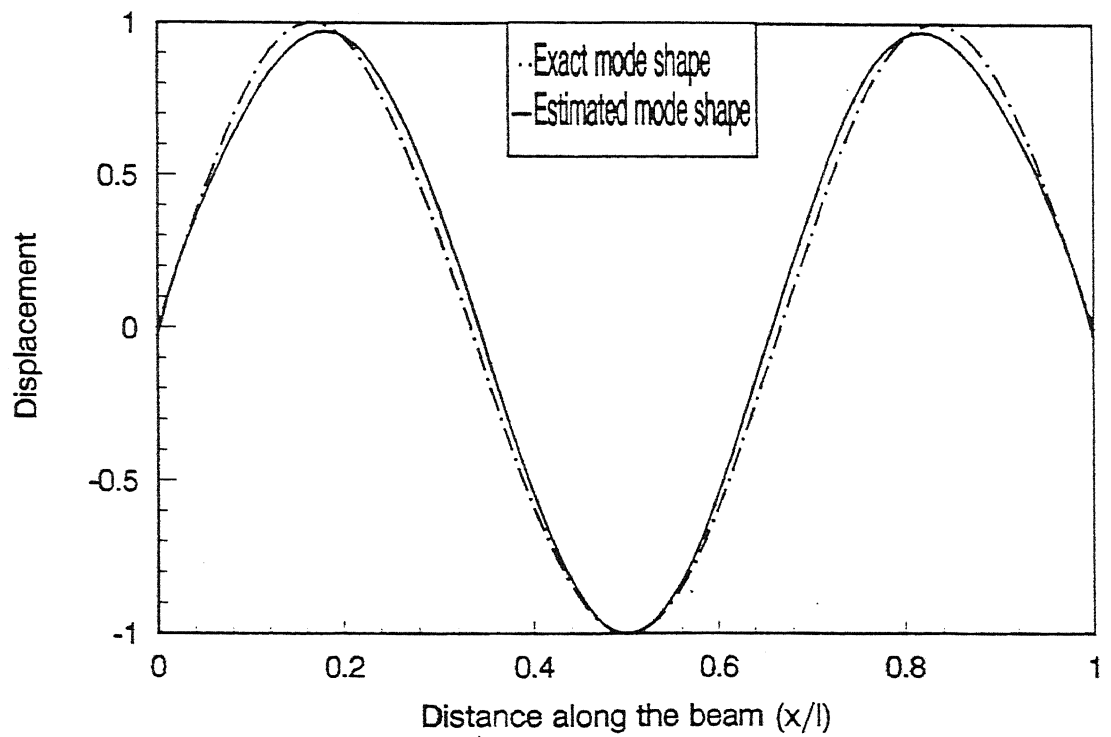


Fig. 3.1 (b) Simulated out of phase response amplitude of simply supported beam ($\kappa=0.1$)



(a) Mode 1



(b) Mode 2

Fig.3.2 Estimated and exact mode shapes of simply supported beam($\kappa=0.1$)

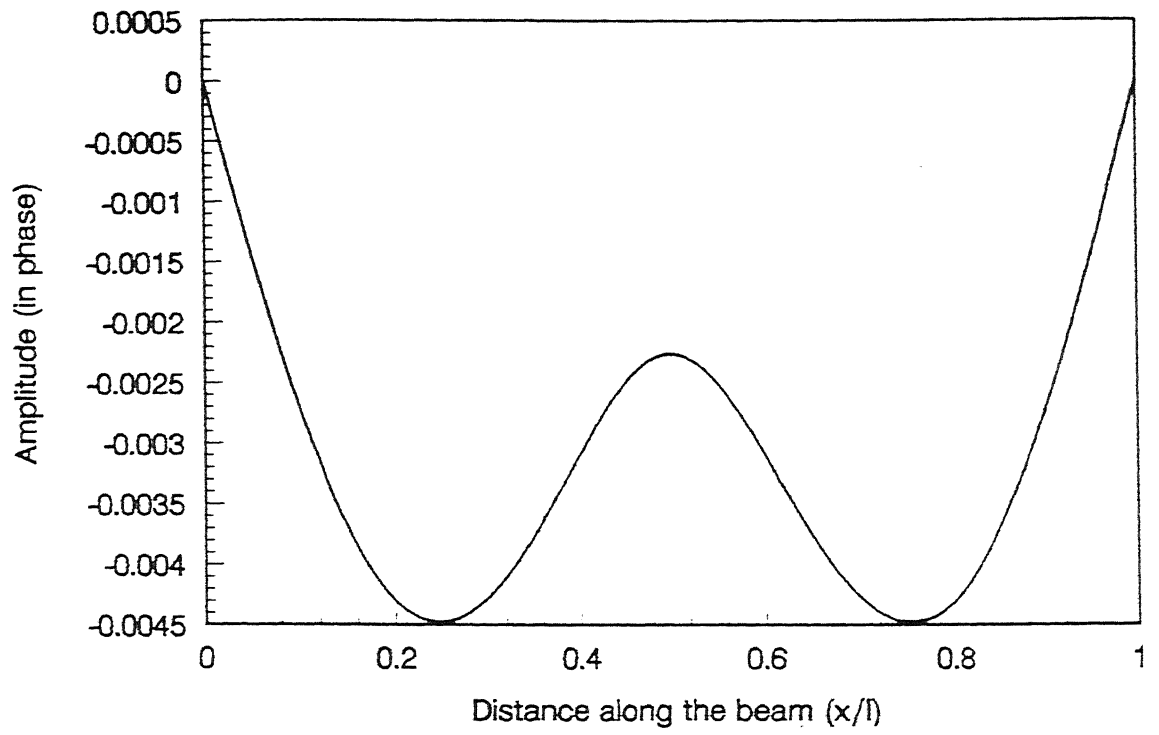


Fig. 3.3 (a) Simulated in phase response amplitude of simply supported beam ($\kappa=1.0$)

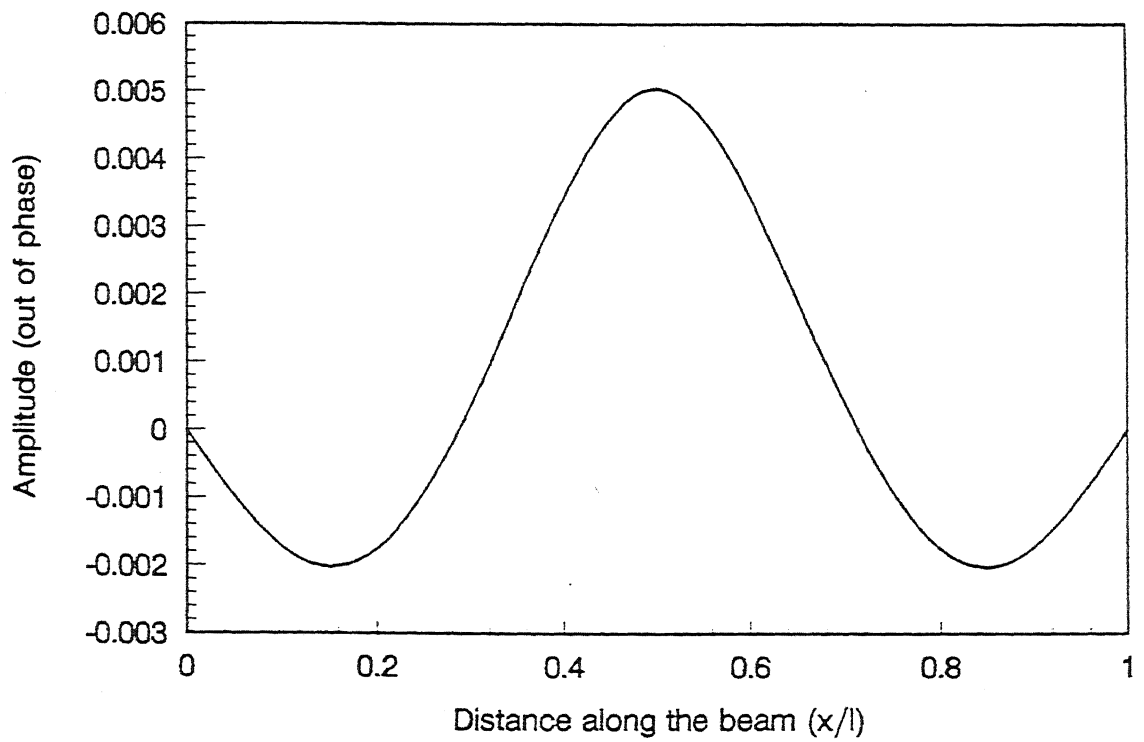
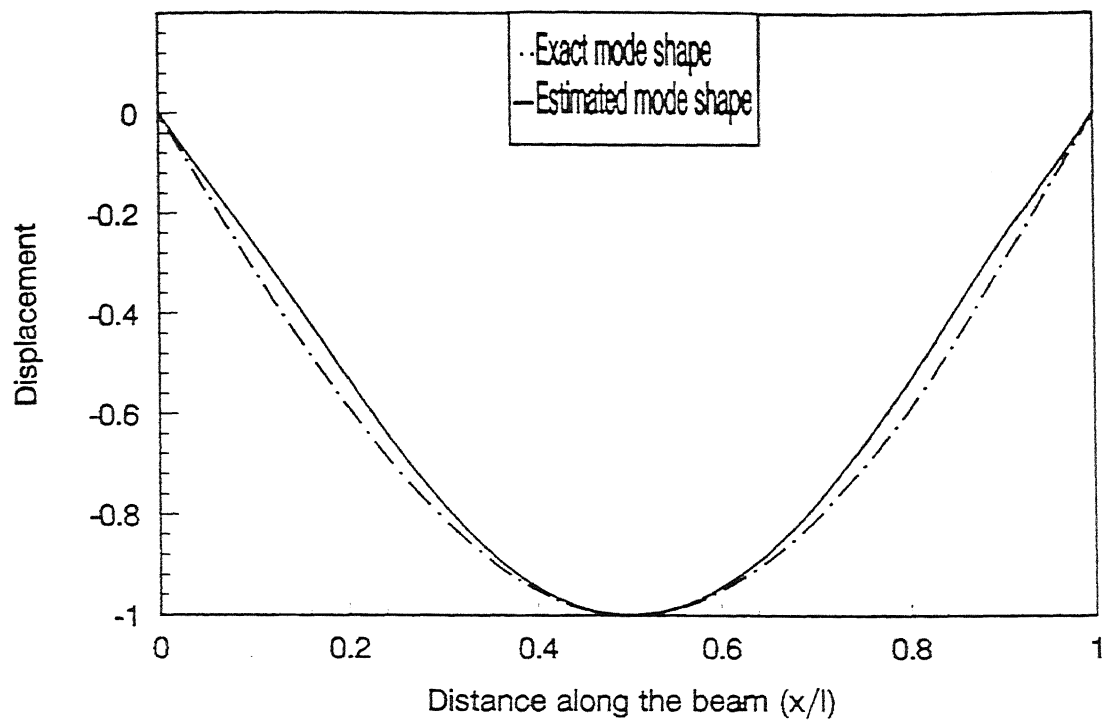
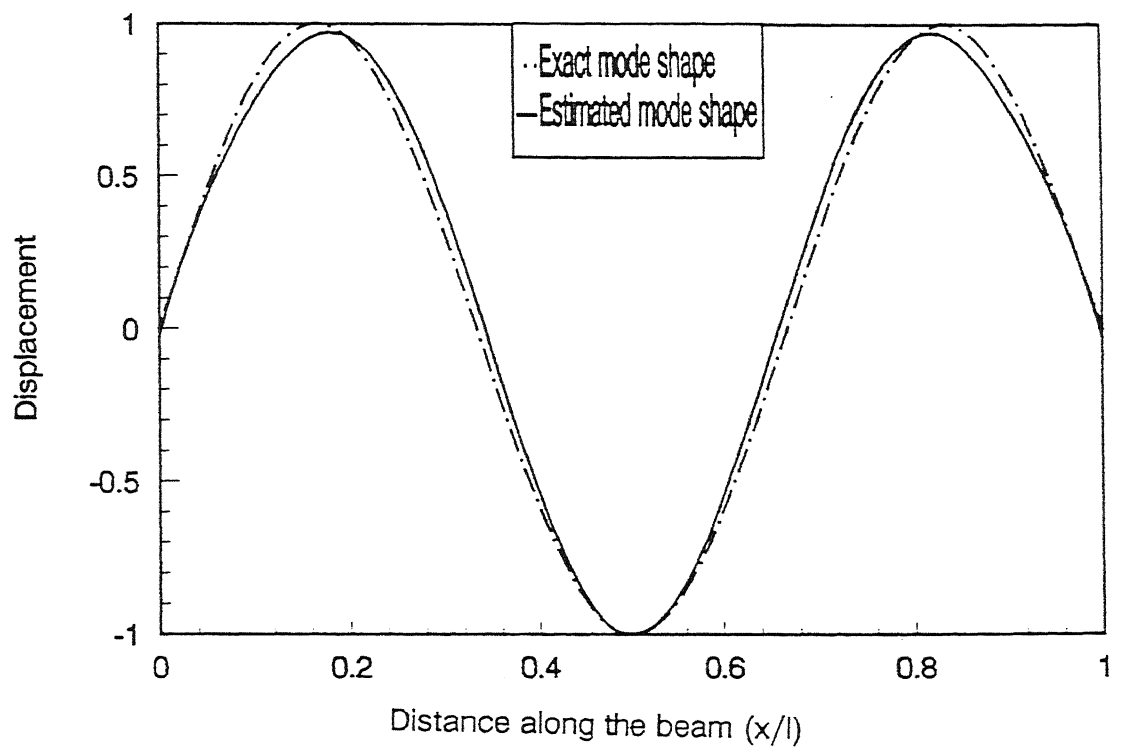


Fig. 3.3 (b) Simulated out of phase response amplitude of simply supported beam ($\kappa=1.0$)



(a) Mode 1



(b) Mode 2

Fig.3.4 Estimated and exact mode shapes of simply supported beam($\kappa=1.0$)

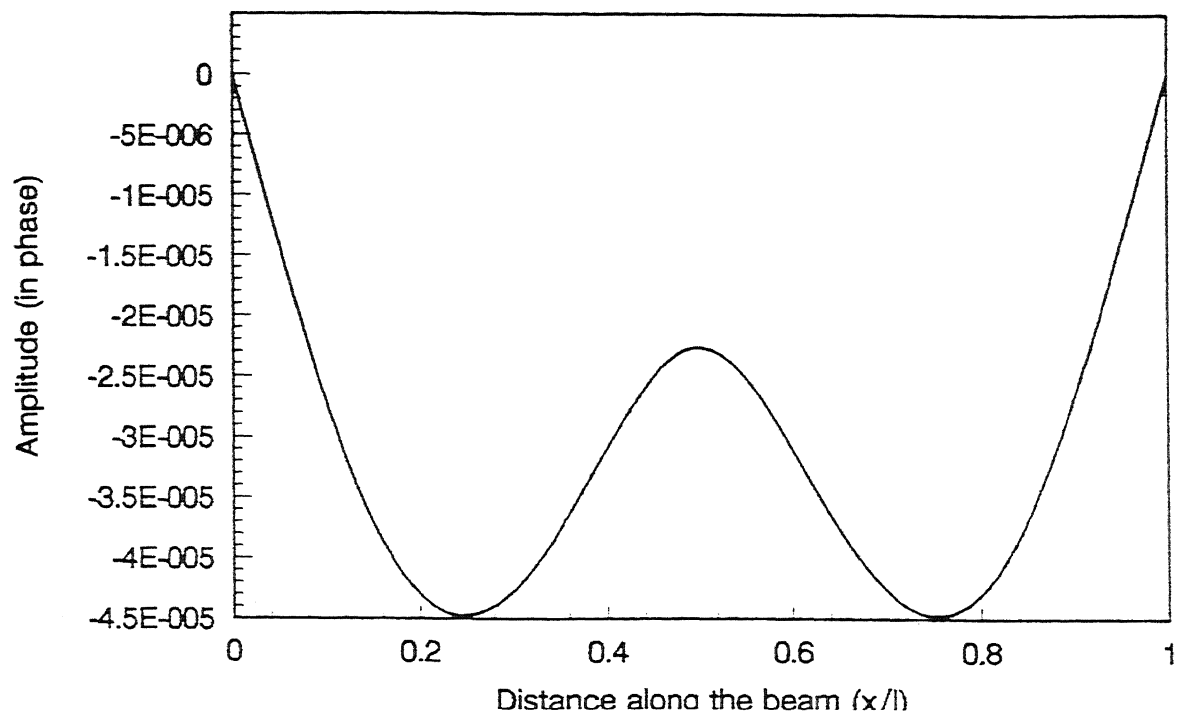


Fig. 3.5 (a) Simulated in phase response amplitude of simply supported beam ($\kappa=10.0$)

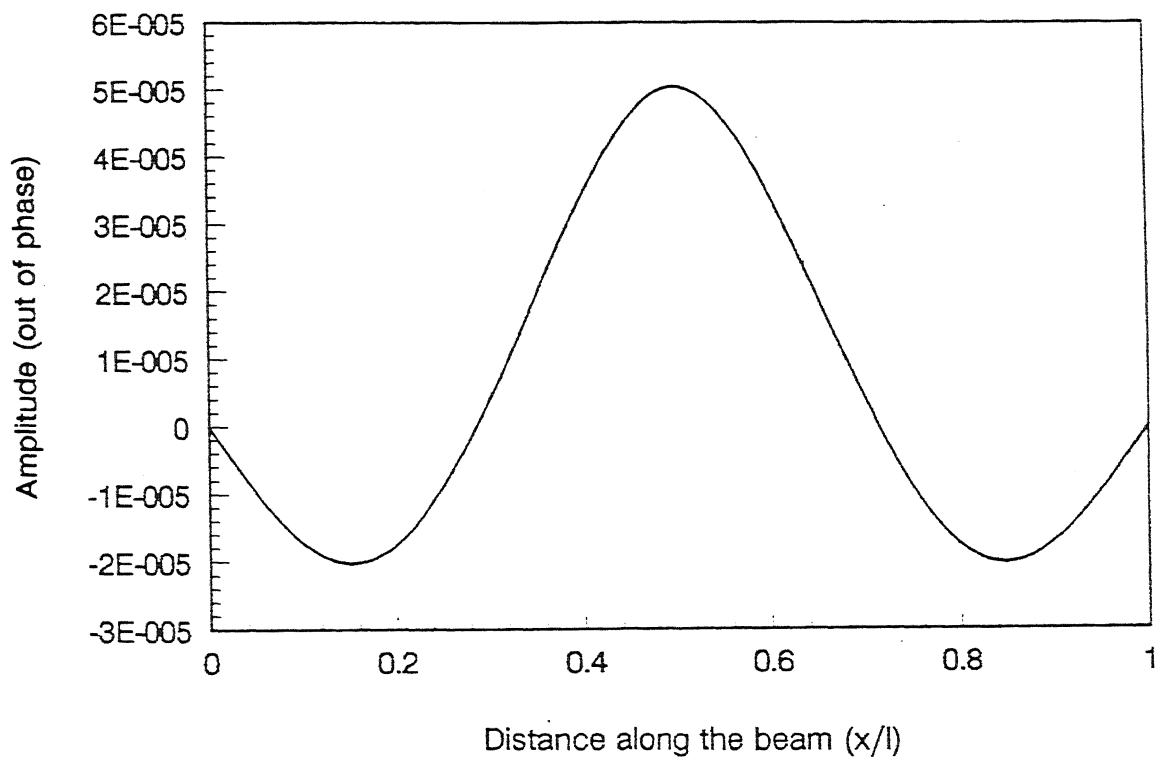
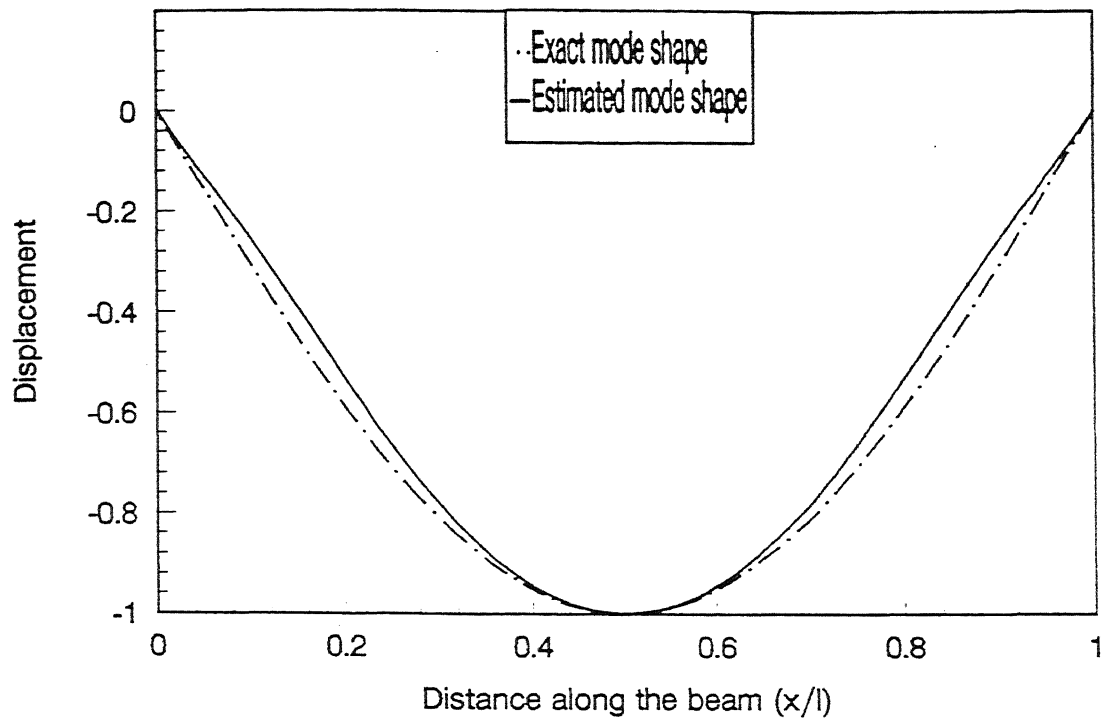
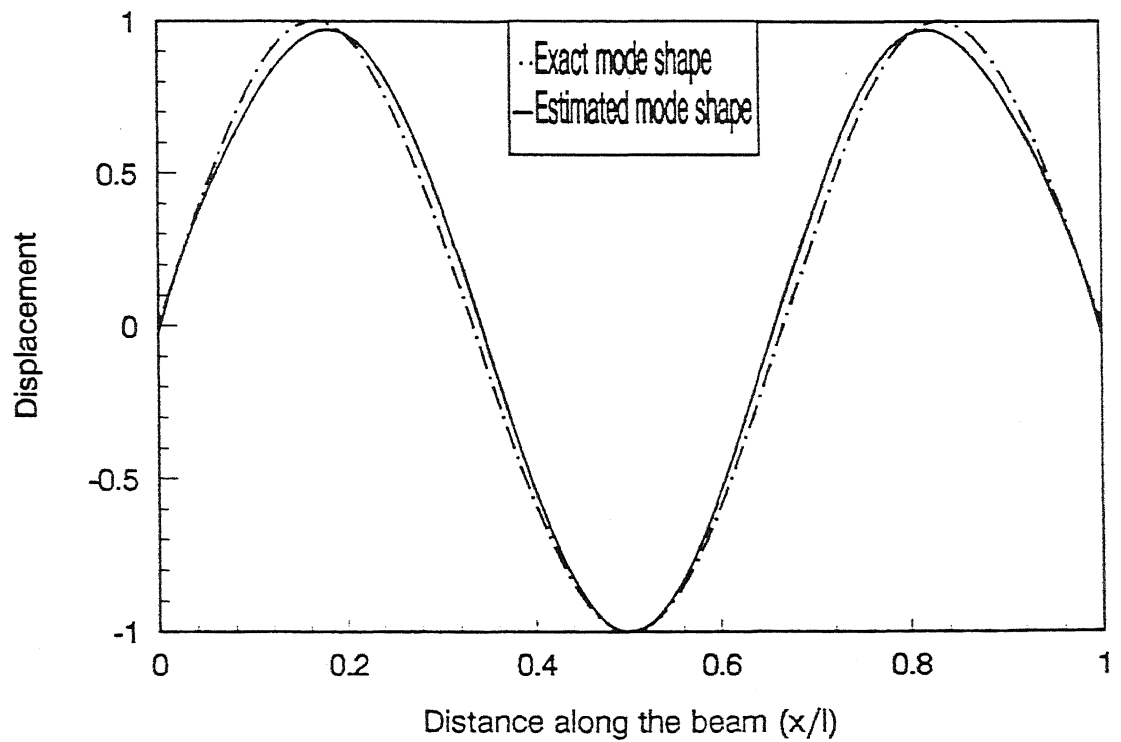


Fig. 3.5 (b) Simulated out of phase response amplitude of simply supported beam ($\kappa=10.0$)



(a) Mode 1



(b) Mode 2

Fig.3.6 Estimated and exact mode shapes of simply supported beam ($\kappa = 10.0$)

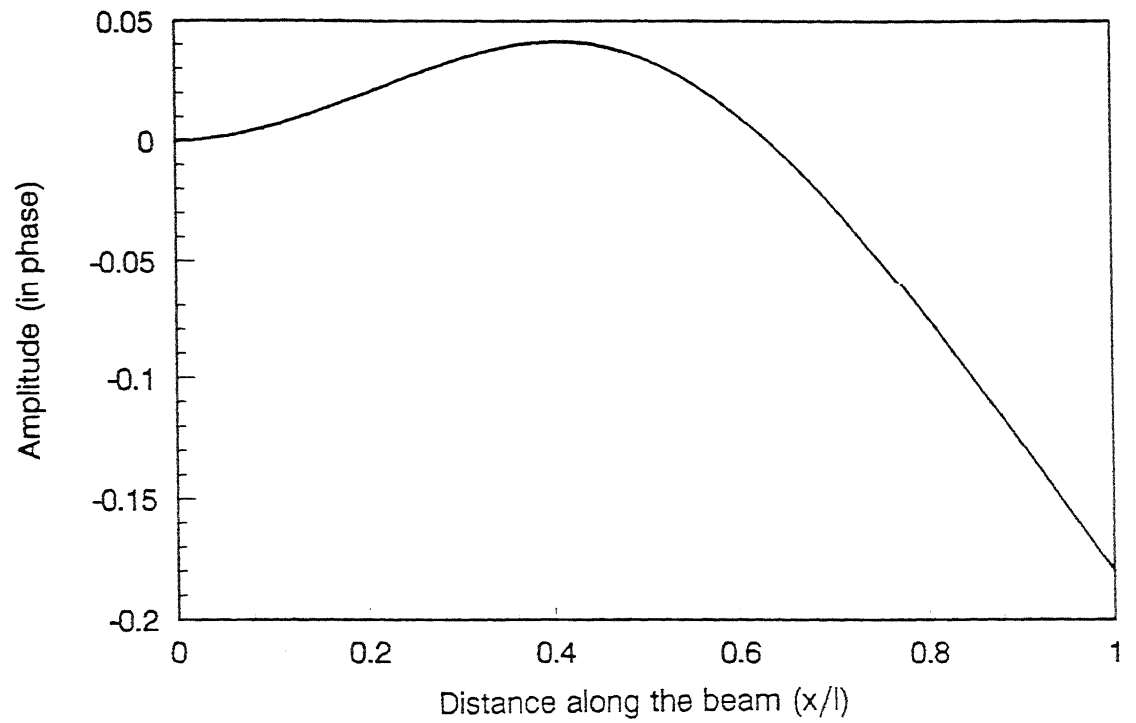


Fig. 3.7 (a) Simulated in phase response amplitude of cantilever beam ($\kappa=1.0$)

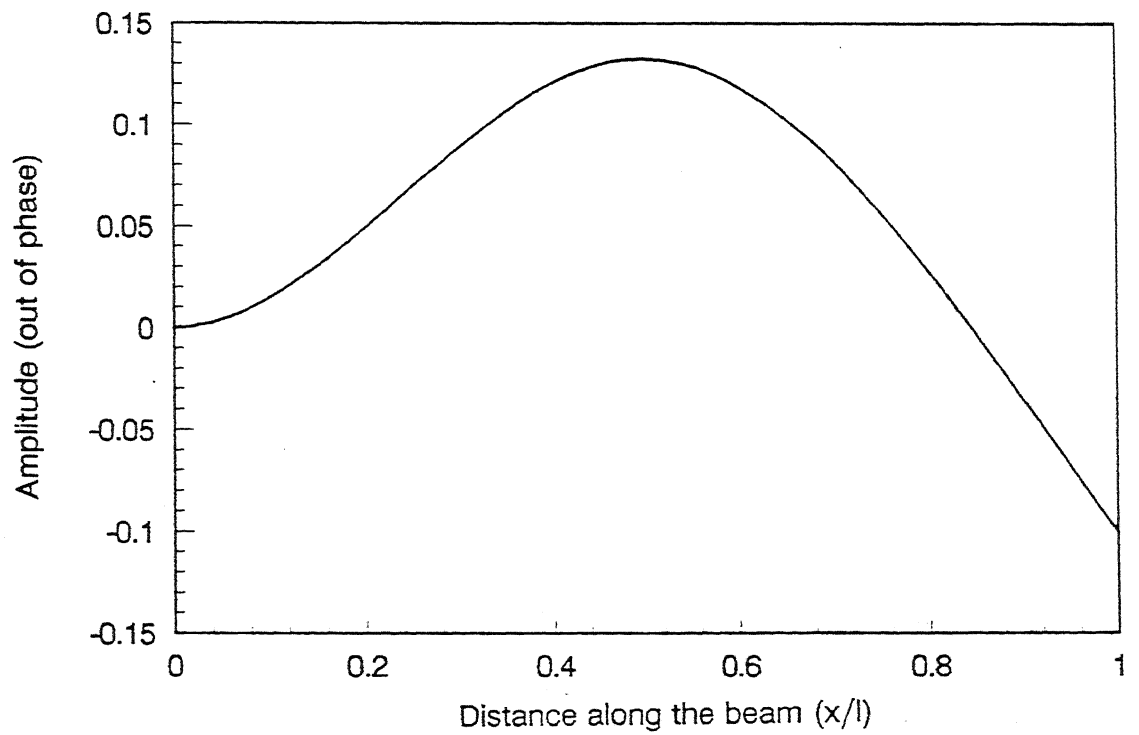
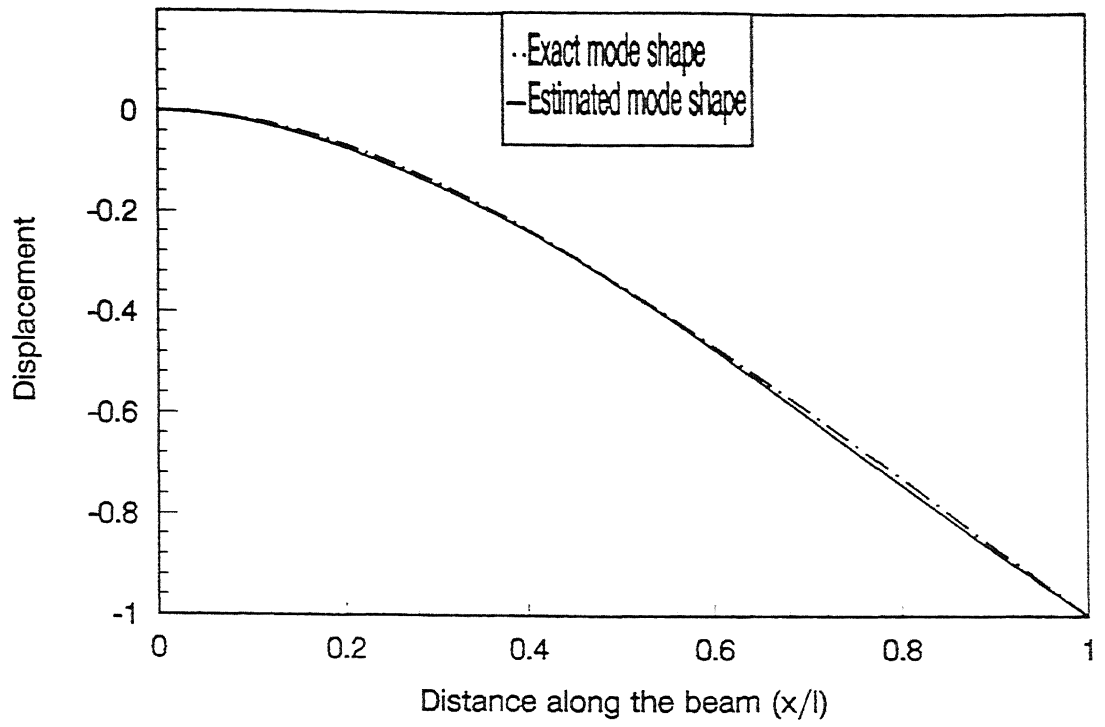
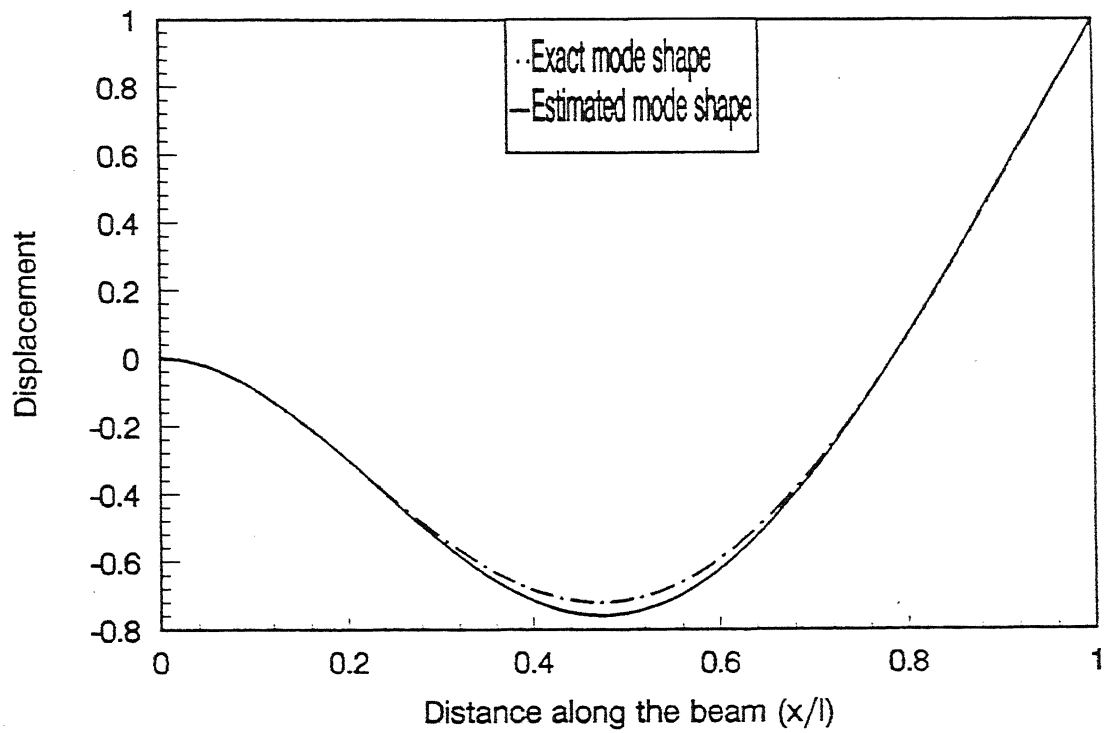


Fig. 3.7 (b) Simulated out of phase response amplitude of cantilever beam ($\kappa=1.0$)



(a) Mode 1



(b) Mode 2

Fig.3.8 Estimated and exact mode shapes of cantilever beam($\kappa=1.0$)

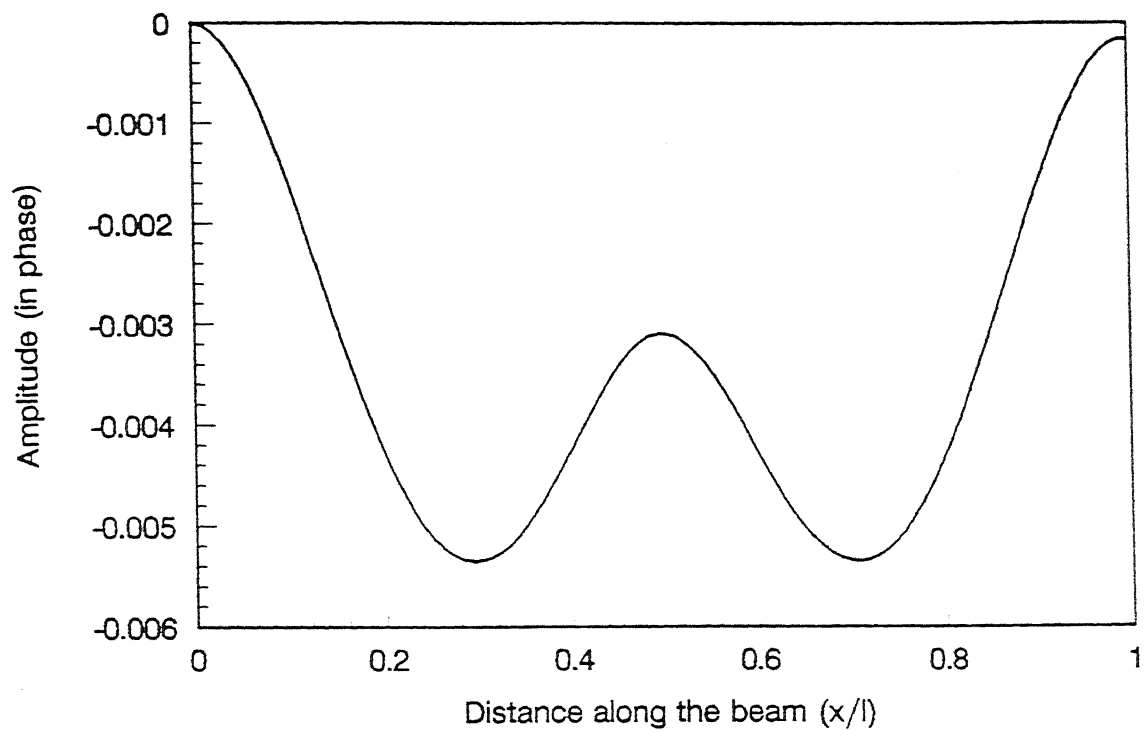


Fig. 3.9 (a) Simulated in phase response amplitude of fixed-fixed beam ($\kappa=1.0$)

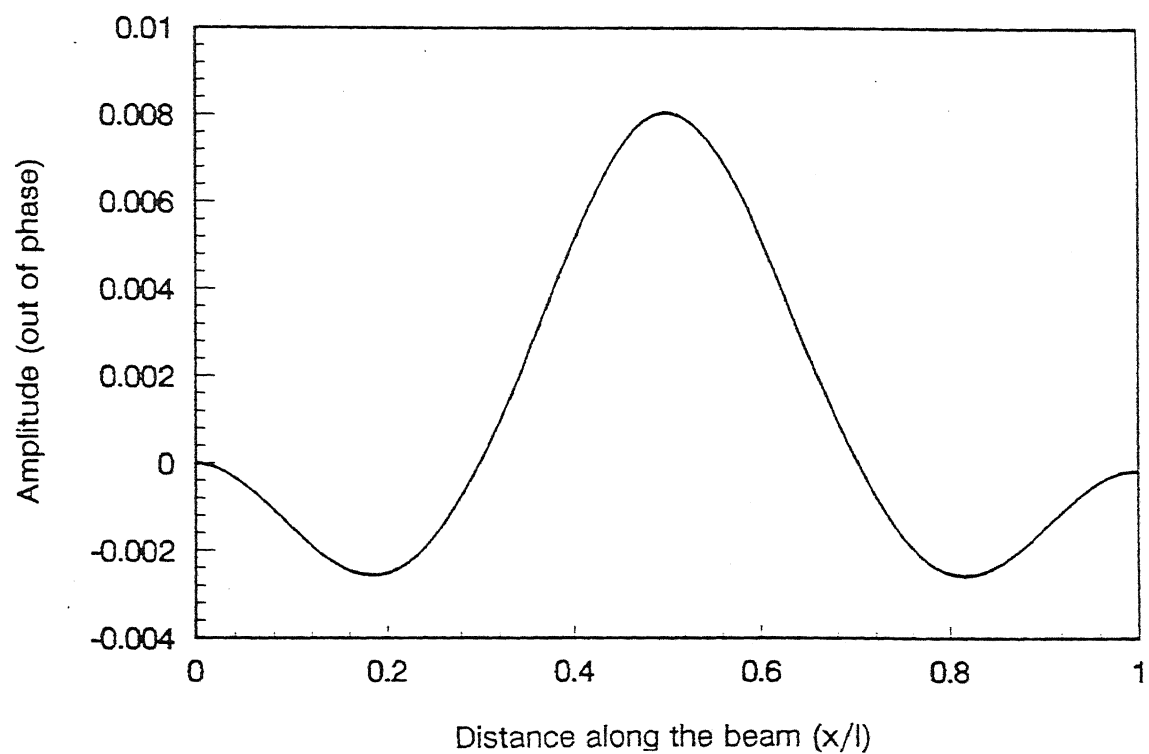
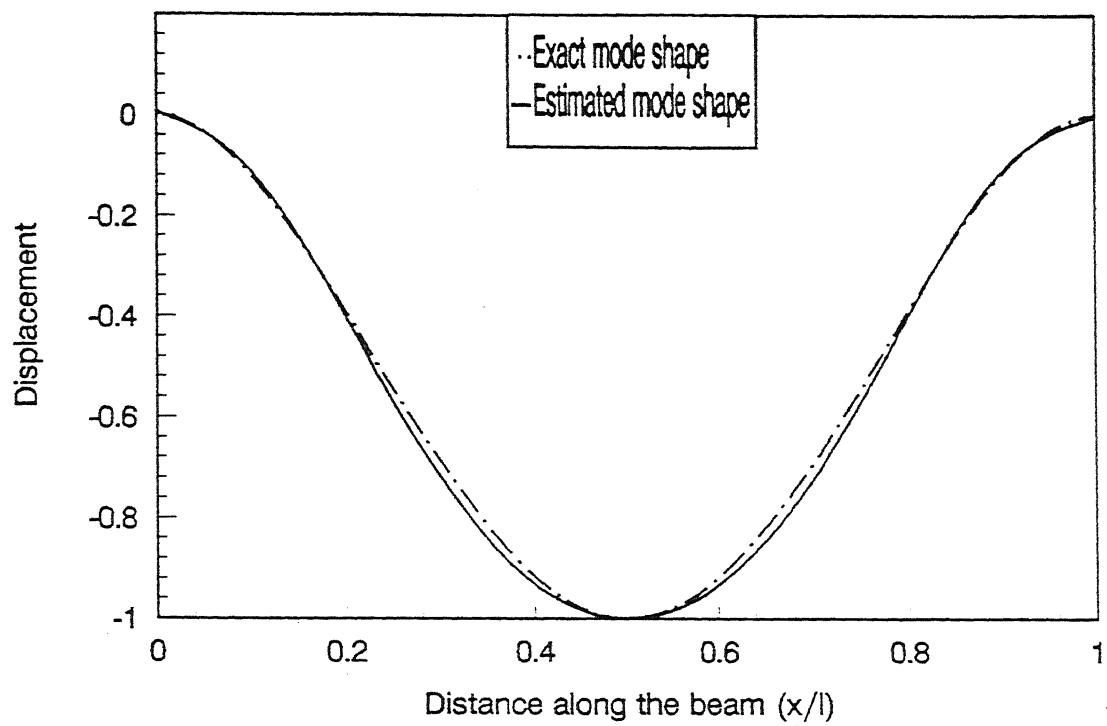
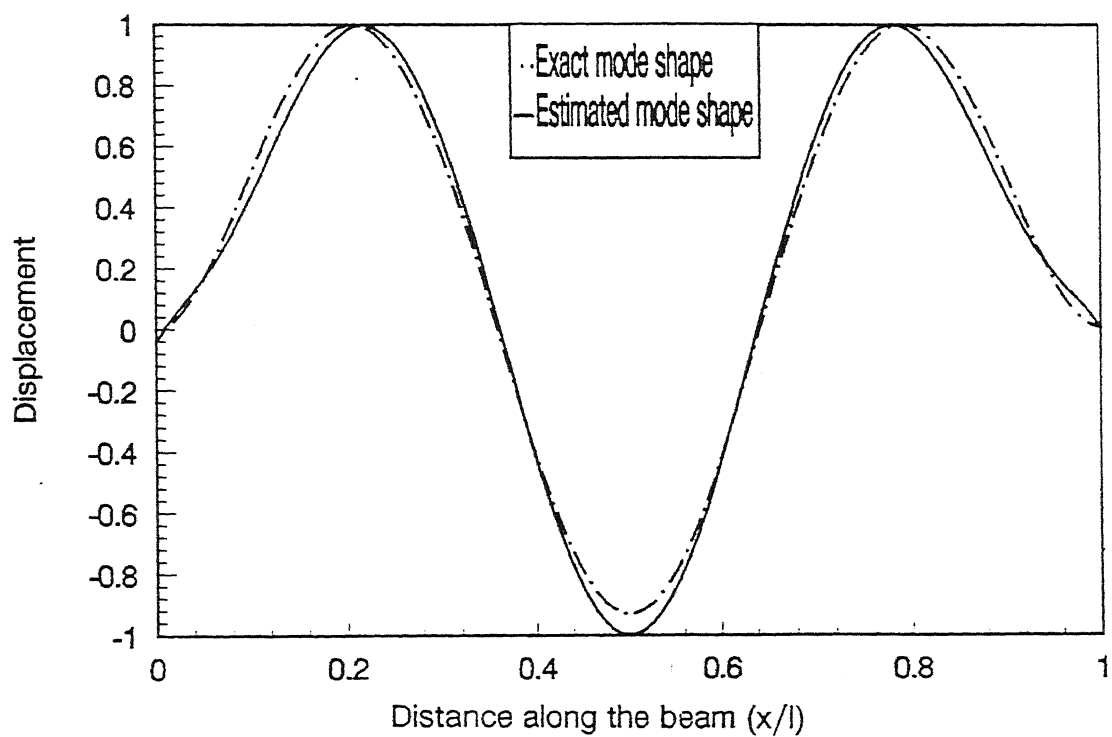


Fig. 3.9 (b) Simulated out of phase response amplitude of fixed-fixed beam ($\kappa=1.0$)



(a) Mode 1



(b) Mode 2

Fig.3.10 Estimated and exact mode shapes of fixed-fixed beam($\kappa=1.0$)

3.3 Influence of the number of measurement stations

The influence of the number of points along the beam, where steady -state vibration amplitudes are measured is studied next. The estimation procedure is carried out for 25, 50 and 100 number of measurement points, for the simply-supported, cantilever and fixed-fixed configurations, with the nondimensional parameter, $\kappa=1.0$. The errors in the mode shapes are computed by comparison with the corresponding exact values available in literature. Figs. 3.11 (a) - (b) show the estimates of the first and third modes for the simply-supported case, with 25, 50 and 100 measurement stations. Fig.3.12 (a) - (b) show the corresponding errors in the estimations. For mode 1, the maximum errors is 12% with 25 measurement stations, which reduces to 6% as the number of stations is increased to 100. For mode 2, similarly the maximum error reduces from 14% to 9%, as the number of measuring stations is increased from 25 to 100. Moreover, it can be seen from the figures that the error gets more evenly spread along the length of the beam as the number of measurement stations is increased. Similar trends can be observed for the cantilever and fixed-fixed boundary conditions, from Figs. 3.13 - 3.16. The maximum error, with 100 number of measuring stations is of the order of 4 %, and is taken to be sufficiently accurate for the present study.

3.4 Effect of measurement error

The influence of possible errors in the measurement of beam response is discussed in this section. The computer simulated response of the beams is adulterated with random noise, with rms value equal to 5 % of the maximum value of the measurement in each case. The random noise is simulated on the computer through an appropriate random number generator. The excitation frequencies and point of application of the excitation force is kept the same as those listed in section 3.1. The value of the nondimensional parameter κ is kept as 1.0 and the number of measurement stations is 100. Figs. 3.17 (a) - (b) show the noisy response input thus fed to the estimation algorithm for simply-supported case. Figs. 3.18 (a) - (b) show the estimated mode shapes. Figs. 3.19(a)-(b) and 3.20(a)-(b) are the inputs and the estimated mode shapes for the cantilever while Figs 3.21(a)-(b) and 3.22(a)-(b) are the corresponding curves for the fixed-fixed boundary conditions. The estimated natural frequencies and damping ratios are listed in

Table 3.4. Comparing the values in Table 3.4 with those in Tables 3.1-3.3 (without noise), reveals a marginal increase in errors in estimates. This illustrates the robustness of the procedure in the presence of measurement noise.

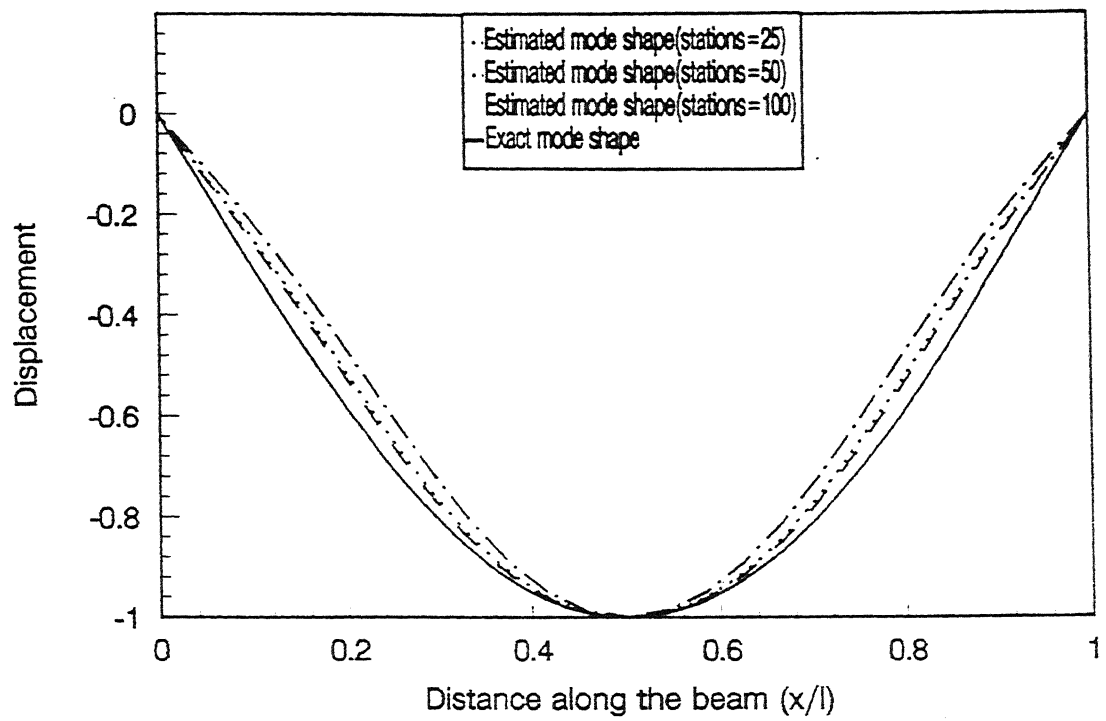
Table 3.4 Exact and Estimated Natural Frequencies and Damping Ratios

Beam	Mode	Natural frequencies			Damping ratios		
		Exact	Estimated	Error	Exact	Estimated	Error
Simply supported ($\kappa=1$)	1	30.910	30.424	1.58	0.02	0.02044	2.20
	3	278.21	273.292	1.76	0.02	0.01962	1.90
Cantilever ($\kappa=1$)	1	11.012	11.367	3.22	0.02	0.01927	3.15
	2	69.014	70.657	2.38	0.02	0.02063	3.65
Fixed-fixed ($\kappa=1$)	1	70.075	73.309	2.87	0.02	0.02078	3.90
	3	378.67	390.279	3.06	0.02	0.02100	5.00

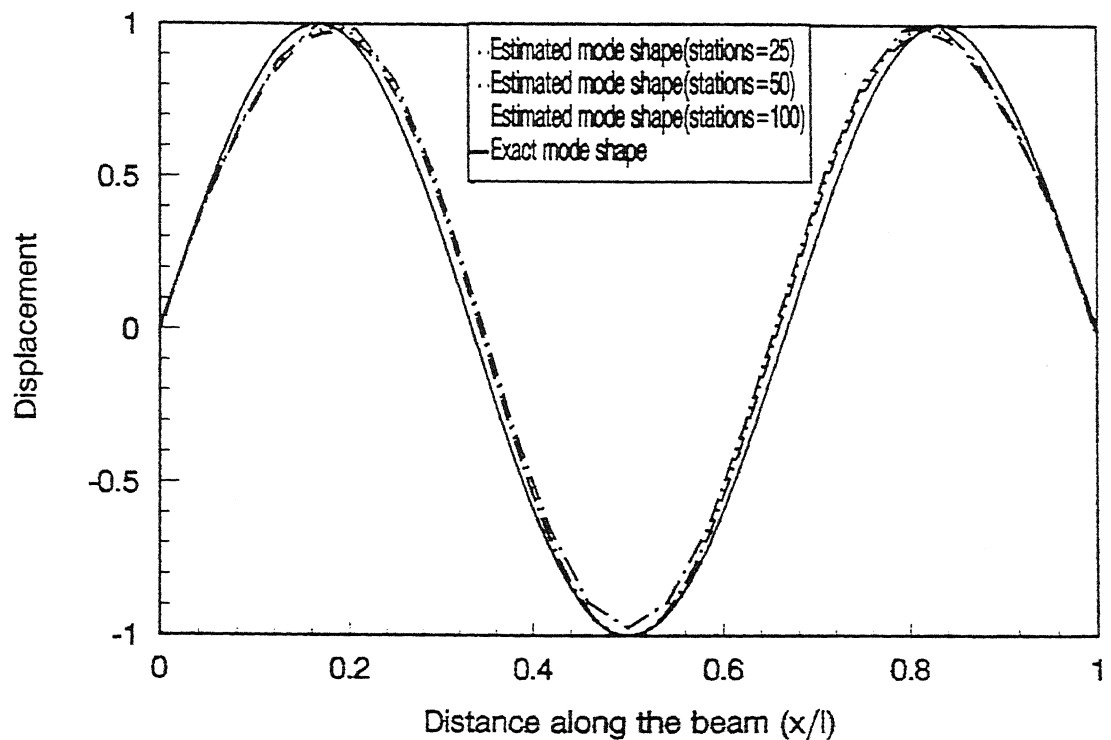
3.5 Influence of error in the point of force application

The accuracy in the point of force application is very crucial for the proposed estimation procedure, for beams with symmetric boundary configurations (e.g. simply-supported, fixed-fixed, free-free etc.). For example, if the force is not applied exactly at the mid-point of a simply-supported beam, in addition to the symmetric modes (i.e. modes 1, 3, 5, 7...), the non-symmetric modes (2, 4, 6...) also get excited and contribute to the beam response. This contribution from the non-symmetric modes does not get accounted for in the proposed estimation procedure. Therefore, a numerical study is carried out to evaluate the influence of such an error.

Fig. 3.23 (a) and (b) show the response of the simply supported beam ($\kappa = 1.0$, measurement stations 100), where the applied force is eccentric with the beam mid-point by 0.5 %. As mentioned above the response (simulated through equation 3.2) comprises of contributions from the non-symmetric modes (2, 4, 6...) in addition to the symmetric modes (1, 3, 5, 7...). Figs. 3.24 (a) and (b) give the estimated mode shapes. The exact mode shapes are also shown in these figures, which reveal that the procedure is sensitive to the point of force application and the error can be significant if accuracy is not observed while locating the excitation force. Similar trends are observed for the fixed-fixed case with 0.5 % error in the point of force application. For the fixed-fixed case Figs. 3.25 (a)-(b) and 3.26 (a)-(b) are the response input and estimated mode shapes, respectively.

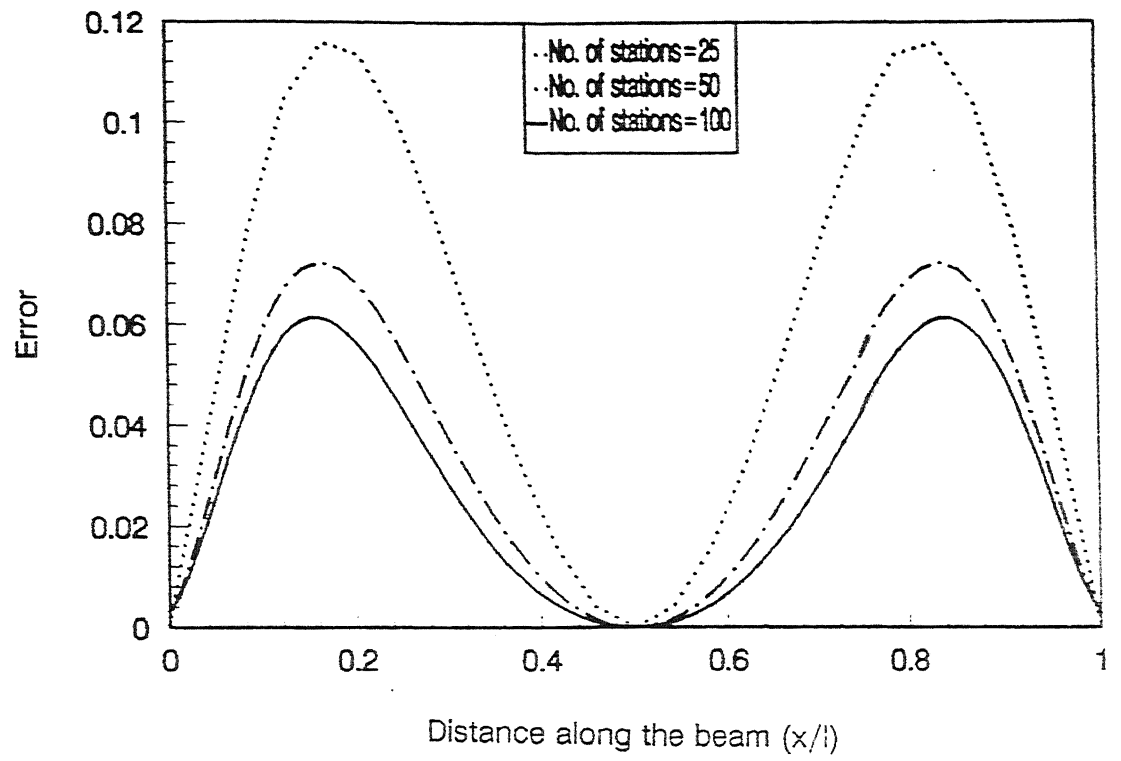


(a) Mode 1

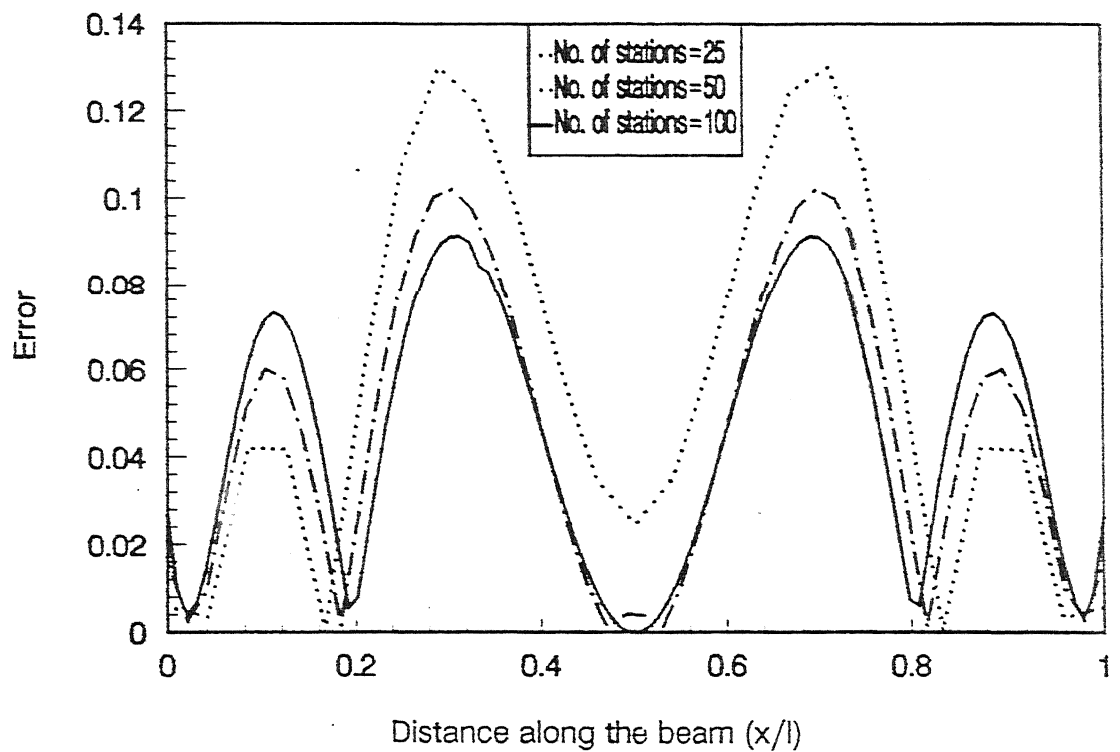


(b) Mode 2

Fig. 3.11 Estimated and exact mode shapes of simply supported beam with the influence of number of stations ($\kappa=1.0$)

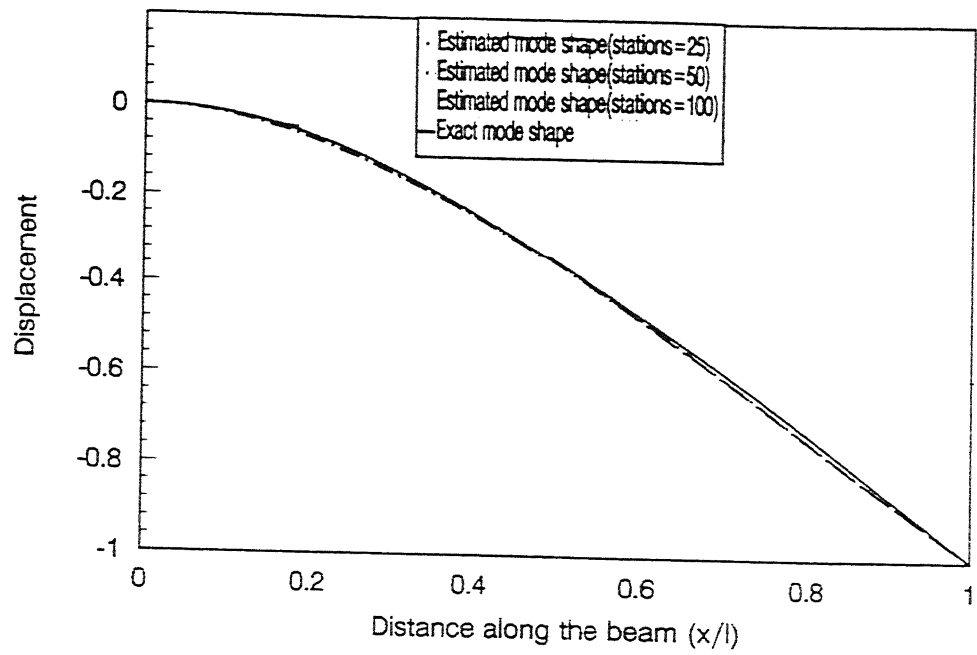


(a) Mode 1

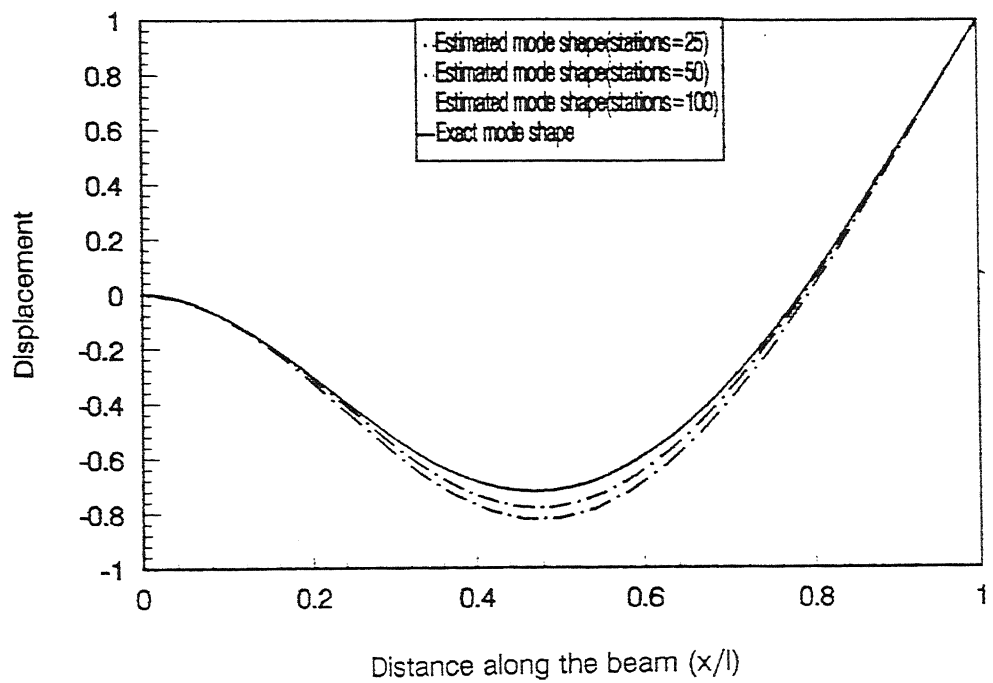


(b) Mode 2

Fig. 3.12 Errors of simply supported beam with the influence of number of stations ($\kappa=1.0$)

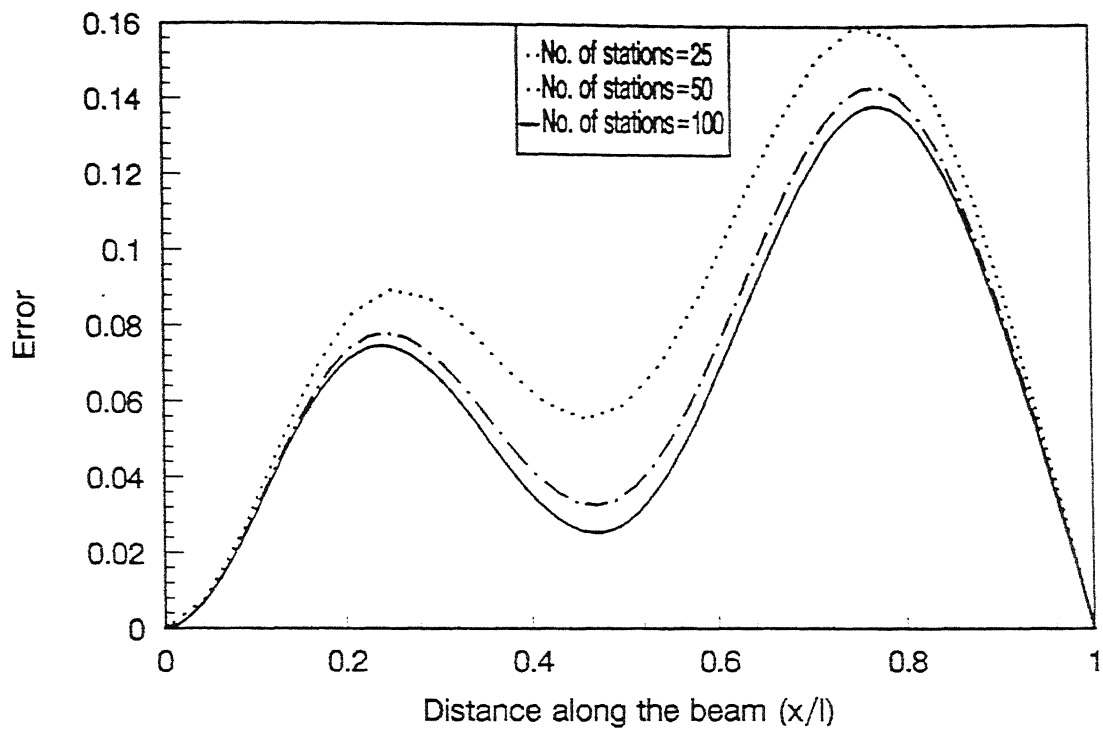


(a) Mode 1

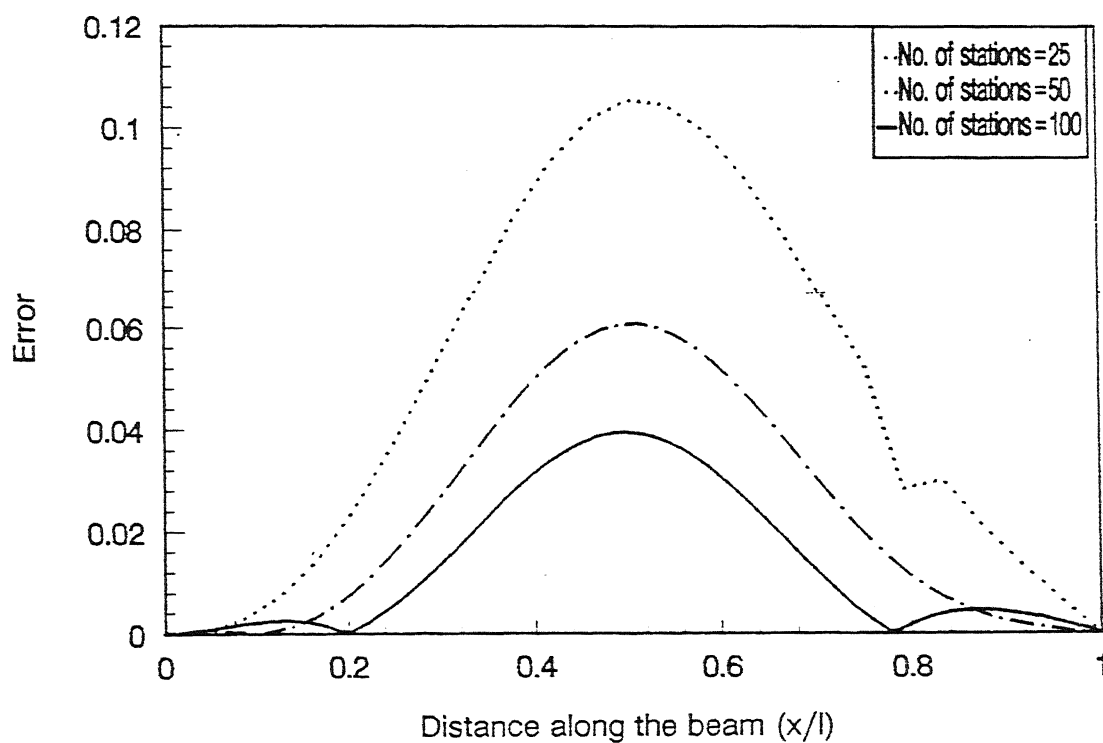


(b) Mode 2

Fig. 3.13 Estimated and exact mode shapes of cantilever beam with the influence of number of stations ($\kappa=1.0$)

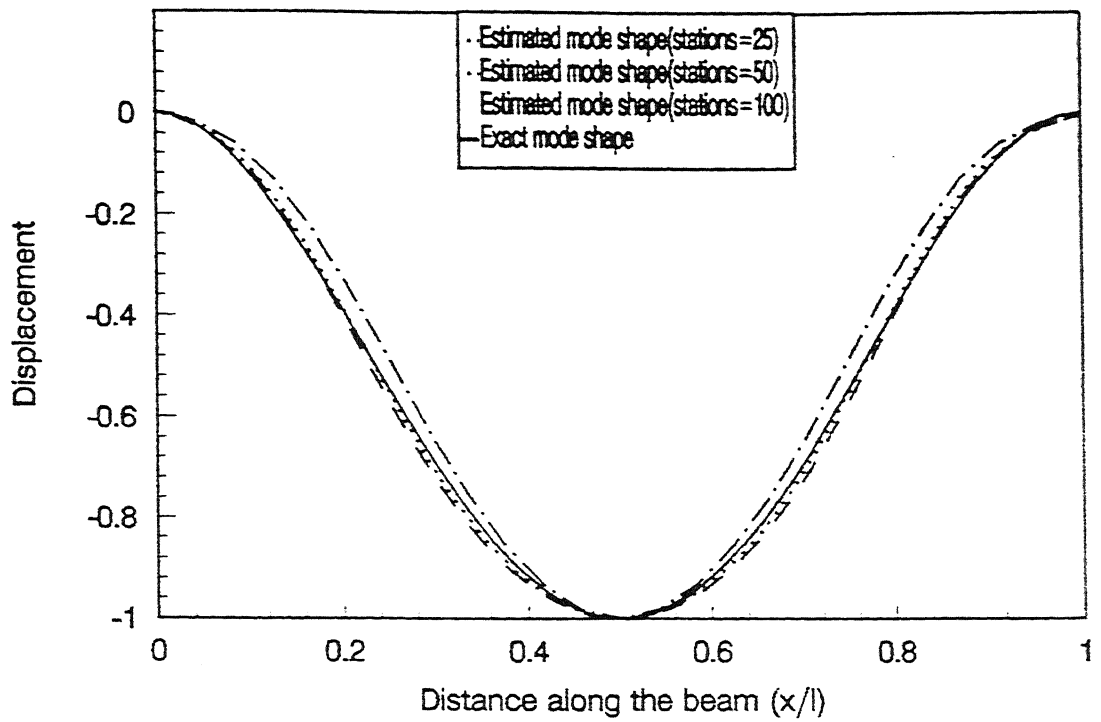


(a) Mode 1

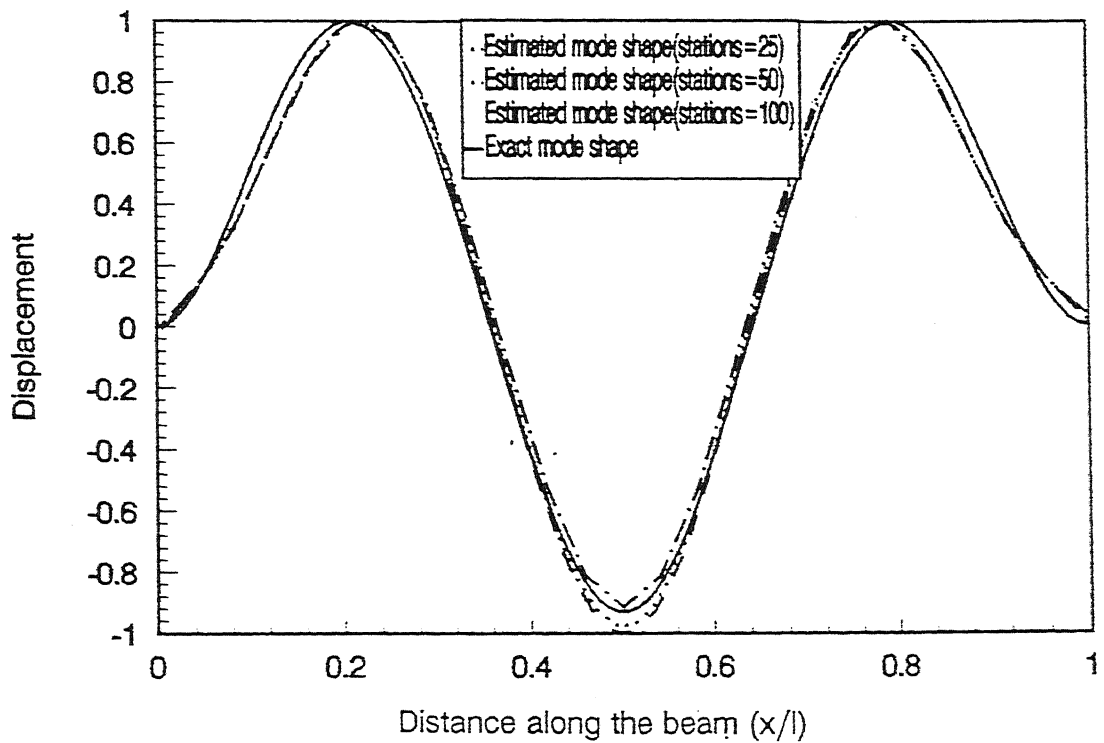


(b) Mode 2

Fig. 3.14 Errors of cantilever beam with the influence of number of stations ($\kappa=1.0$)

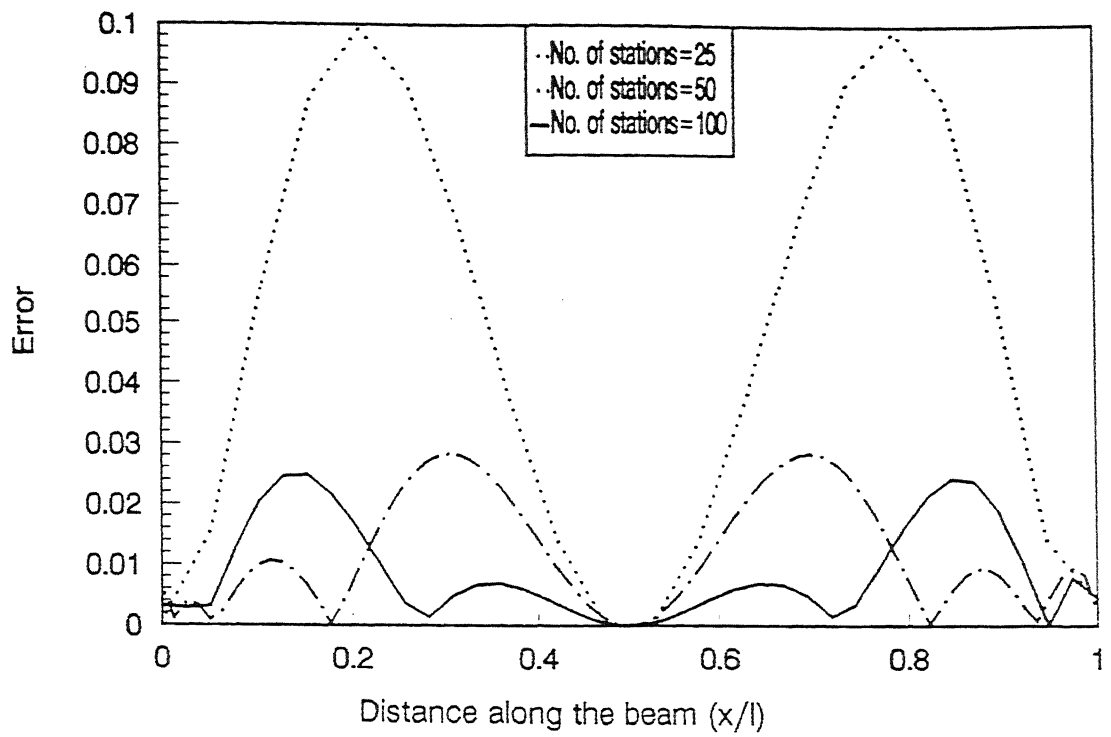


(a) Mode 1

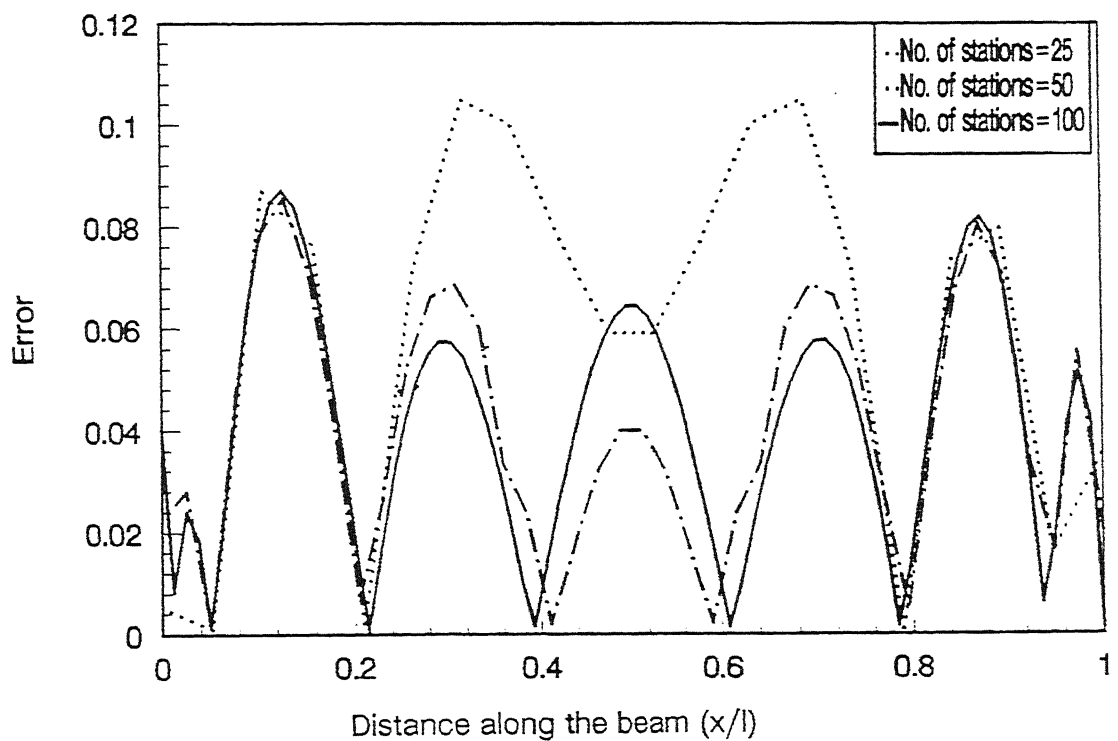


(b) Mode 2

Fig. 3.15 Estimated and exact mode shapes of fixed-fixed beam with the influence of number of stations ($\kappa=1.0$)



(a) Mode 1



(b) Mode 2

Fig. 3.16 Errors of fixed-fixed beam with the influence of number of stations ($\kappa=1.0$)

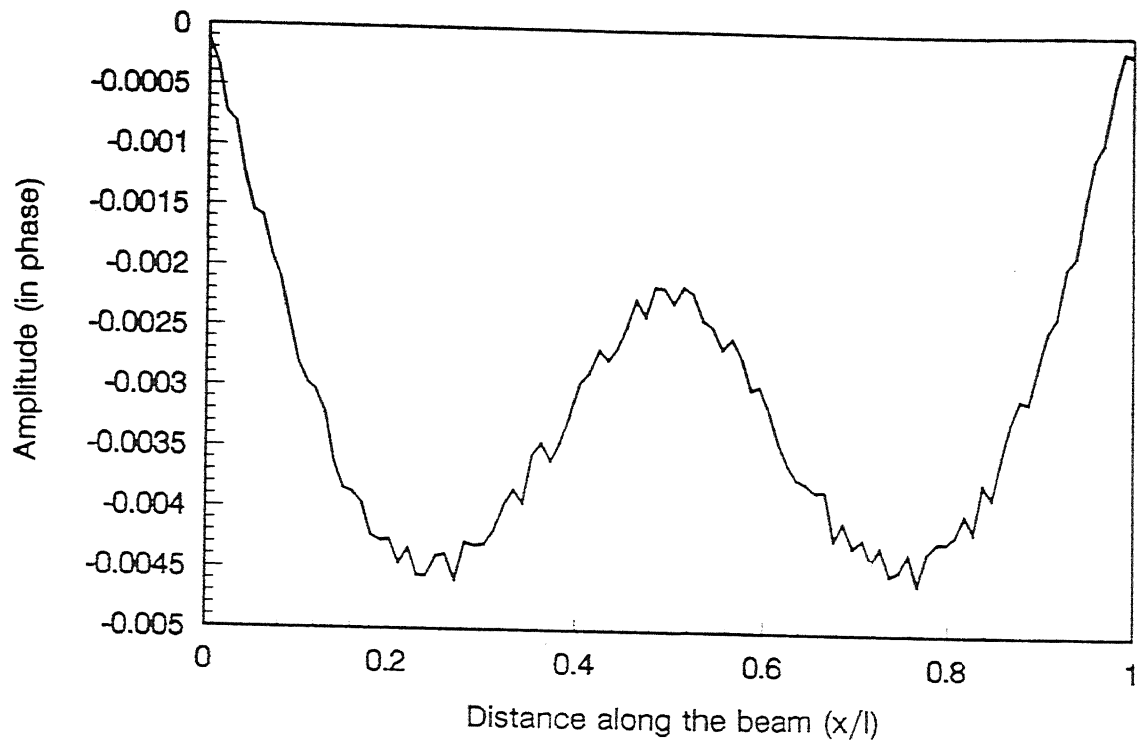


Fig. 3.17 (a) Simulated in phase response amplitude of simply supported beam with 5% noise($\kappa=1.0$)

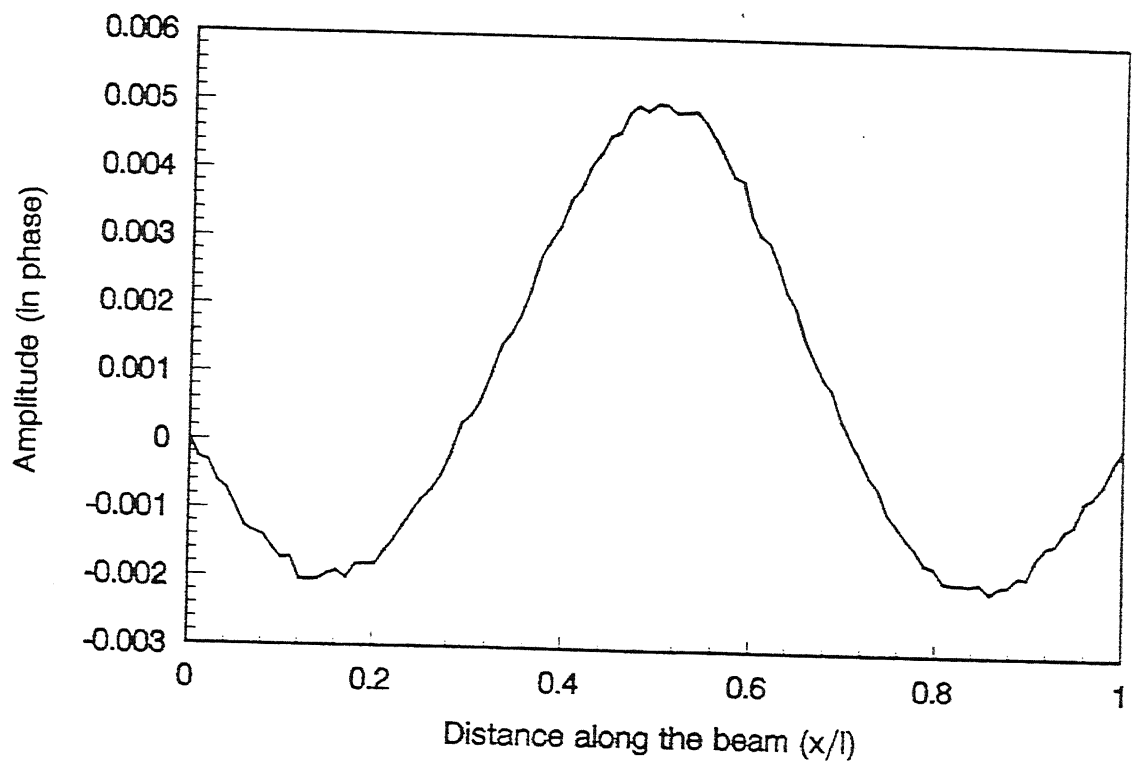
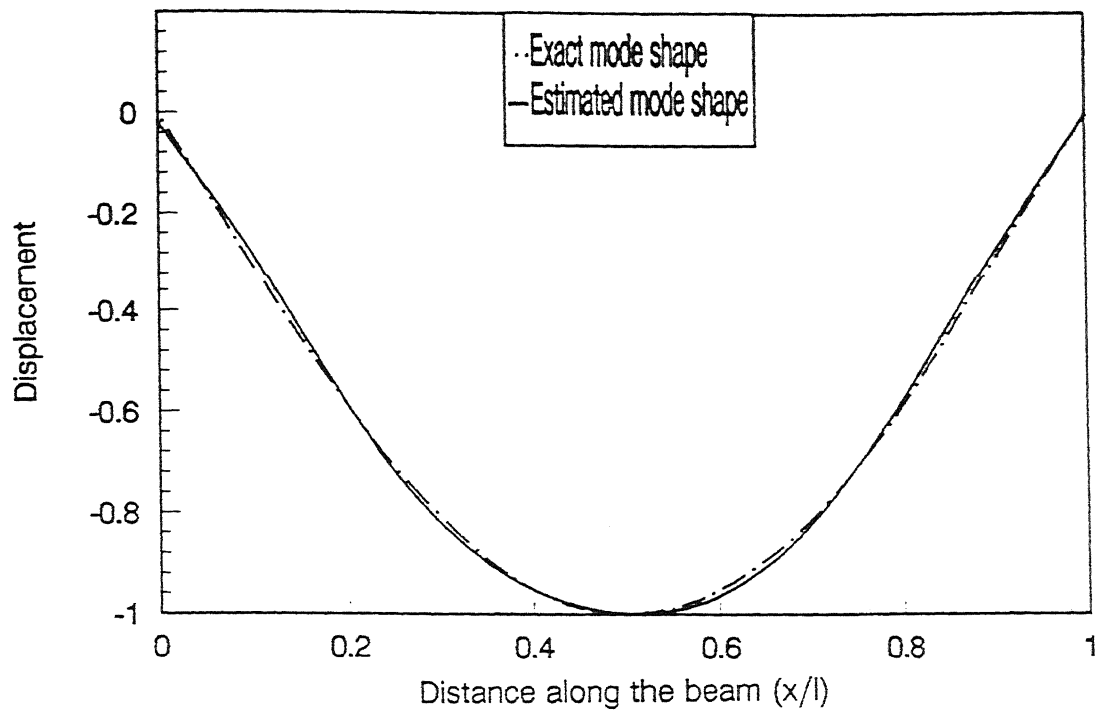
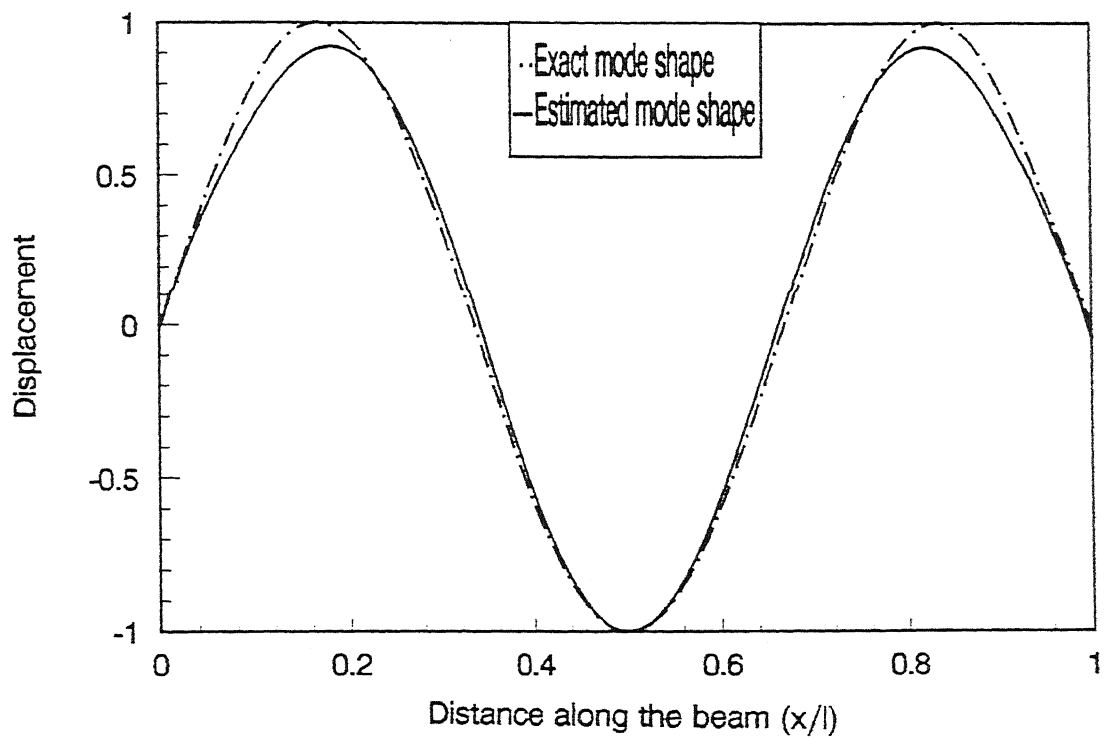


Fig. 3.17 (b) Simulated out of phase response amplitude of simply supported beam with 5% noise($\kappa=1.0$)



(a) Mode 1



(b) Mode 2

Fig.3.18 Estimated and exact mode shapes of simply supported beam with 5% noise ($\kappa=1.0$)

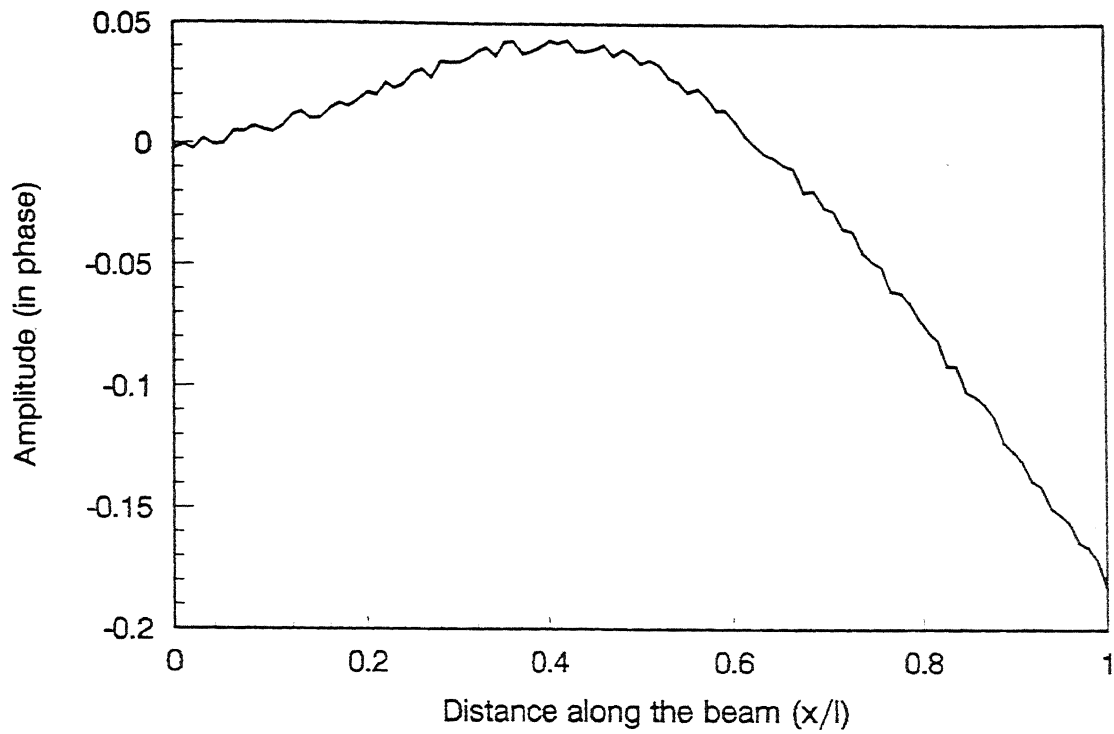


Fig. 3.19 (a) Simulated in phase response amplitude of cantilever beam with 5% noise($\kappa=1.0$)

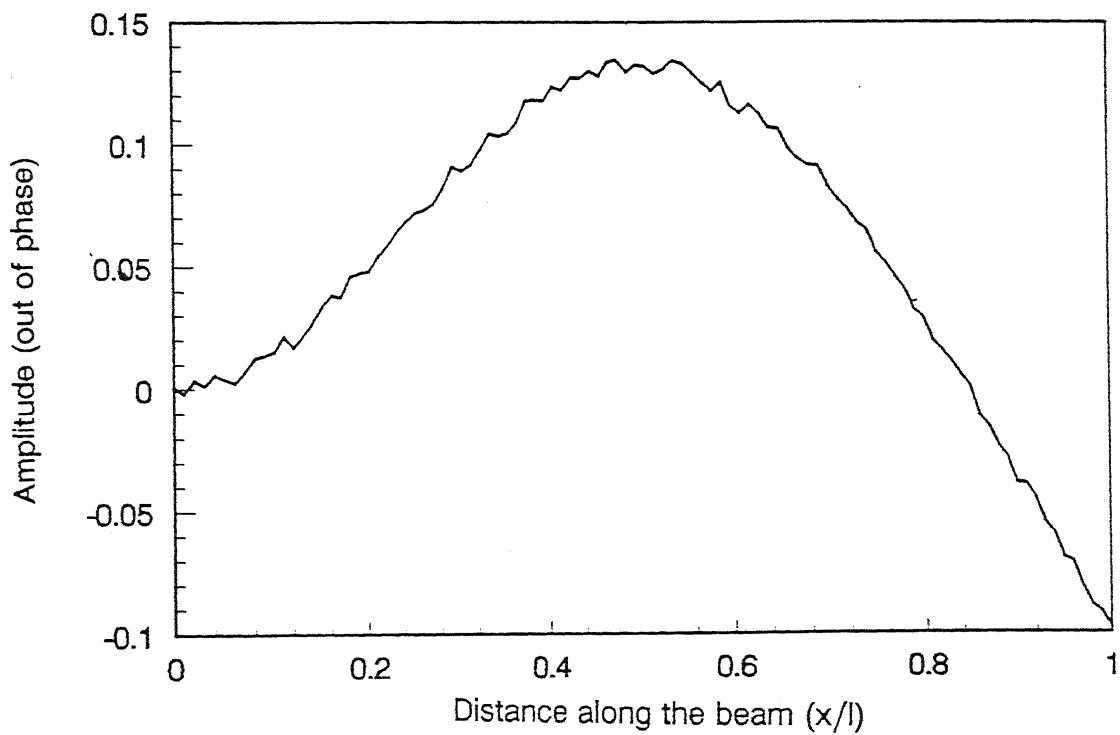
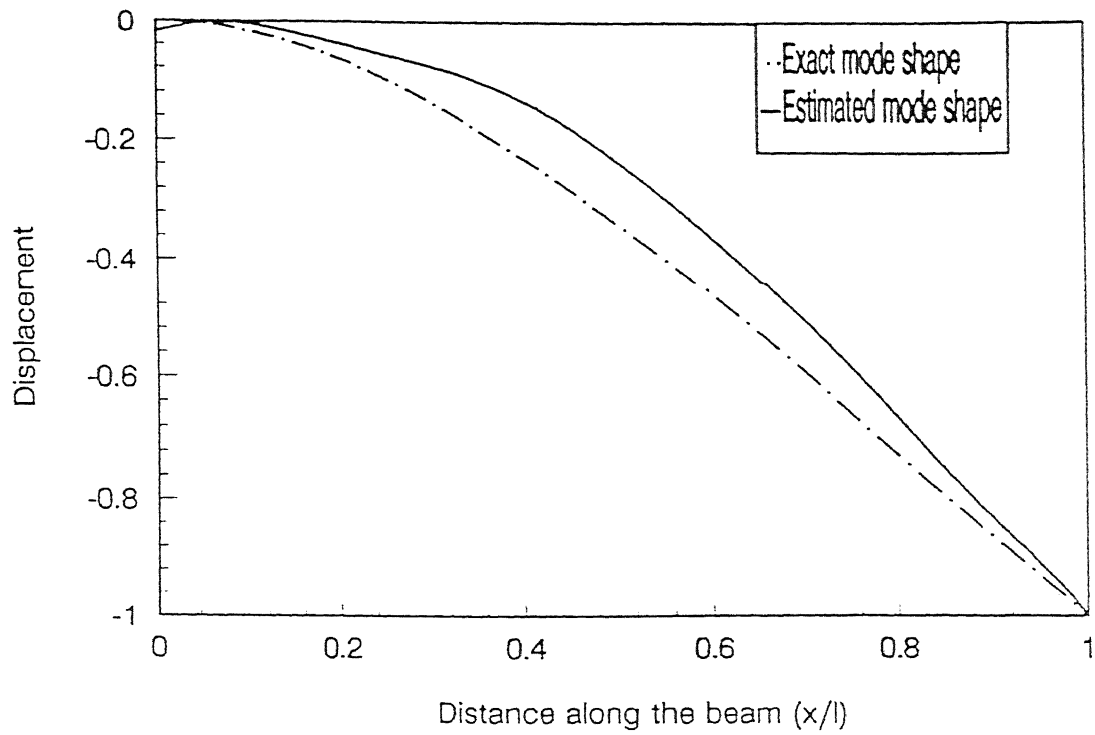
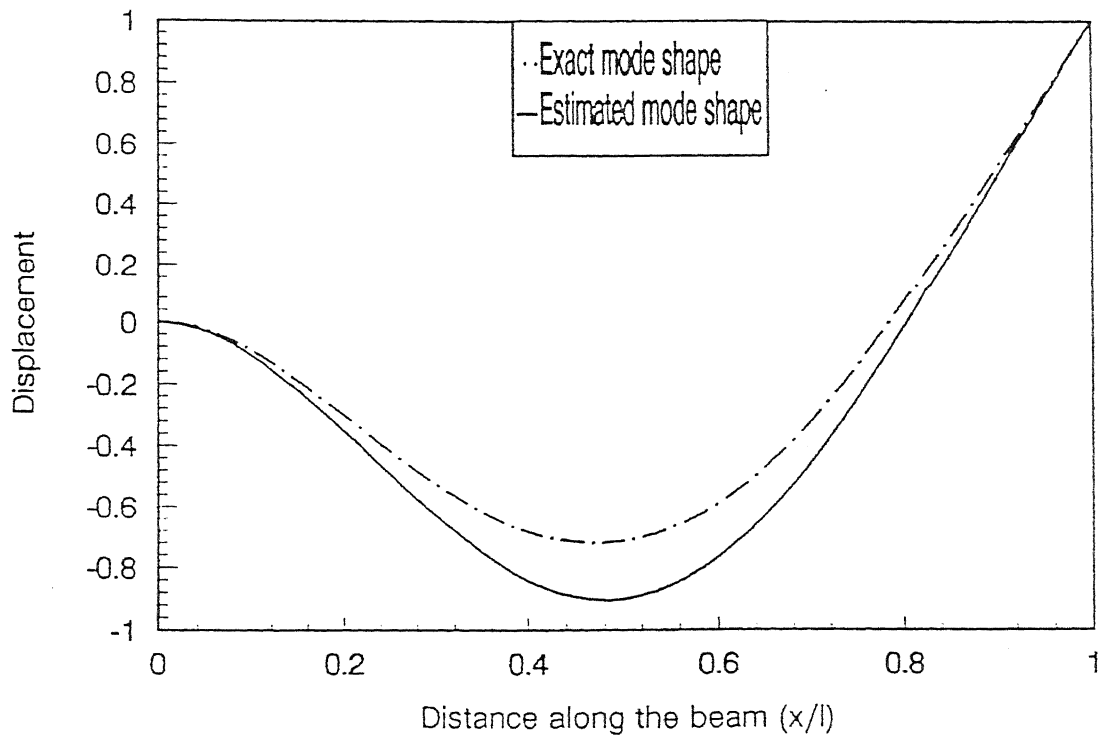


Fig. 3.19 (b) Simulated out of phase response amplitude of cantilever beam with 5% noise($\kappa=1.0$)



(a) Mode 1



(b) Mode 2

Fig.3.20 Estimated and exact mode shapes of cantilever beam with 5% noise($\kappa=1.0$)

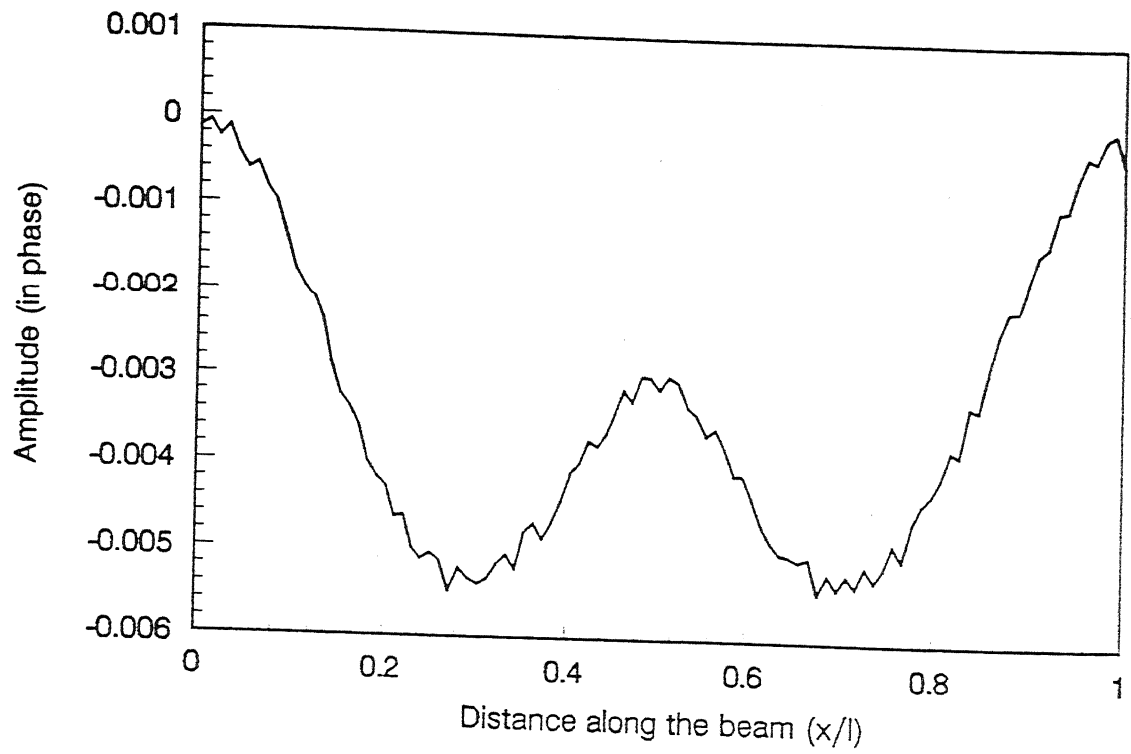


Fig. 3.21 (a) Simulated in phase response amplitude of fixed-fixed beam with 5% noise($\kappa=1.0$)

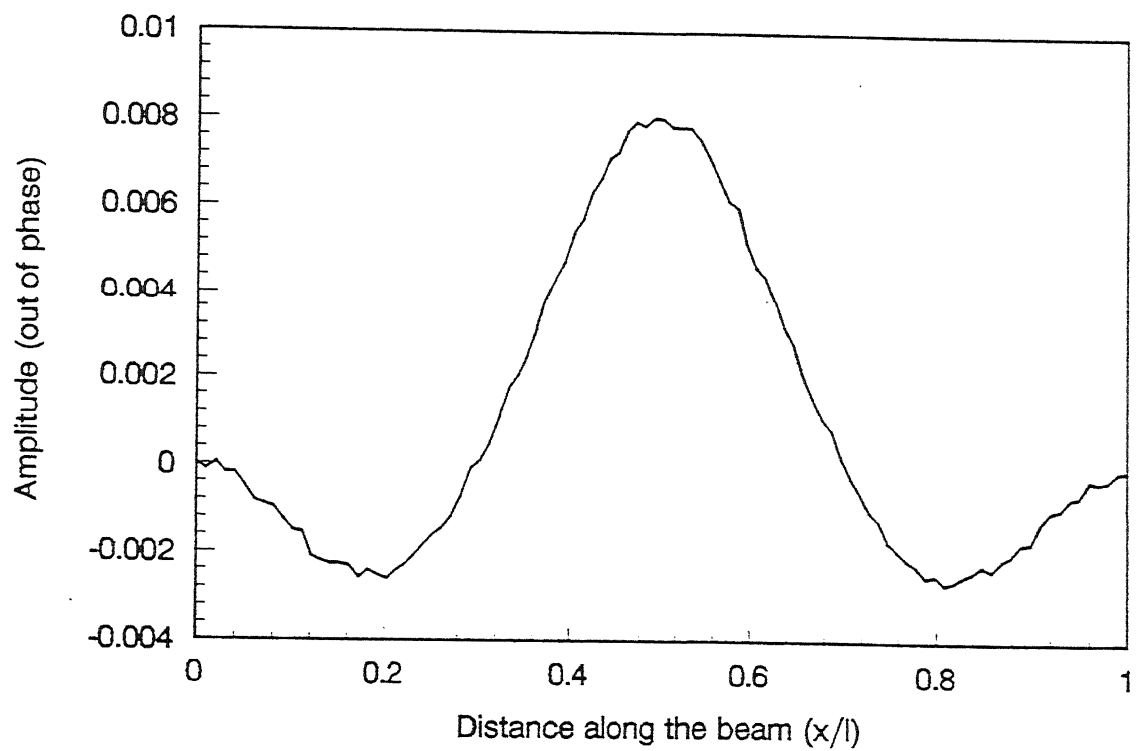
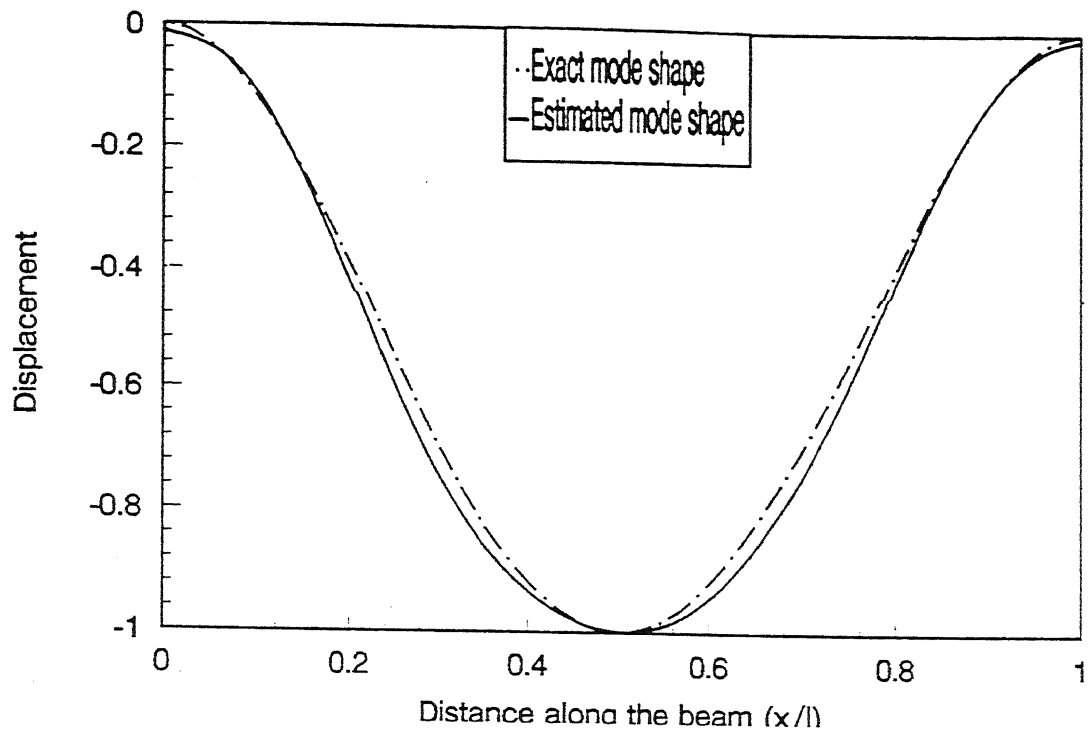
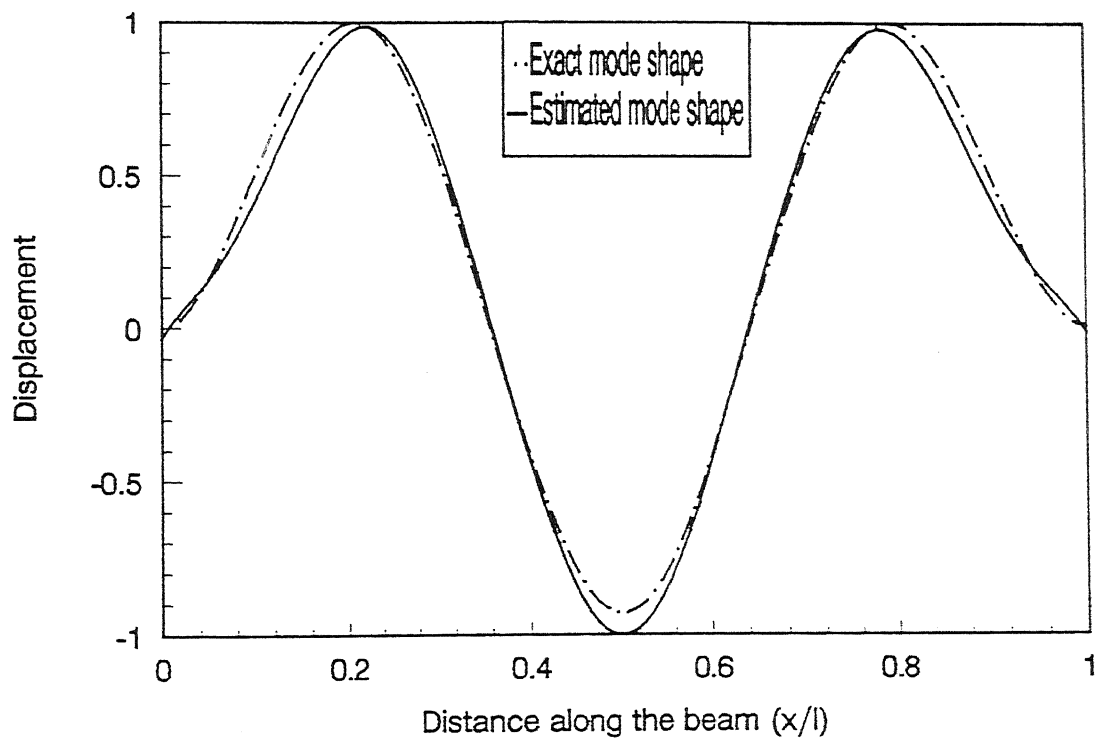


Fig. 3.21 (b) Simulated out of phase response amplitude of fixed-fixed beam with 5% noise($\kappa=1.0$)



(a) Mode 1



(b) Mode 2

Fig.3.22 Estimated and exact mode shapes of fixed-fixed beam with 5% noise($\kappa=1.0$)

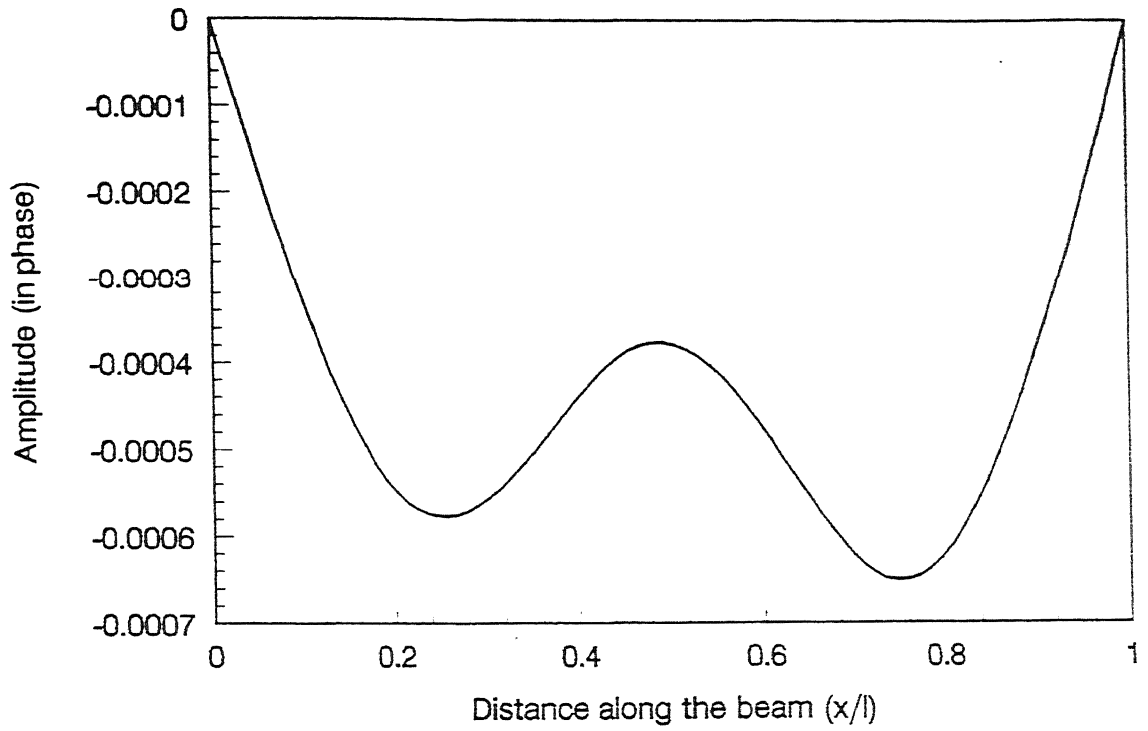


Fig. 3.23 (a) In phase response amplitude of simply supported beam with 0.5% error in point of force application ($\kappa=1.0$)

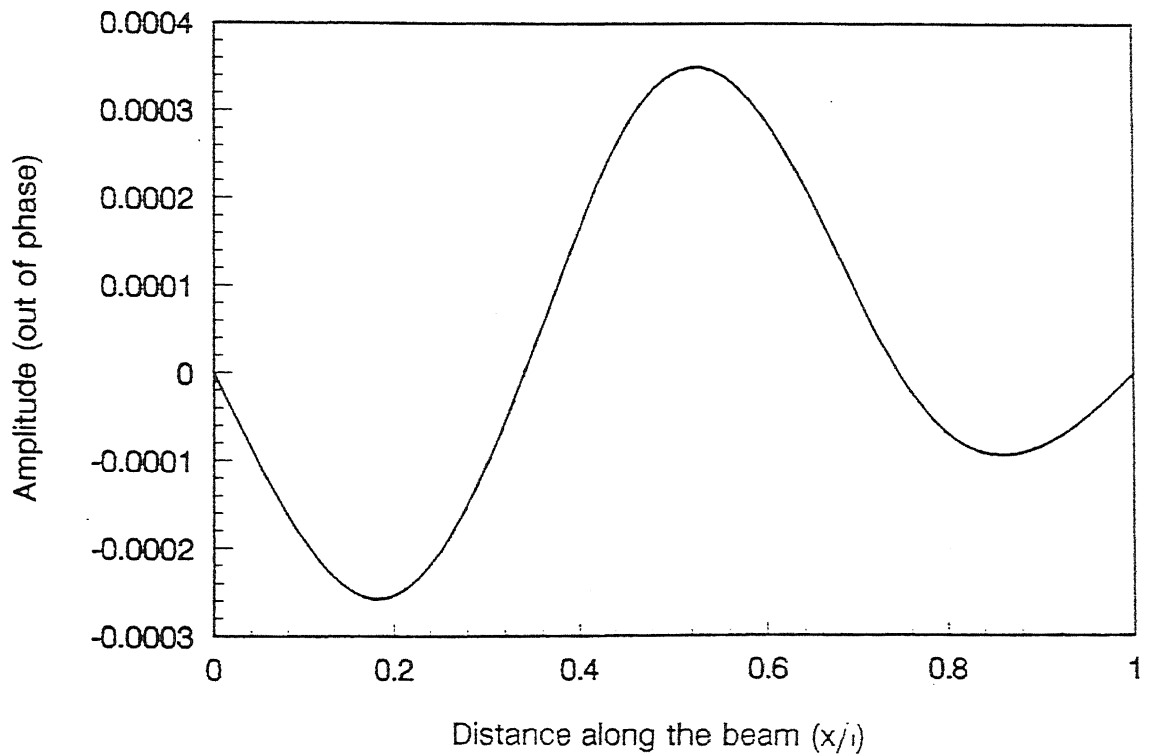
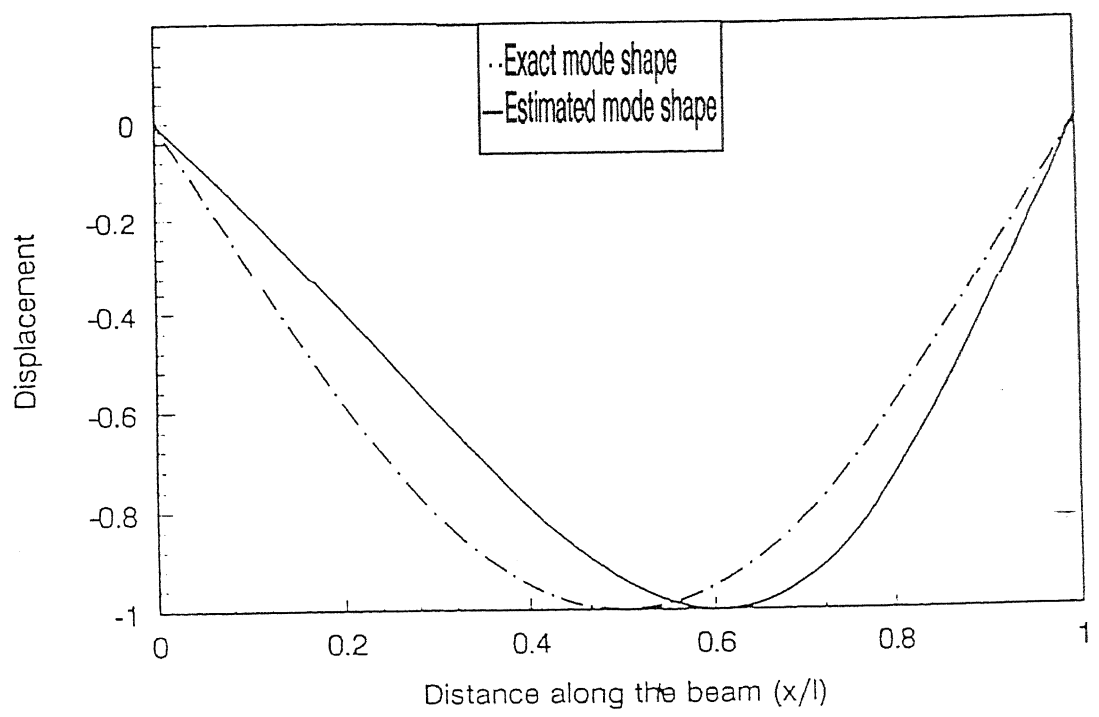
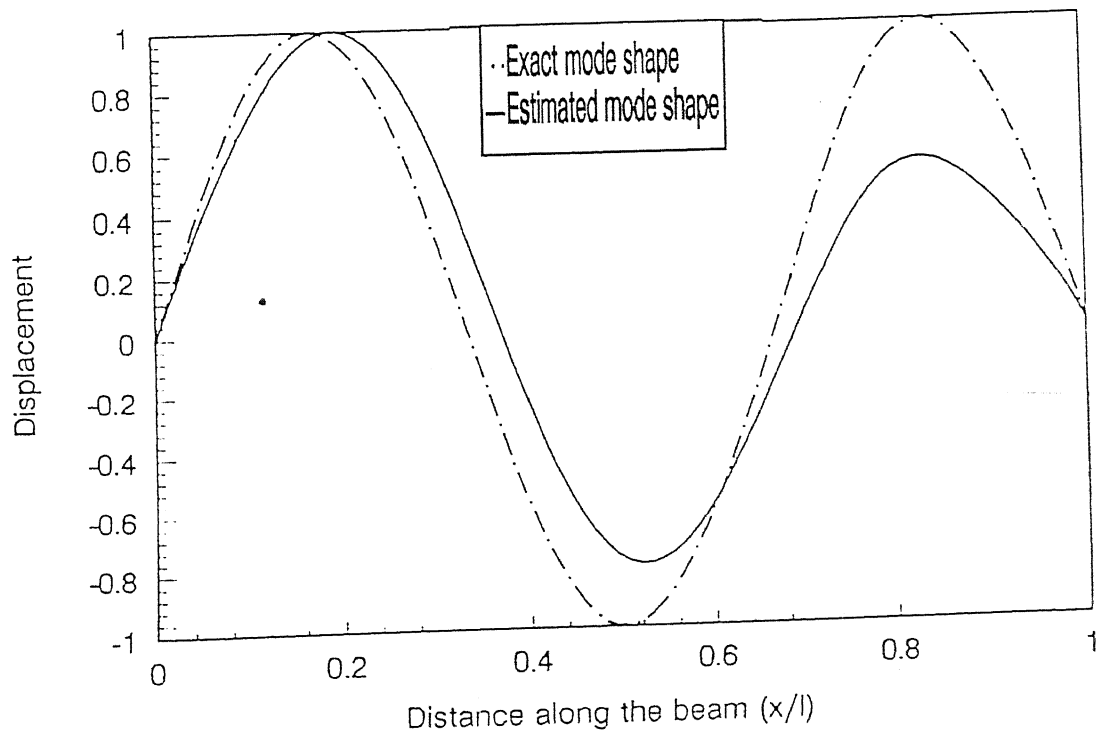


Fig. 3.23 (b) Out of phase response amplitude of simply supported beam with 0.5% error in point of force application ($\kappa=1.0$)



(a) Mode 1



(b) Mode 2

Fig. 3.24 Mode shapes of simply supported beam with 0.5% error in point of force application ($\kappa=1.0$)

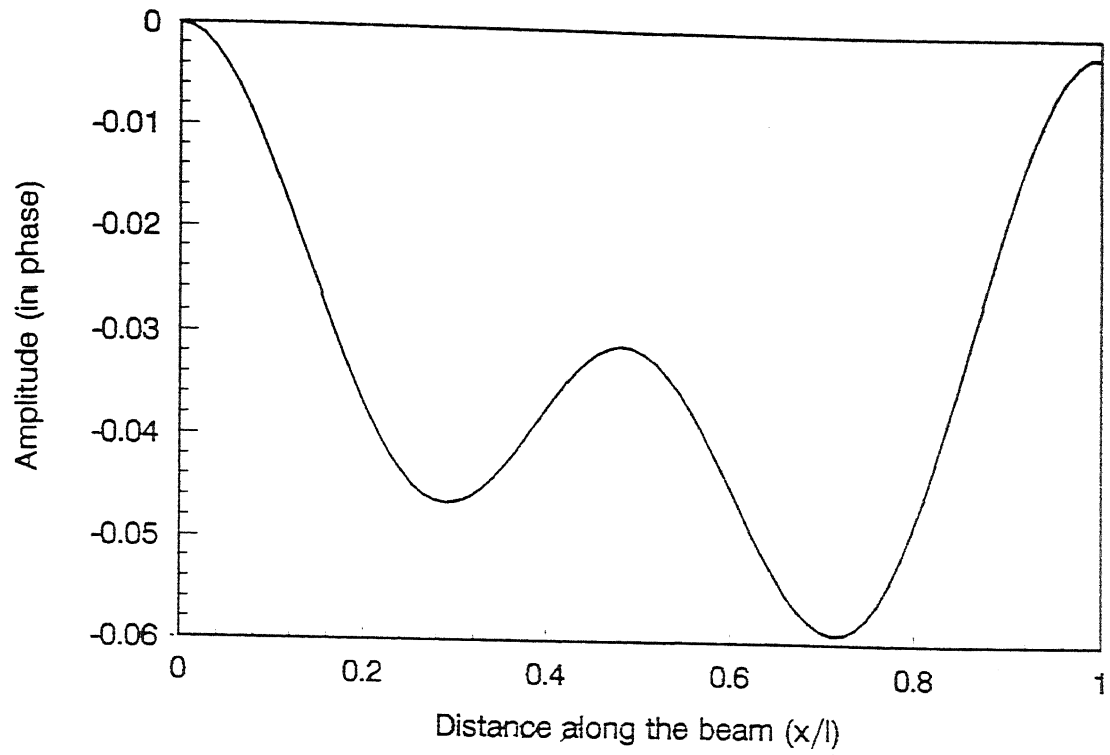


Fig. 3.25 (a) In phase response amplitude of fixed-fixed beam with 0.5% error in point of force application($\kappa=1.0$)

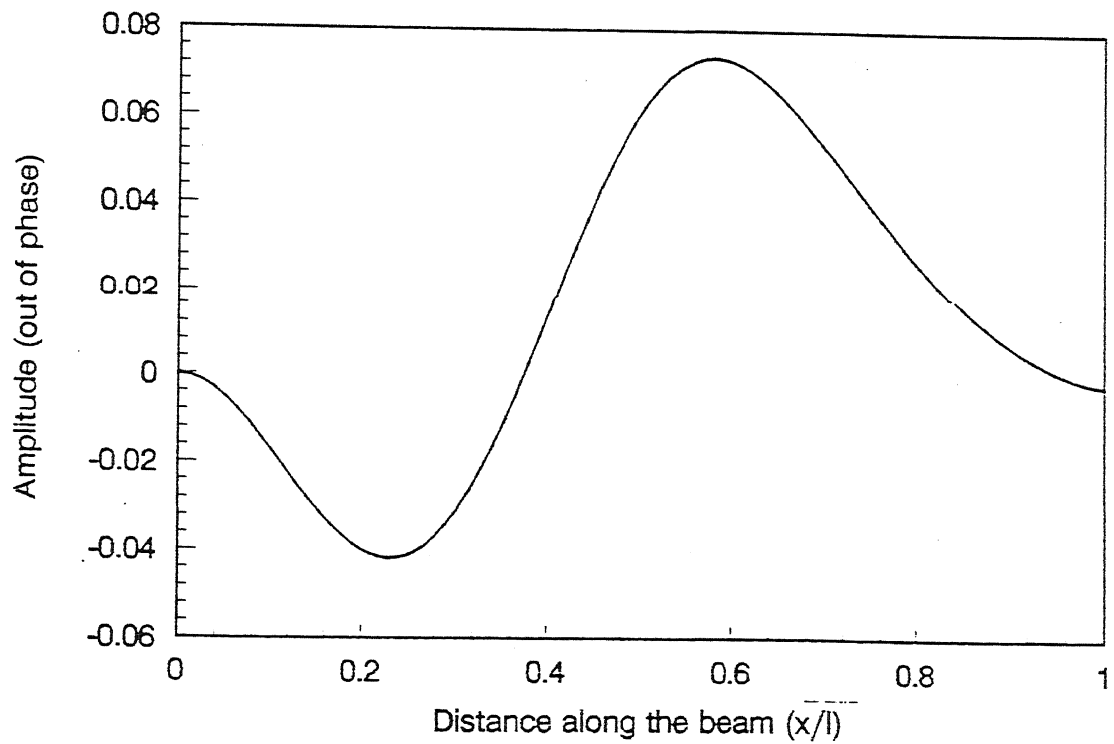
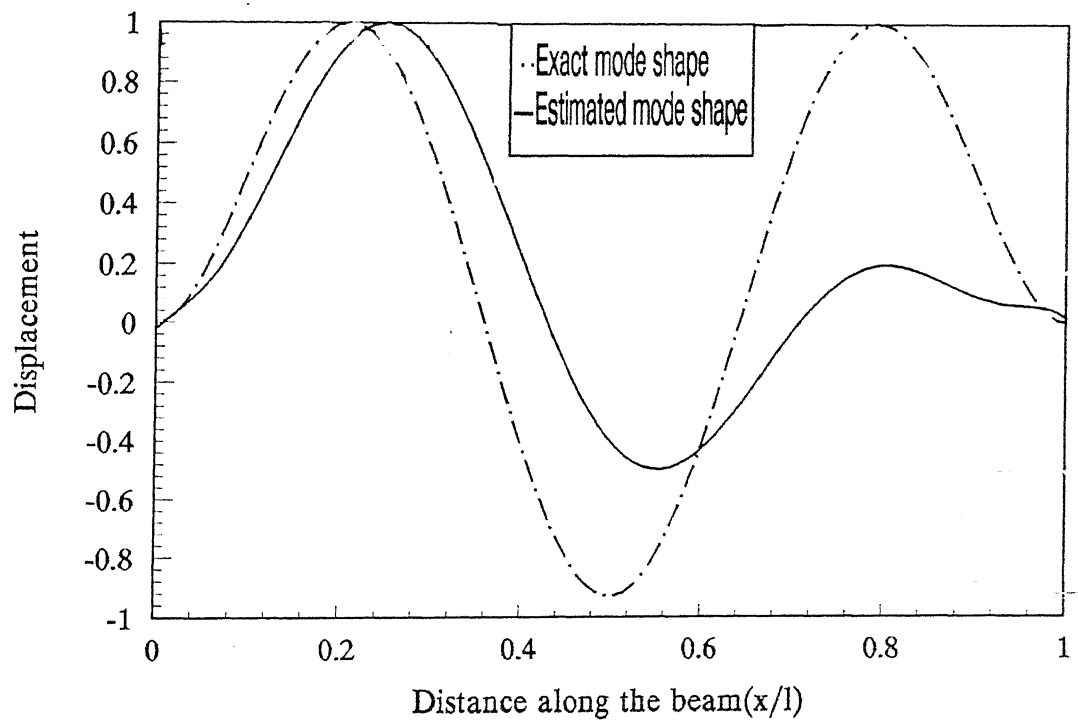
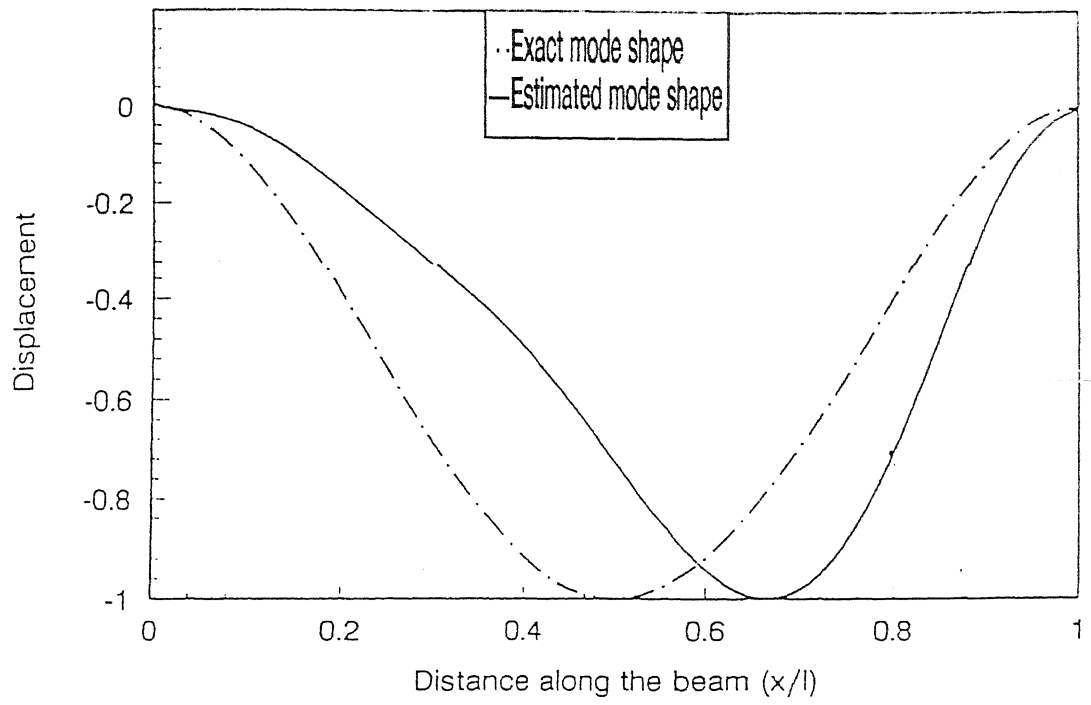


Fig. 3.25 (b) Out of phase response amplitude of fixed-fixed beam with 0.5% error in point of force application($\kappa=1.0$)



(b) Mode 2

Fig. 3.26 Mode shapes of fixed-fixed beam with 0.5% error in point of force application ($\kappa=1.0$)

3.6 Remarks

The numerical simulation amply validates the developed procedure. The participation of modes adjacent to the excitation frequency is correctly estimated from the measured spatial data. As expected, the accuracy of the estimates increases with increasing the number of measurement points. The procedure is fairly robust and does not become unstable in the presence of measurement noise. However, the procedure is quite sensitive to errors in the point of force application, which need to be located carefully.

CHAPTER 4

EXPERIMENTAL INVESTIGATIONS

Experimental investigations have been carried out, in addition to numerical simulation described in the previous chapter, to validate further, the applicability and appropriateness of the developed spatial modal analysis procedures. The experimental investigations are however handicapped due to the usage of standard accelerometers as sensors. Spatial Modal analysis procedures are ideally suited for Laser Vibrometer sensors, which employ the Laser beam and the Doppler effect for vibration sensing. This is a non-contact type of sensing device and the entire structure can be scanned with great accuracy to provide measurements at a very large number of points. Standard accelerometers on the other hand, are contact type pick-ups which can provide measurements only at very limited number of stations on the vibrating structure. Also the location of the accelerometer cannot be as accurate as the aim of the Laser beam.

The investigations have been carried out on the available beam set-ups in the laboratory. Simply-supported and fixed-fixed configurations shown in Figs 4.1 and 4.2 have been chosen for this experimental study. The excitation to the beams is provided through locally fabricated electromagnets. These electromagnets are located on the base supporting the beam and their position can be varied along the base, as desired. A function generator (PM5132, Philips make) is used in conjunction with a power amplifier (SS250, IMV make) to energize the electromagnets at a desired frequency.

The excitation force is measured with the help of a force transducer (B&K make, Type 8200). The force transducer is attached to the beam through a threaded stud. The response is picked up through an accelerometer (B&K make, Type 4374). The response from the accelerometer is taken through a charge amplifier (B&K make, Type 2635) to a digital storage oscilloscope (DSS 6521). In order to reduce the weight

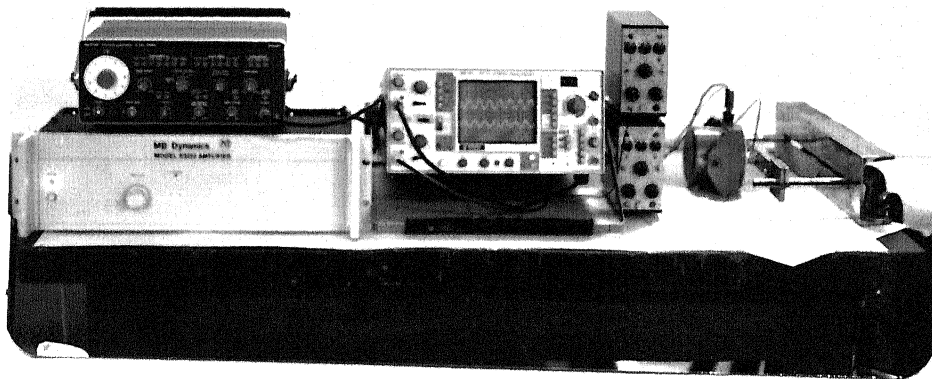


Fig. 4.1 Experimental setup-overall view

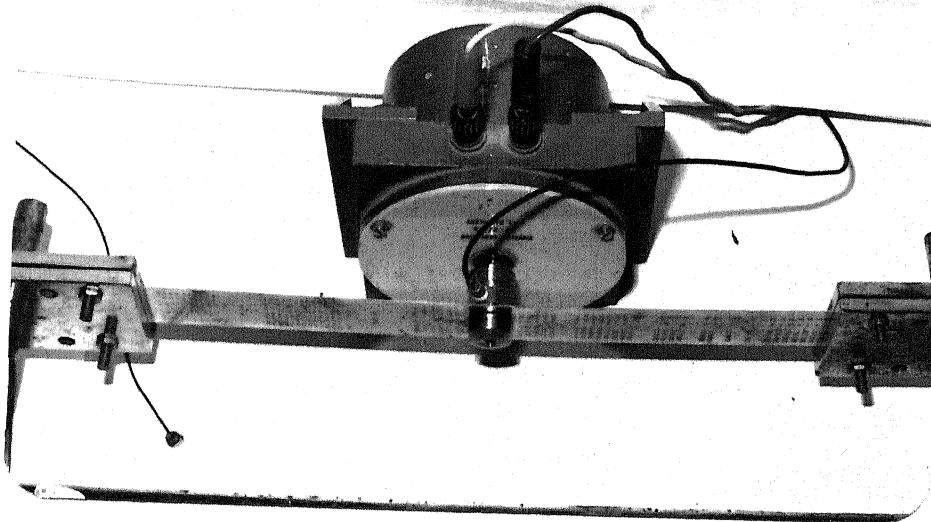


Fig. 4.2 Experimental setup

effect of the tightening nut and the accelerometer, the setups are mounted horizontally.

Fig. 4.3 shows the details of the instrumentation.

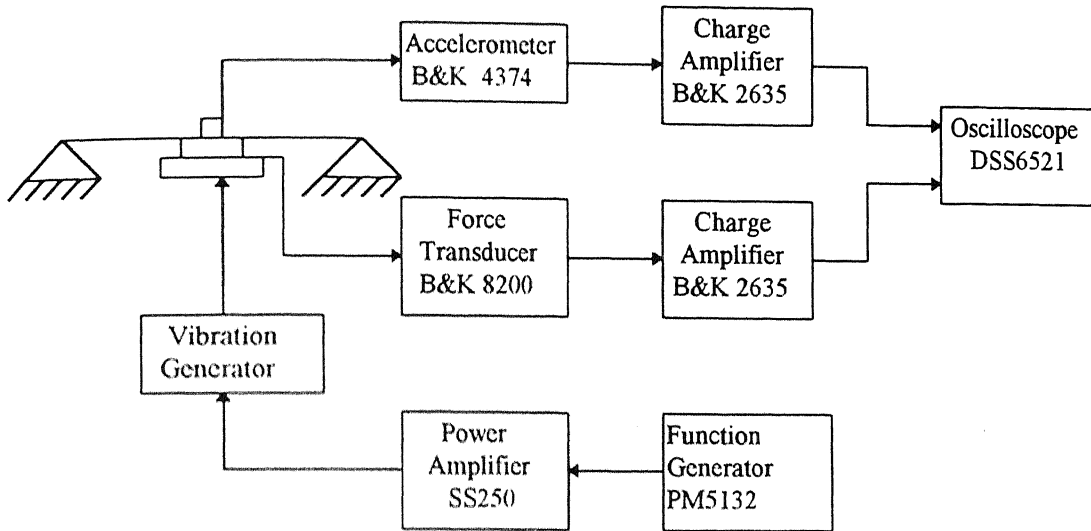


Fig 4.3 Details of Instrumentation

Identical steel beams are taken for study in the simply-supported and fixed-fixed configurations. The beams have a length of 265 mm, thickness of 0.3735 mm and width equal to 25.4 mm. Taking the Modulus of Elasticity to be 2.1×10^{11} Pa. And the density of steel as 7810 kg/cubic meter the first three natural frequencies of the beams are readily calculated using standard formulae as :

Simply-Supported: 3.86 Hz, 15.43 Hz and 34.73 Hz.

Fixed-Fixed: 8.75 Hz, 26.31 Hz and 47.28 Hz.

The simply-supported beam is excited at its mid-point at a frequency of 35 Hz, while the excitation frequency is chosen as 25 Hz in the case of the fixed-fixed beam. The amplitude of the applied force is maintained constant at 1.0 N. The accelerometer is placed at various locations along the beam and the steady state response amplitude and the difference in its phase with the applied sinusoidal force is noted. As mentioned earlier, the measurements could be taken at a small limited number of points, with the accelerometer. Two cases are illustrated here - one with 10 measurement stations and the other with 20 measurement stations. Fig. 4.4 (a) and (b), respectively show the amplitude and phase of the response of the simply-supported beam with 10 measurement points. Figs. 4.5 (a) and (b) show the in-phase and out-of-phase

amplitude responses computed from the measurements of Figs 4.4 (a)-(b). These are fed as inputs to the estimation algorithm. The first and third mode shapes, thus estimated are shown in Figs 4.6 (a)-(b). The errors in the mode shapes are given in Figs. 4.7 (a)-(b). Figs 4.8 (a)-(b) show the measured amplitude and phase, Figs. 4.9 (a)-(b) give the computed in-phase and out-of-phase response, Figs. 4.10 (a)-(b) show the estimated mode shapes, while Figs. 4.11 (a)-(b) depict the errors involved, when the procedure is repeated for 20 measuring points. The maximum error in the estimated mode shapes is about 12 % for the first mode and about 45 % for the second mode. The errors can be seen to reduce when the number of measuring stations is increased. The estimated natural frequencies and the errors are listed in Table 4.1. The errors in the natural frequencies are between 5 to 6 %. From these results it is obvious that more number of measurement stations with a more sophisticated sensor will be required for implementation of a spatial modal analysis procedure of the type developed. Other sources of error can be the improper location of the excitation force and also importantly non-ideal boundary conditions of the set-ups employed.

Similar experimental illustration is carried out with a fixed-fixed configuration of the beam. With 10 number of measuring stations Figs 4.12 (a)-(b) give the amplitude and phase of the measured response. Fig. 4.13 (a)-(b) show the computed in-phase and out-of-phase response. The estimated mode shapes are shown in Figs 4.14 (a)-(b), while the errors are shown in Figs. 4.15 (a)-(b). Again, with 20 measurement stations, the measured amplitude and phase response is shown in Figs. 4.16 (a)-(b). The computed in-phase and out-of-phase response is given in Figs. 4.17 (a)-(b). The estimated mode shapes and the corresponding errors are shown in Figs. 4.18 (a)-(b) and 4.19 (a)-(b) respectively. The estimated natural frequencies and the errors in comparison with the exact values are listed in Table 4.2. The findings and the causes of errors are similar to those mentioned for the simply supported beam.

Table 4.1 **Exact and estimated natural frequencies of simply supported beam**

No. of stations	Mode	Natural frequencies		
		Exact	Estimated	Error
10	1	3.859	3.601	6.70
	3	34.739	32.598	6.13
20	1	3.859	3.654	5.33
	3	34.739	32.980	5.06

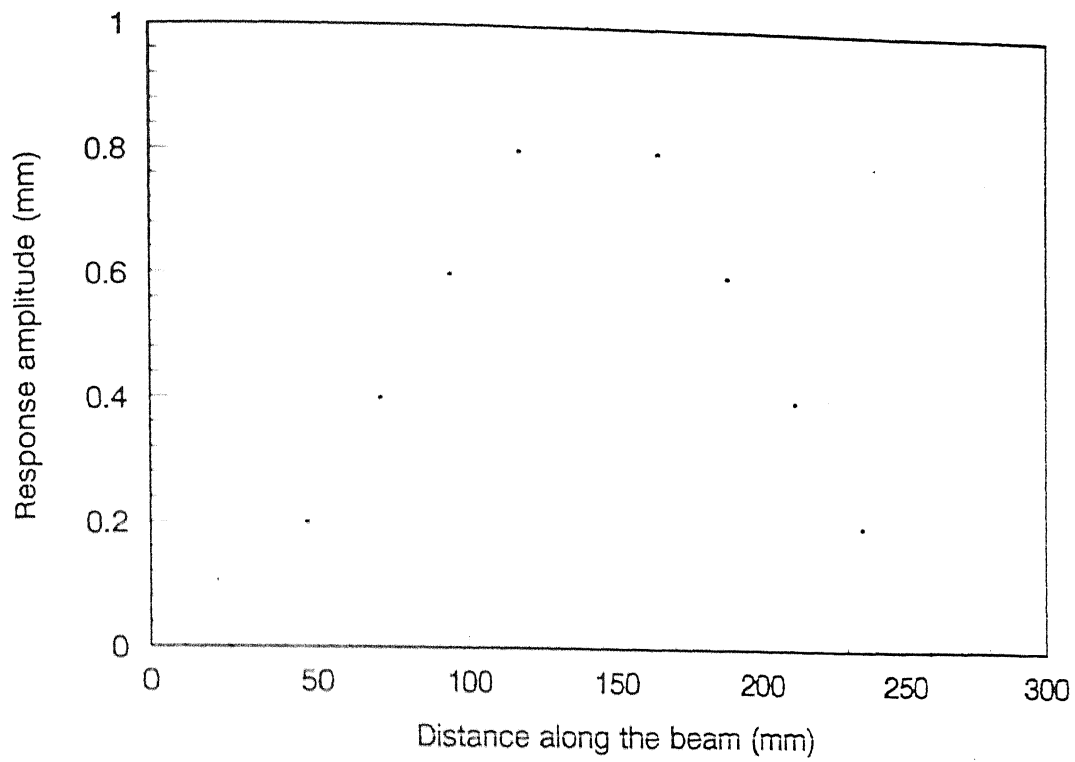


Fig. 4.4(a) Response amplitude of simply supported beam with 10 number of stations ($\kappa=1.2769$)

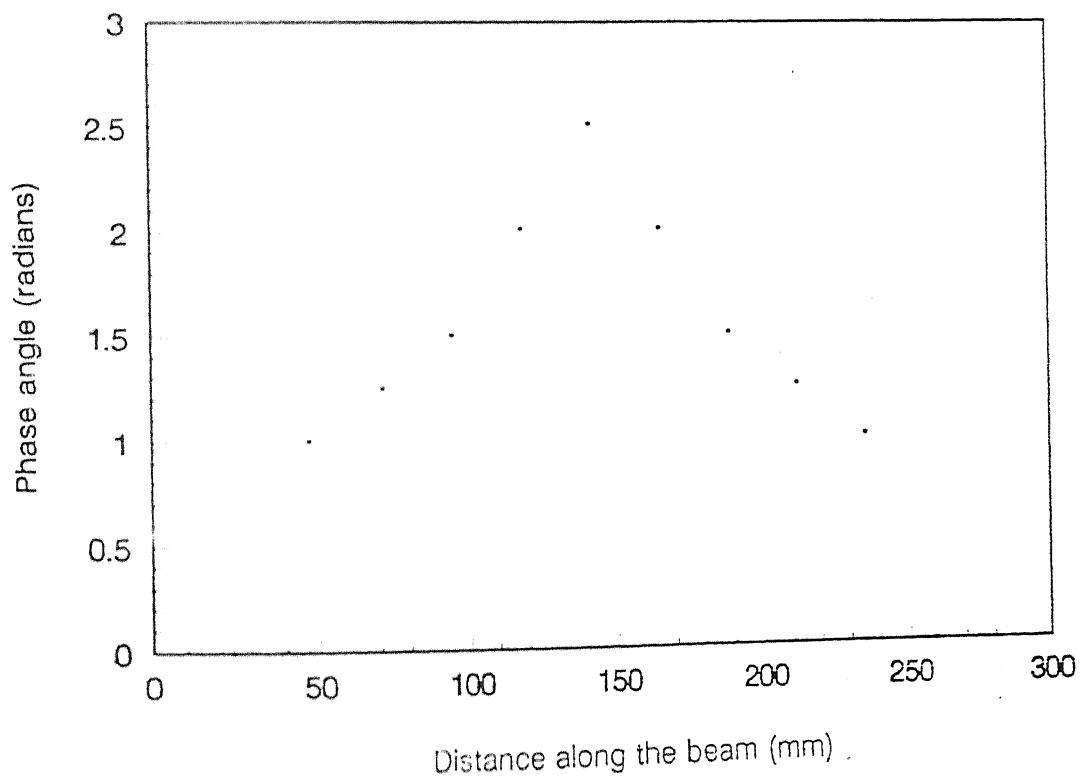


Fig. 4.4(b) Phase angle of simply supported beam with 10 number of stations ($\kappa=1.2769$)

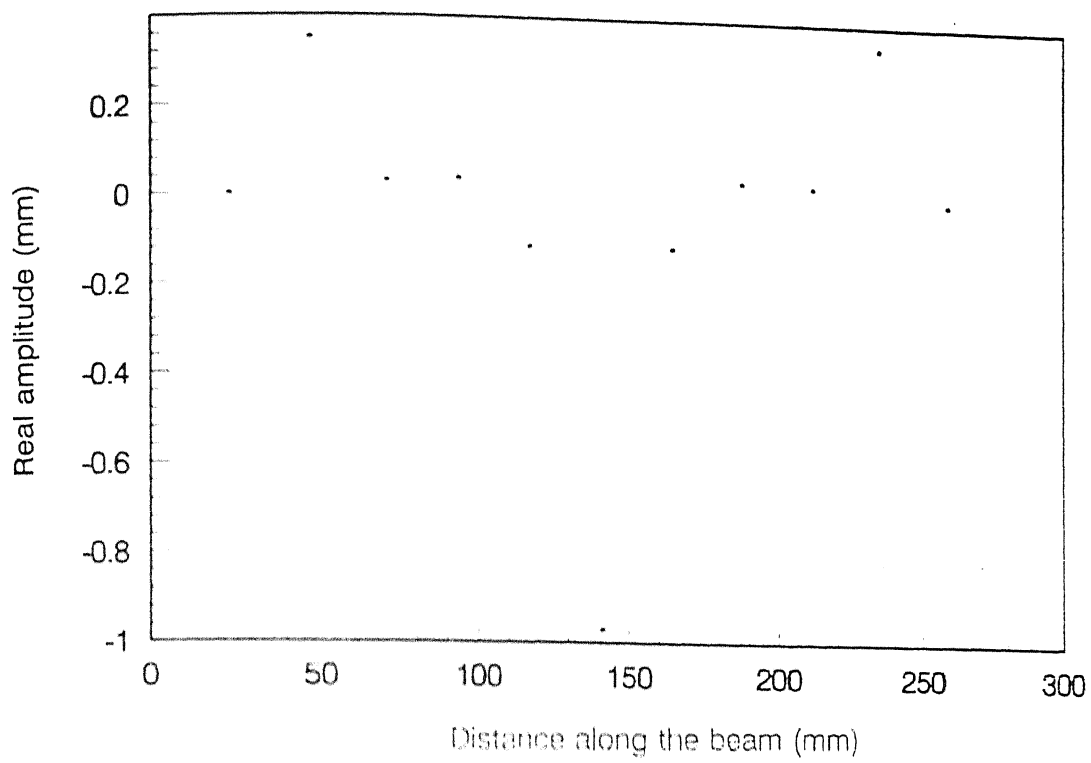


Fig. 4.5(a) In phase response amplitude of simply supported beam with 10 number of stations ($\kappa=1.2769$)

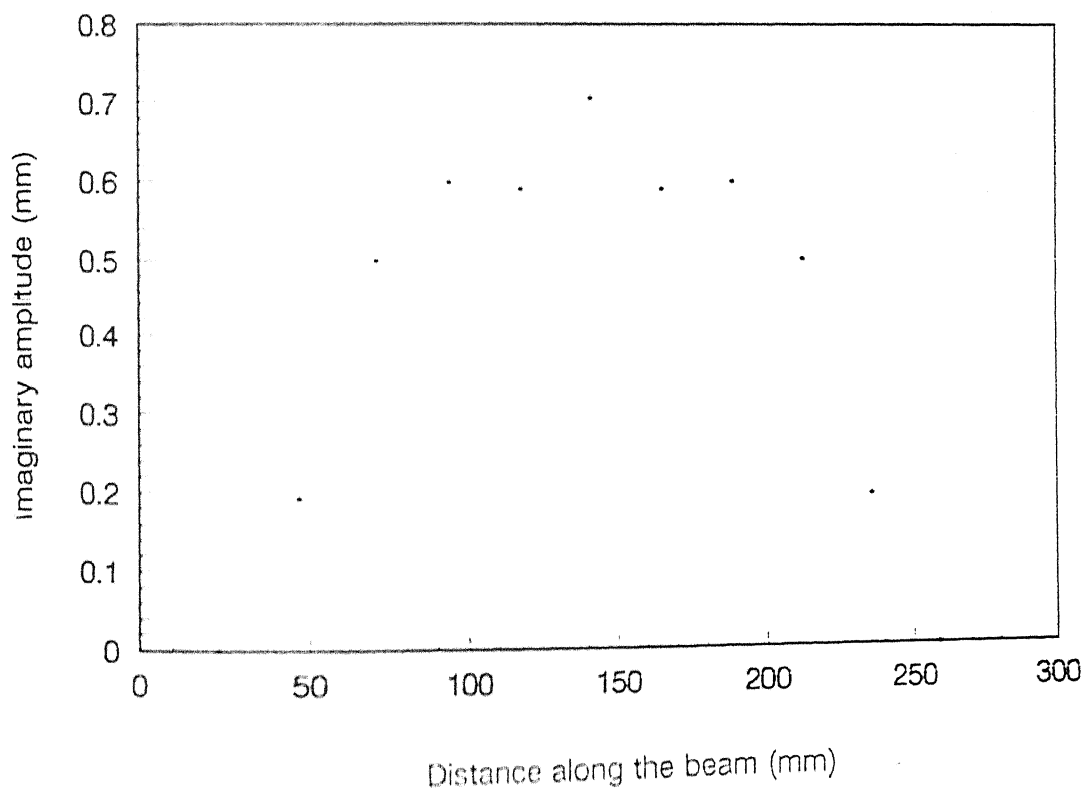
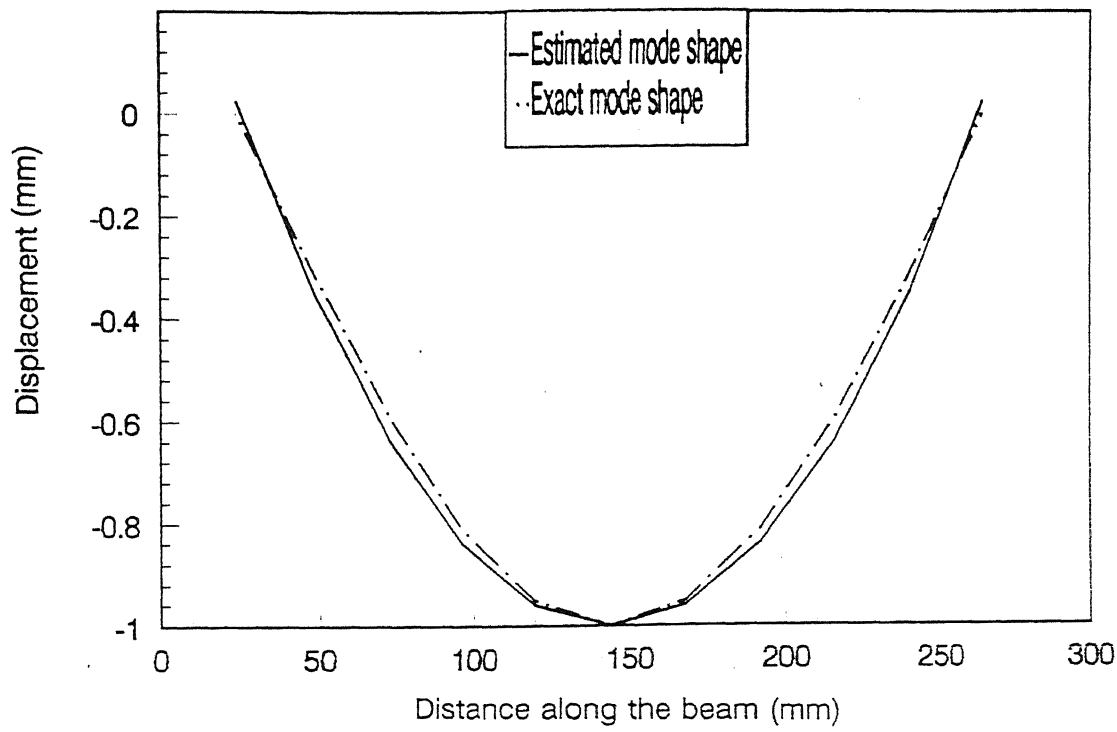
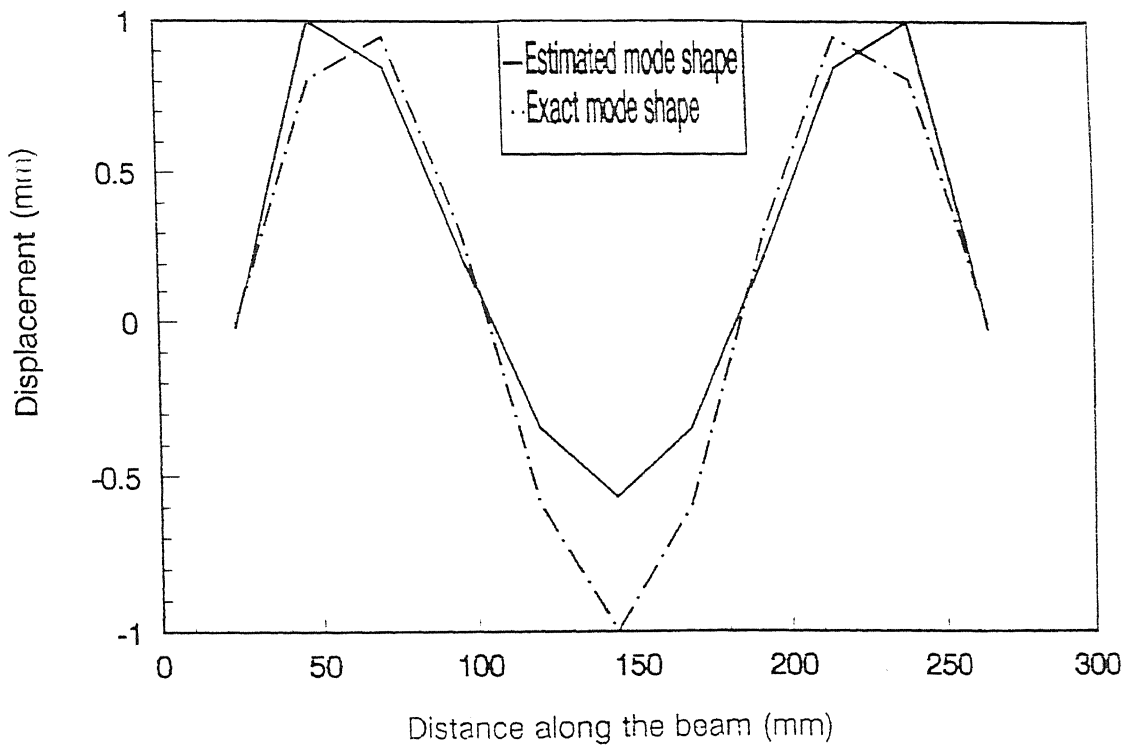


Fig. 4.5(b) Out of phase amplitude of simply supported beam with 10 number of stations ($\kappa=1.2769$)

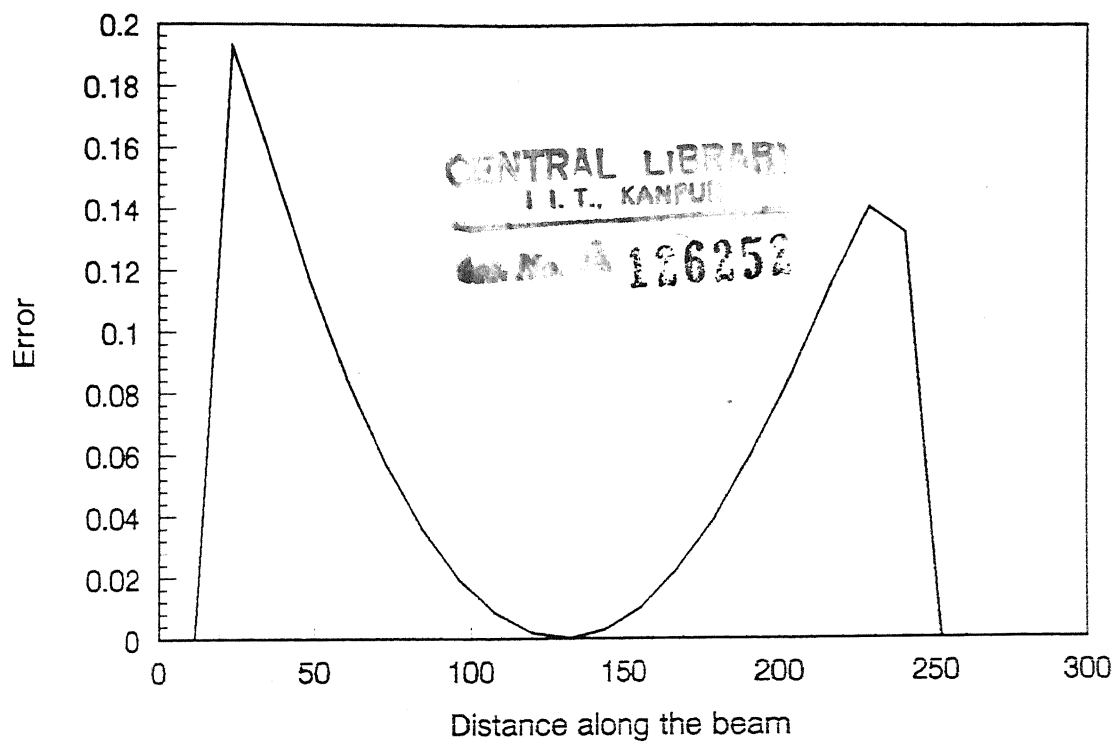


(a) Mode 1

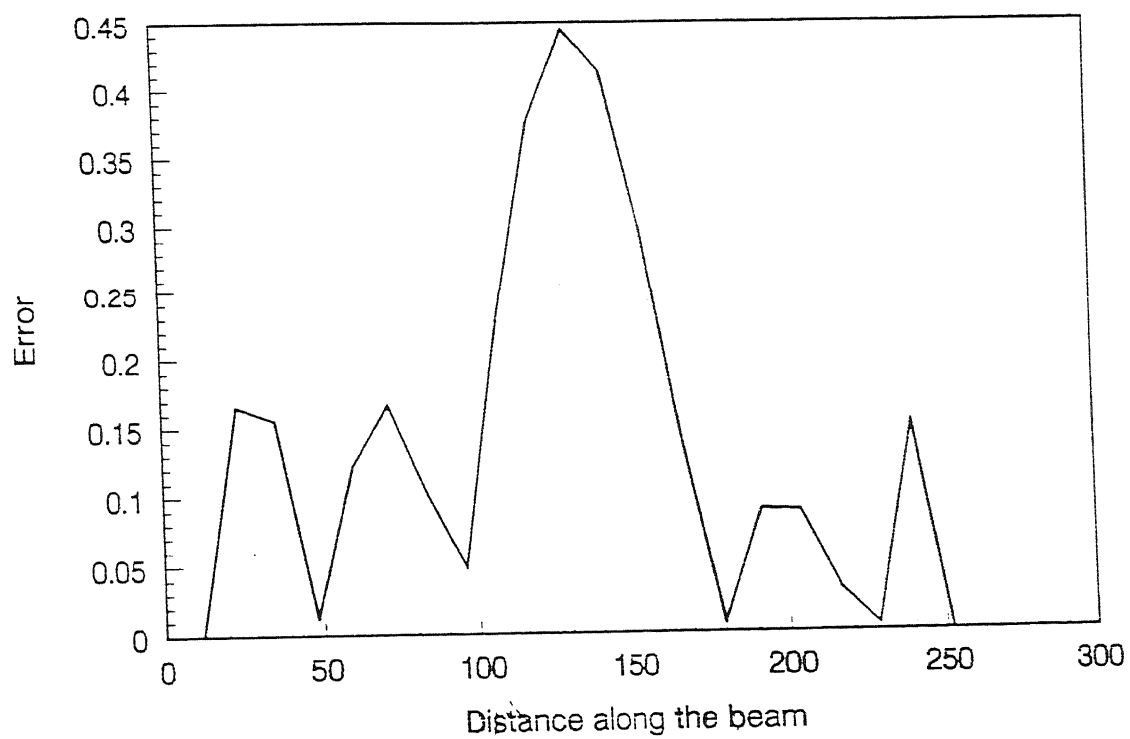


(b) Mode 2

Fig. 4.6 Estimated and exact mode shapes of simply supported beam with 10 number of stations ($\kappa=1.2769$)



(a) Mode 1



(b) Mode 2

Fig. 4.7 Errors of simply supported beam with 10 number of stations ($\kappa=1.2769$)

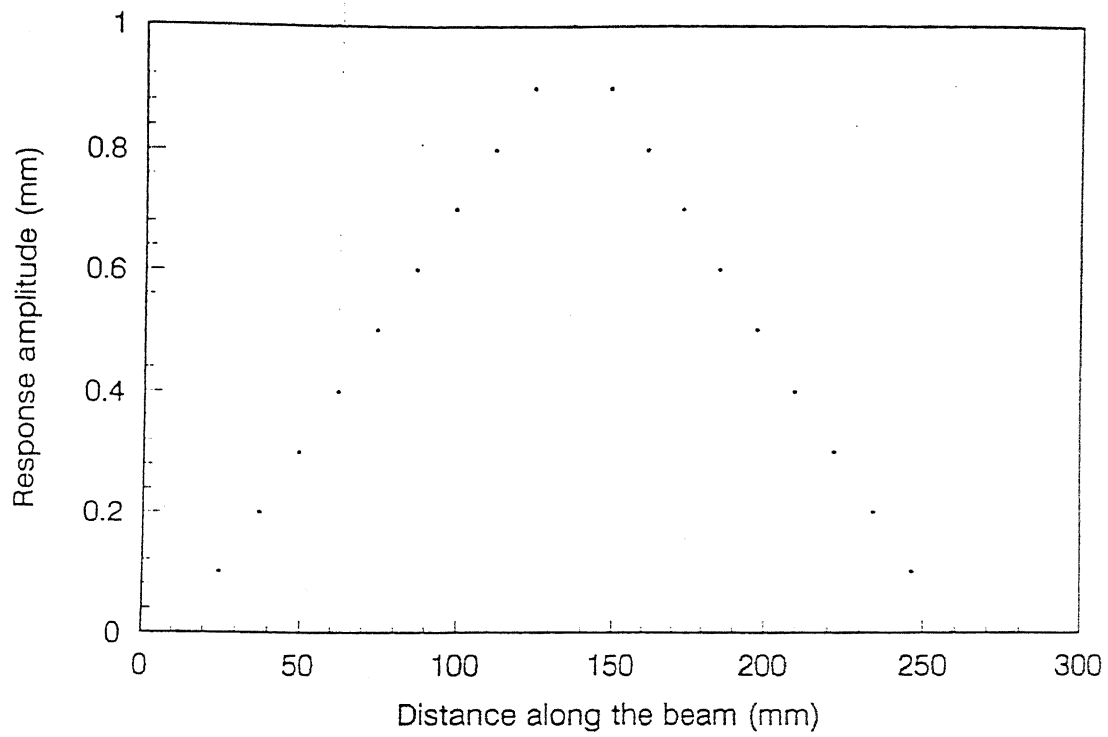


Fig. 4.8(a) Response amplitude of simply supported beam with 20 number of stations ($\kappa=1.2769$)

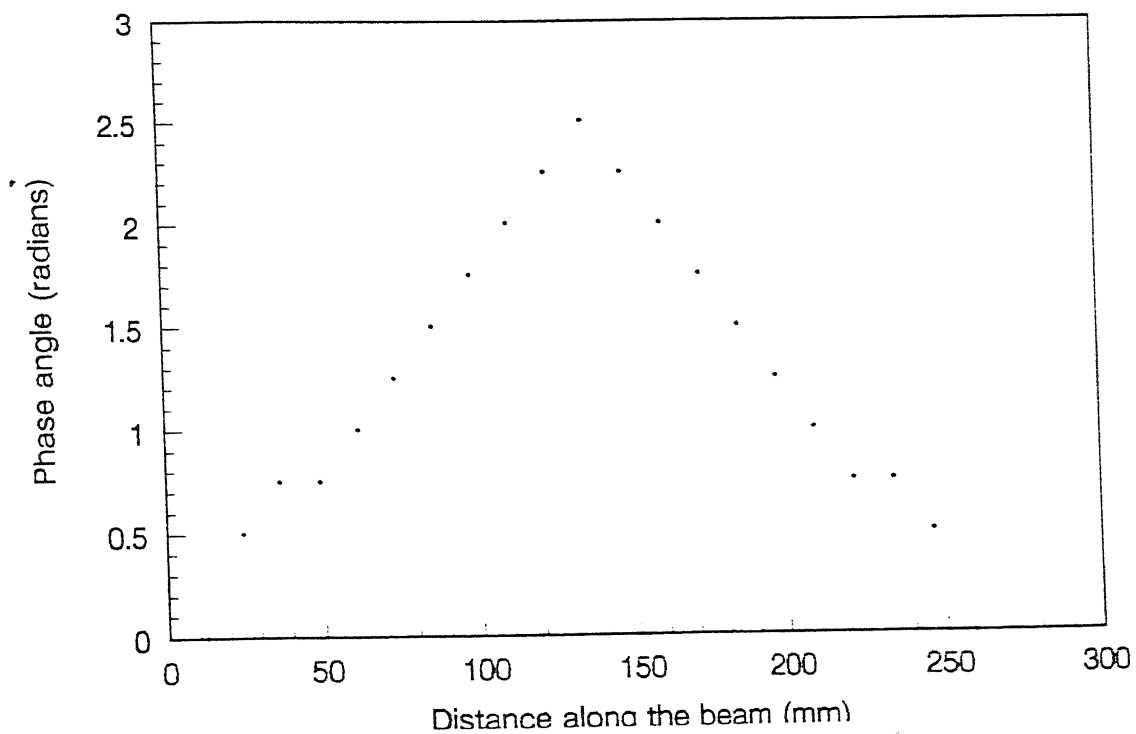


Fig. 4.8(b) Phase angle of simply supported beam with 20 number of stations ($\kappa=1.2769$)

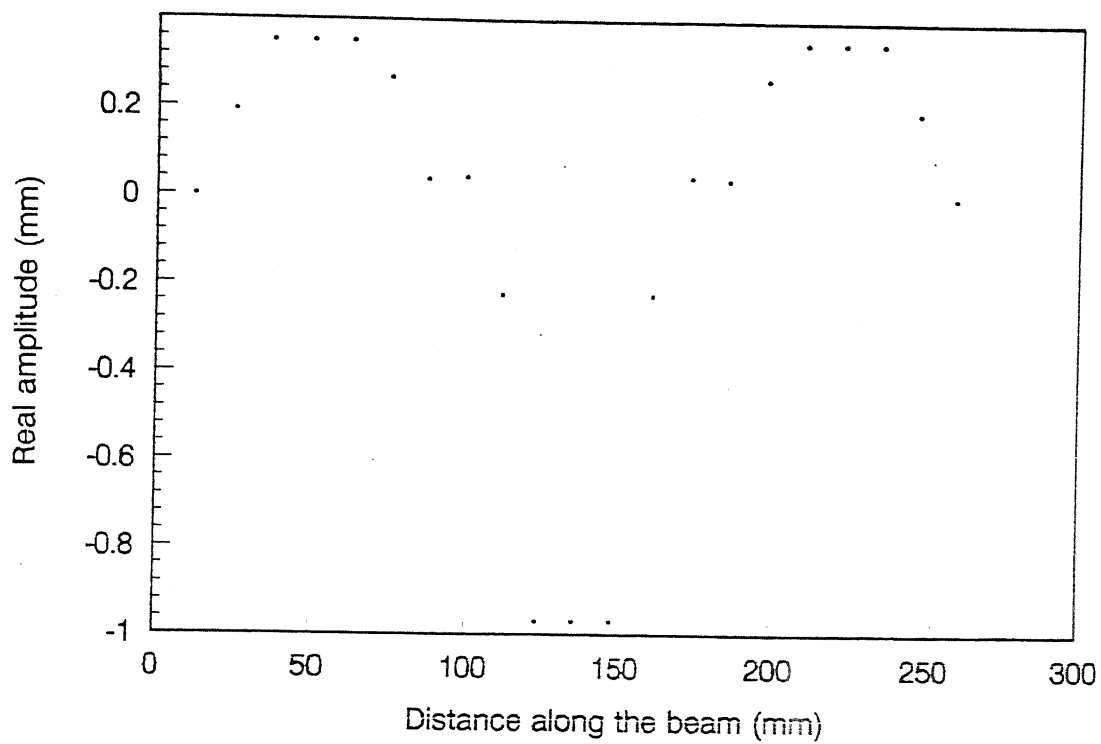


Fig. 4.9(a) In phase response amplitude of simply supported beam with 20 number of stations ($\kappa=1.2769$)

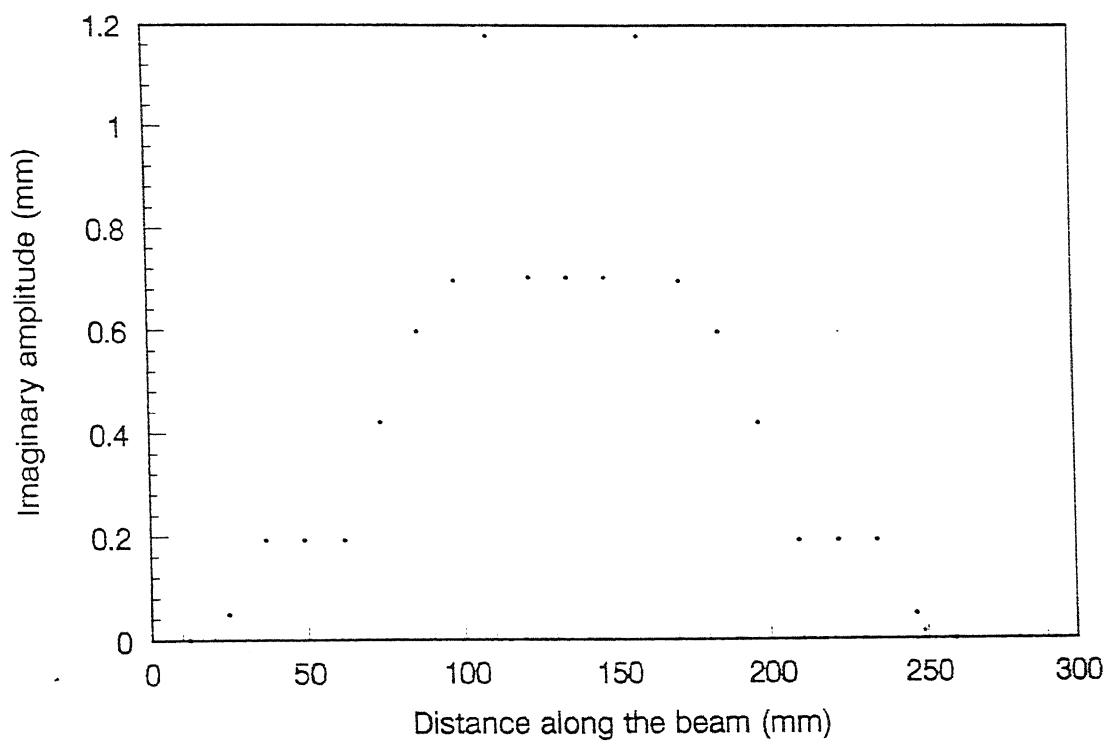
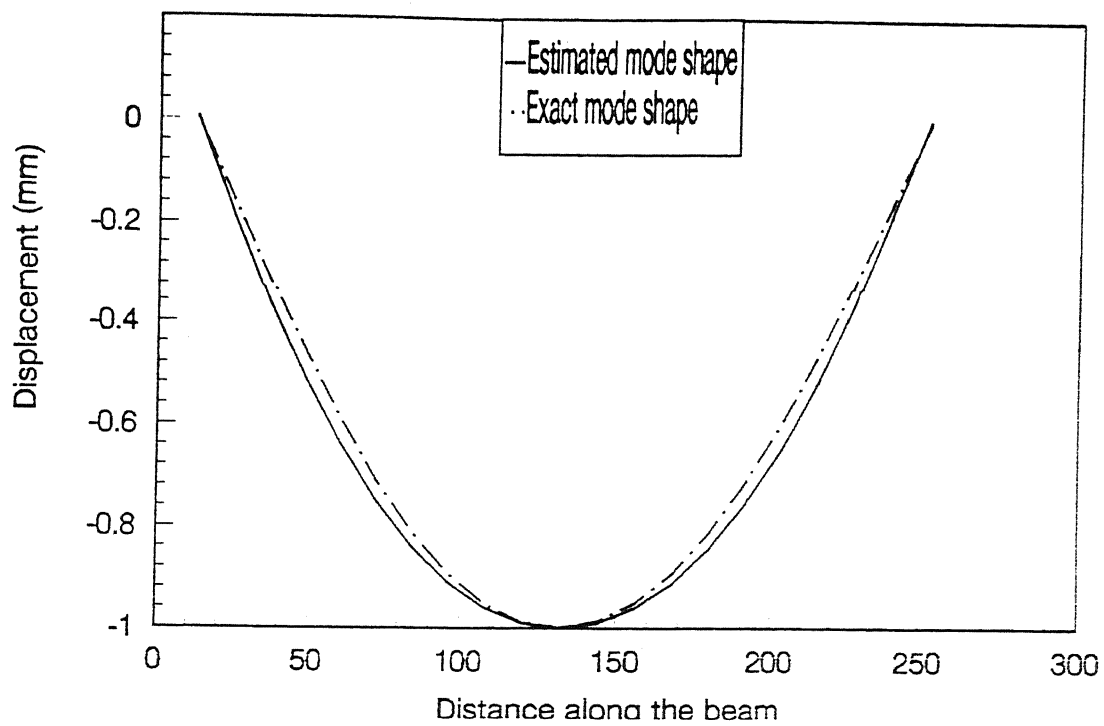
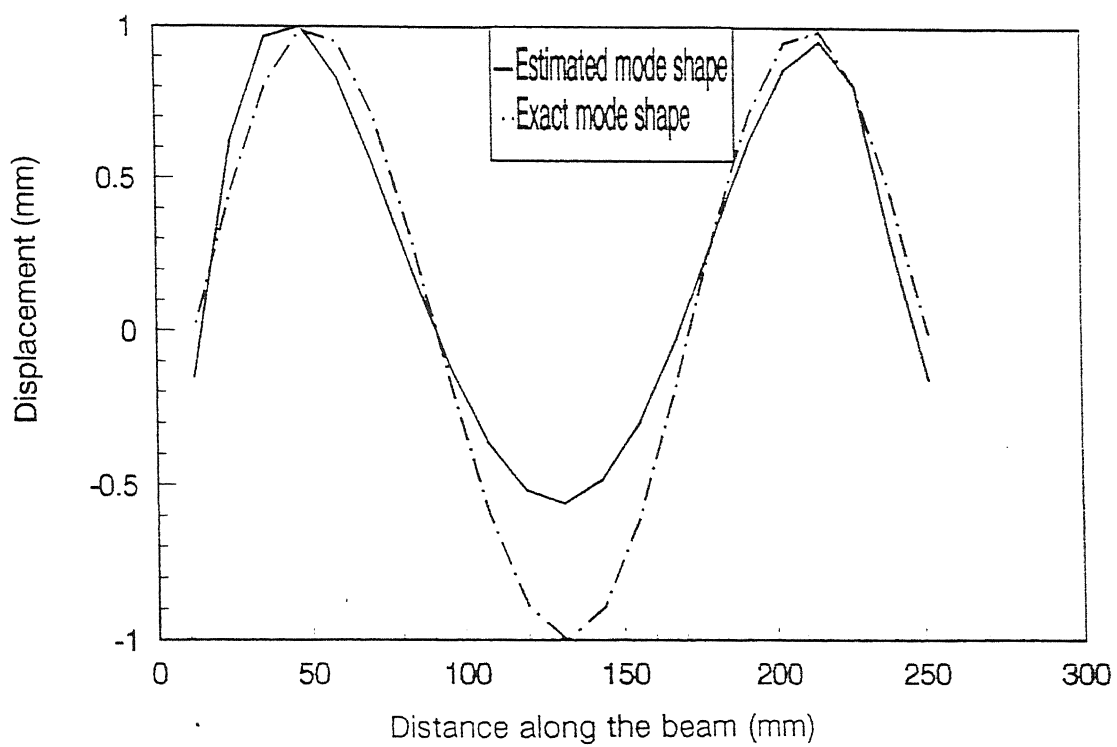


Fig. 4.9(b) Out of phase amplitude of simply supported beam with 20 number of stations ($\kappa=1.2769$)

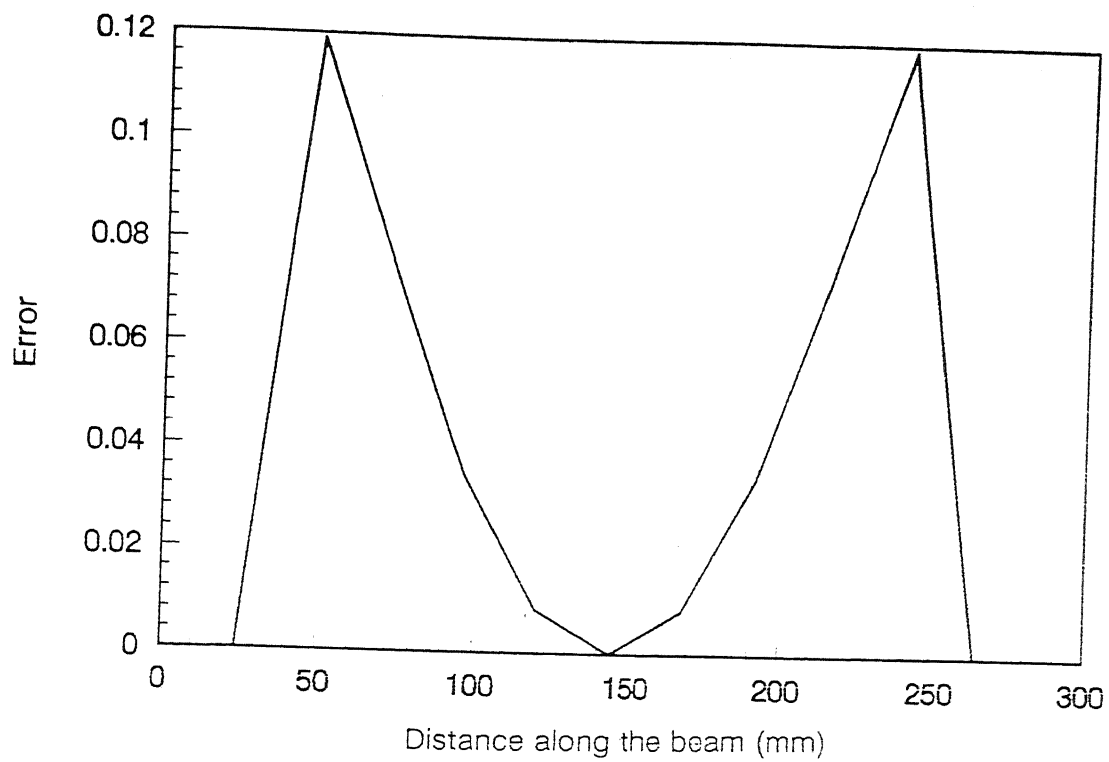


(a) Mode 1

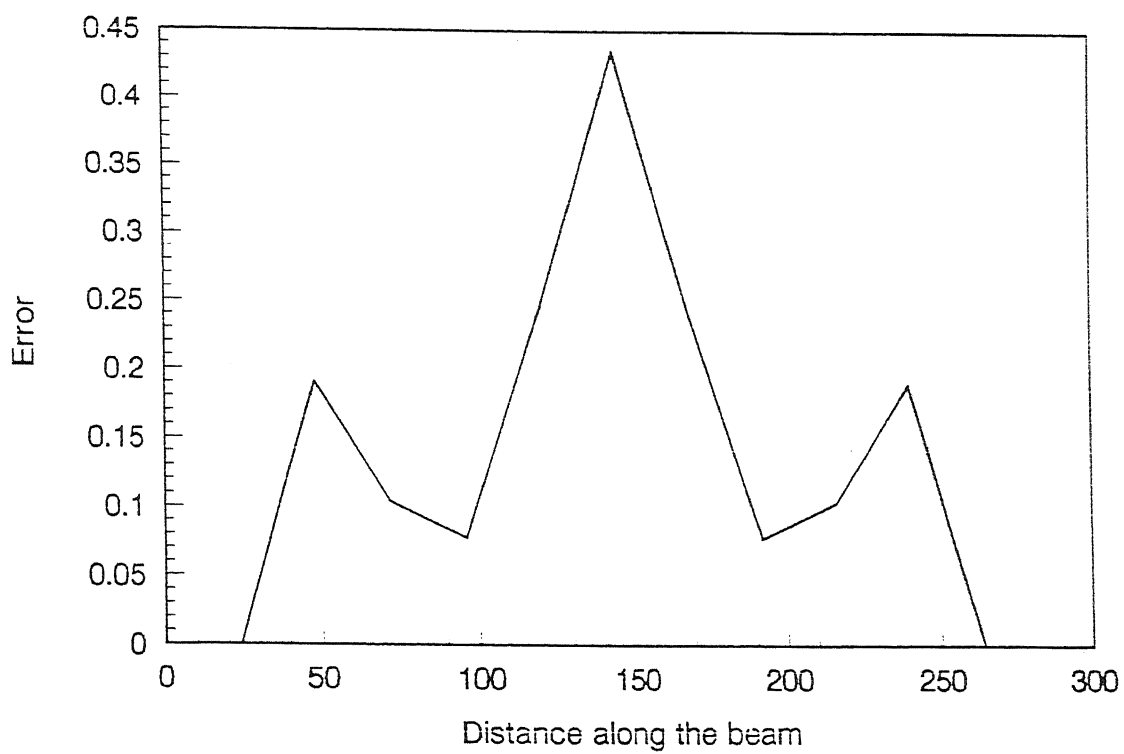


(b) Mode 2

Fig. 4.10 Estimated and exact mode shapes of simply supported beam with 20 number of stations ($\kappa=1.2769$)



(a) Mode 1



(b) Mode 2

Fig. 4.11 Errors of simply supported beam with 20 number of stations ($\kappa=1.2769$)

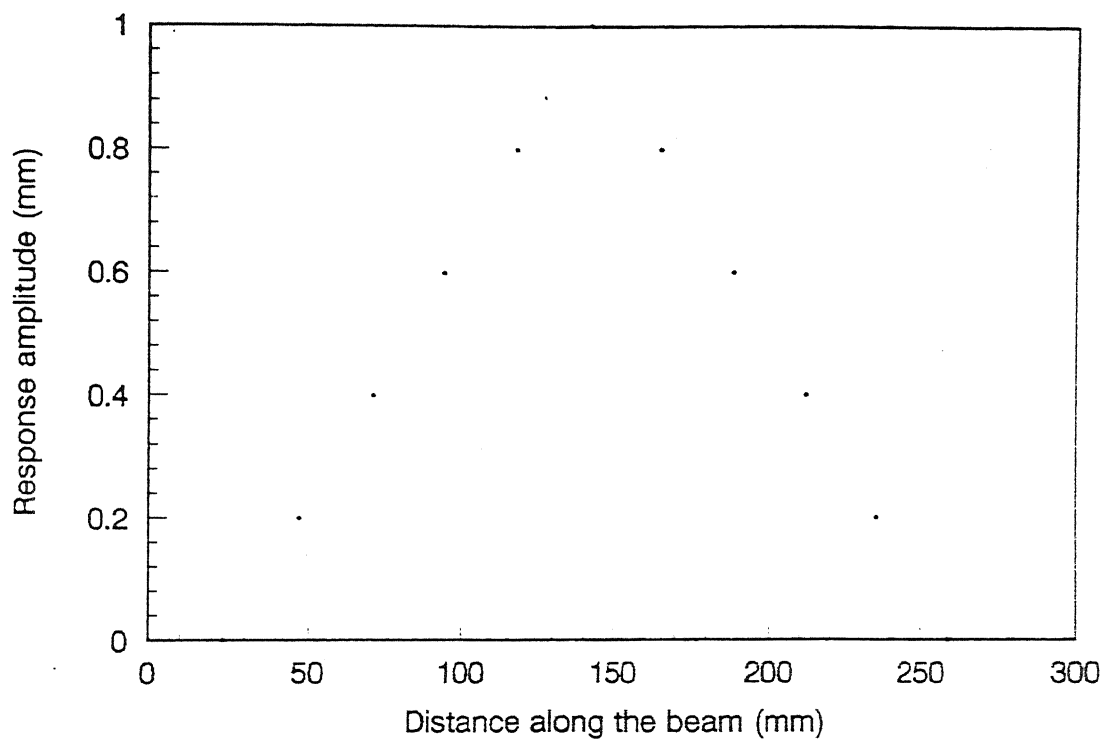


Fig. 4.12(a) Response amplitude of fixed-fixed beam with 10 number of stations ($\kappa=1.2769$)

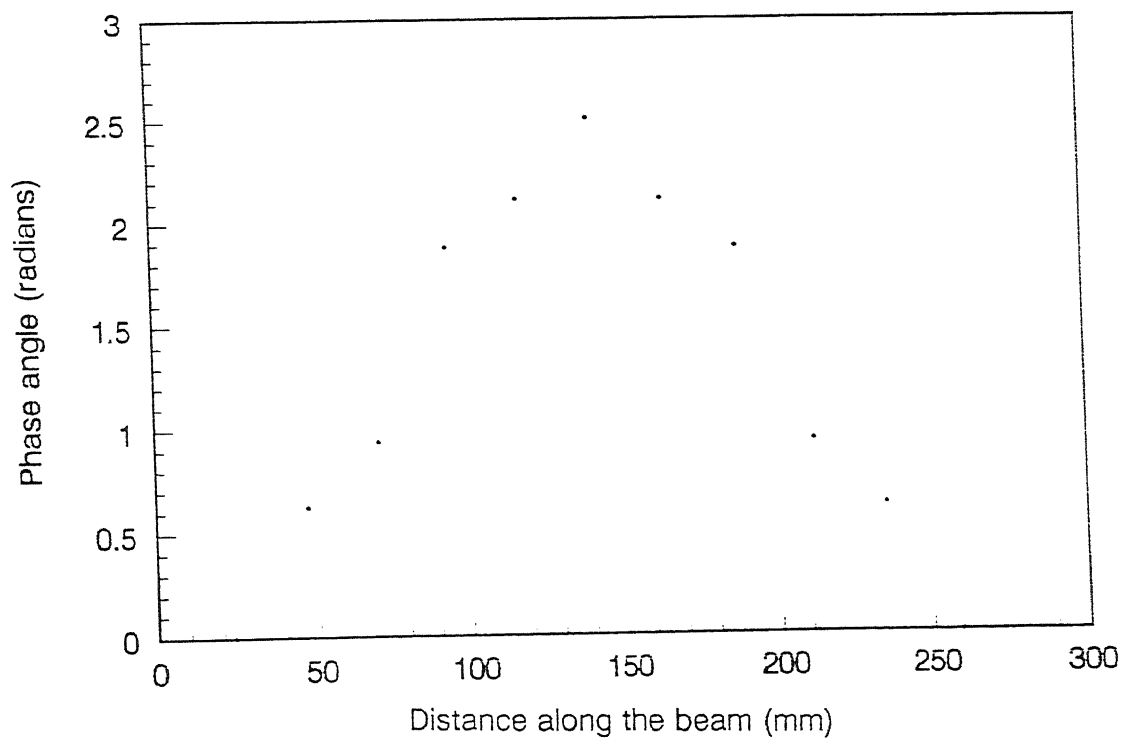


Fig. 4.12(b) Phase angle of fixed-fixed beam with 10 number of stations ($\kappa=1.2769$)

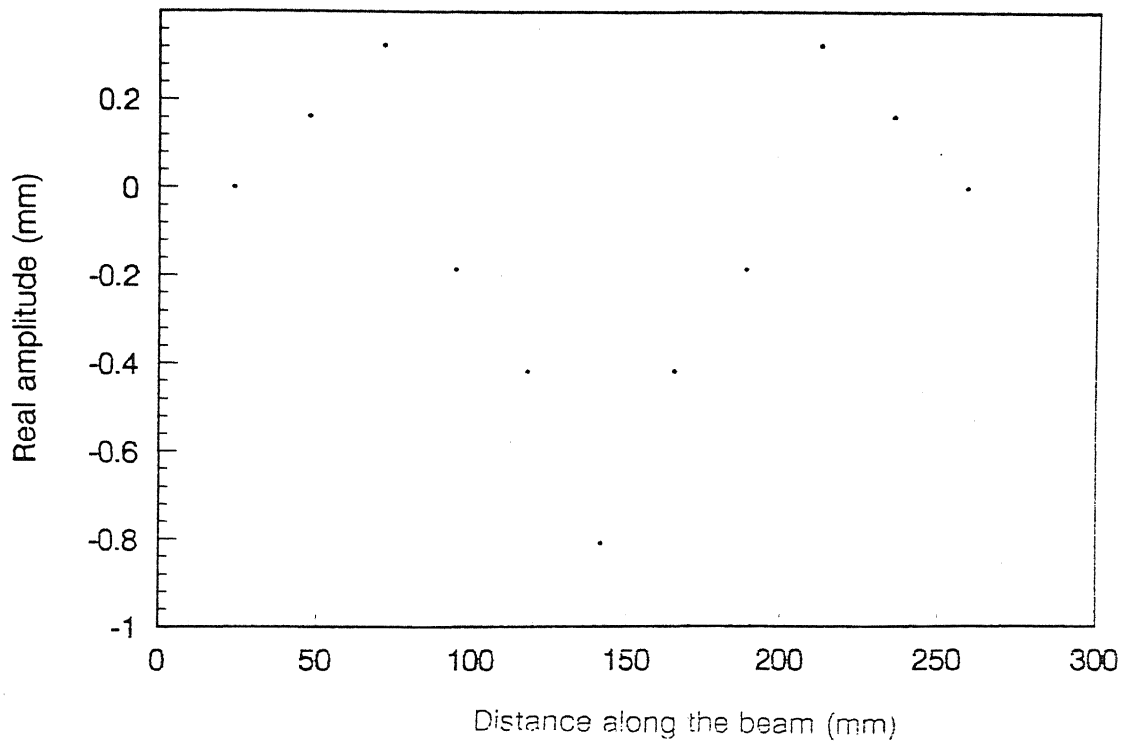


Fig. 4.13(a) In phase response amplitude of fixed-fixed beam with 10 number of stations ($\kappa=1.2769$)

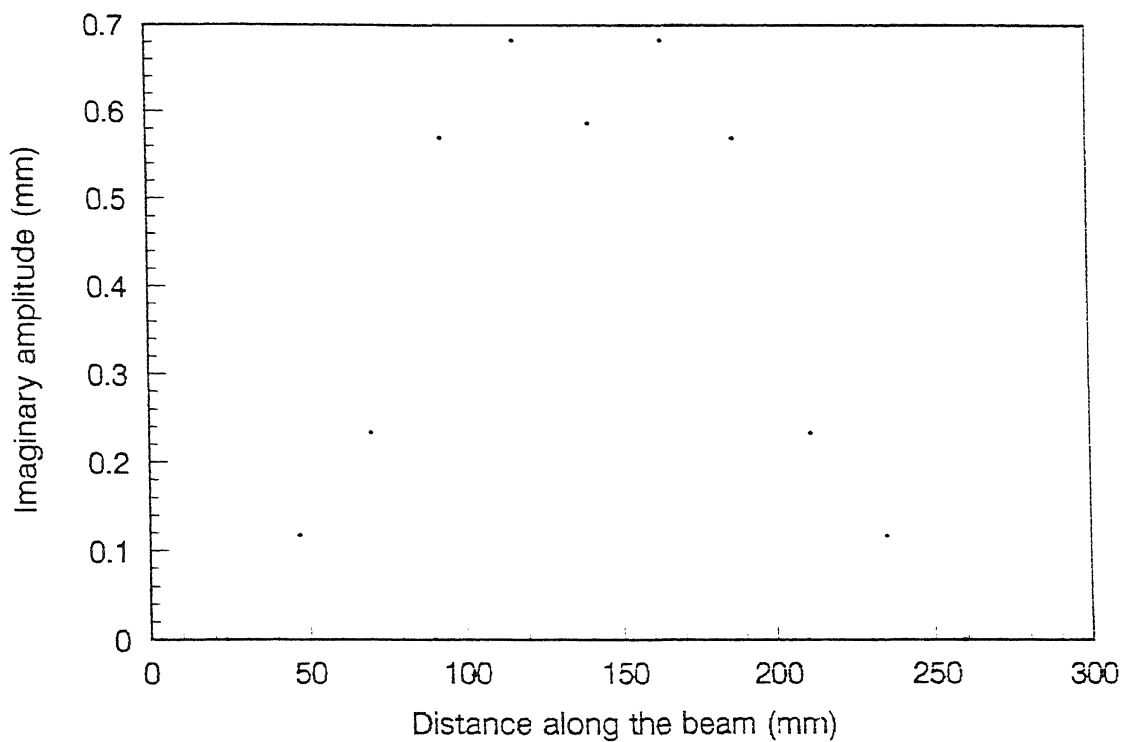
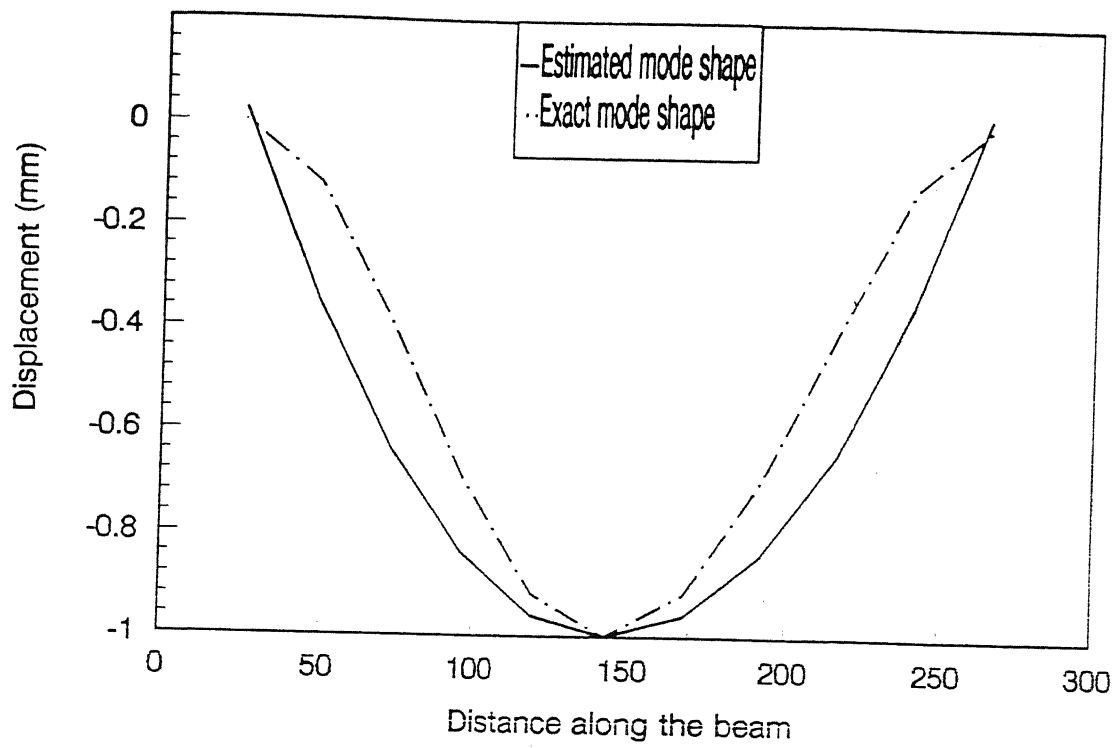
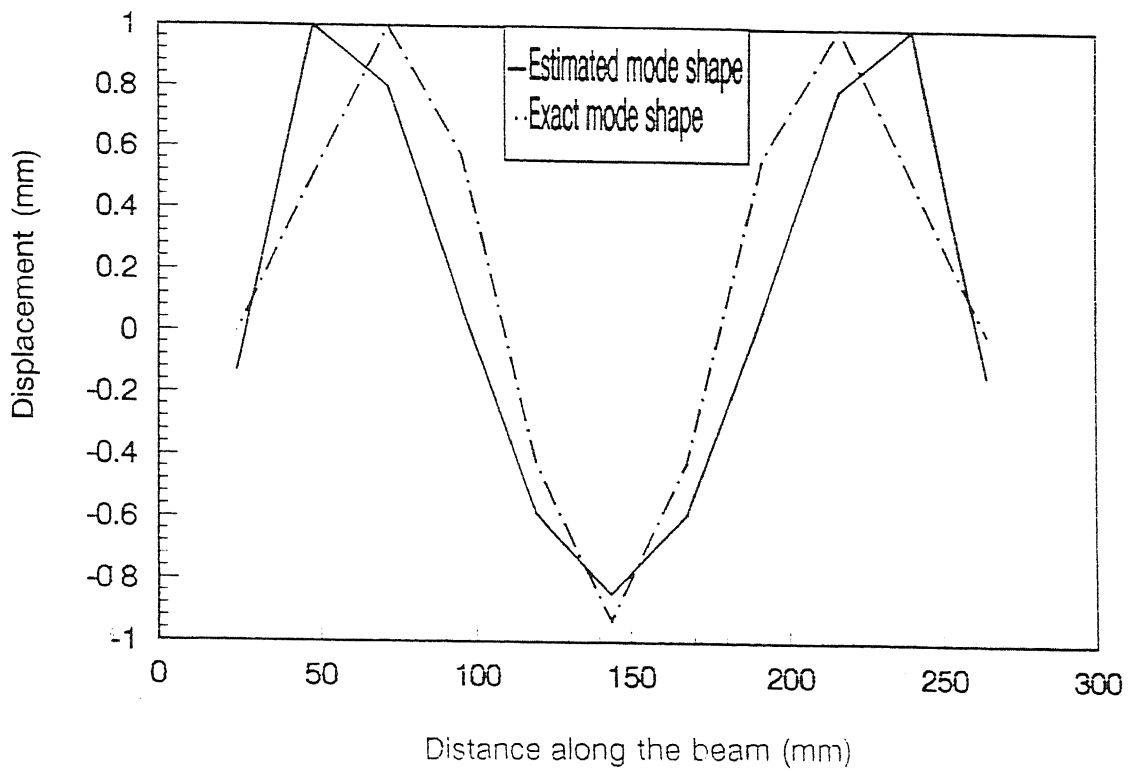


Fig. 4.13(b) Out of phase amplitude of fixed-fixed beam with 10 number of stations ($\kappa=1.2769$)

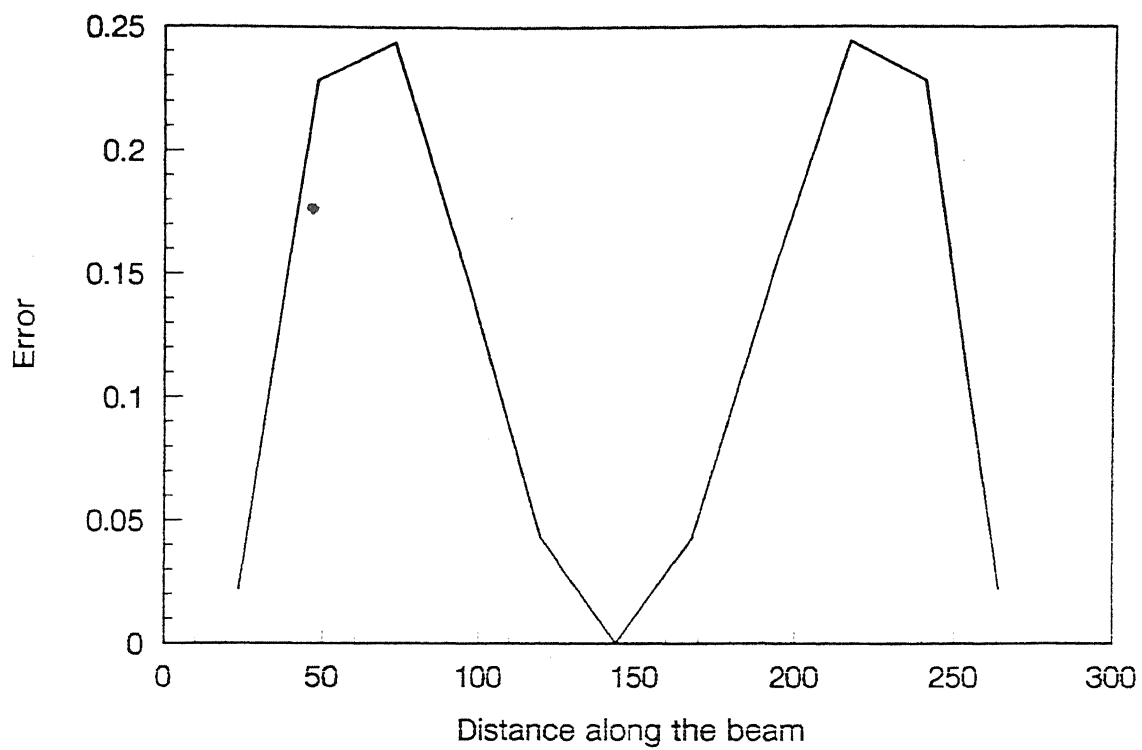


(a) Mode 1

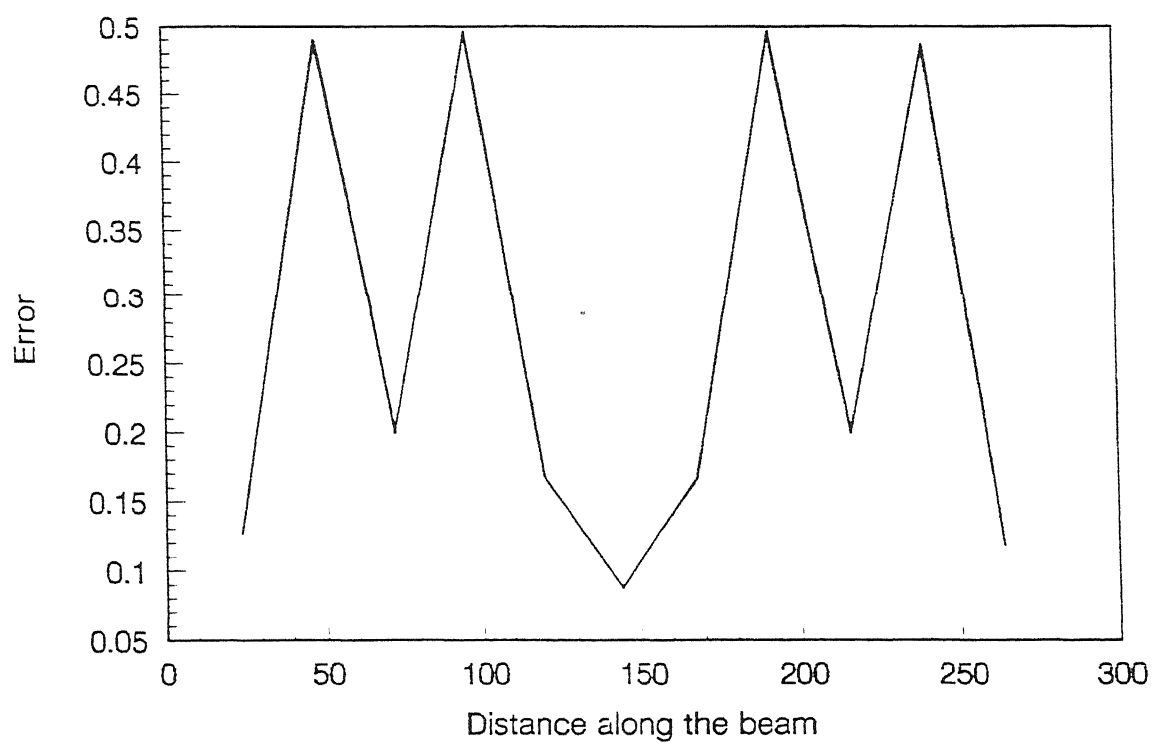


(b) Mode 2

Fig. 4.14 Estimated and exact mode shapes of fixed-fixed beam with 10 number of stations ($\kappa=1.2769$)



(a) Mode 1



(b) Mode 2

Fig. 4.15 Errors of fixed-fixed beam with 10 number of stations ($\kappa=1.2769$)

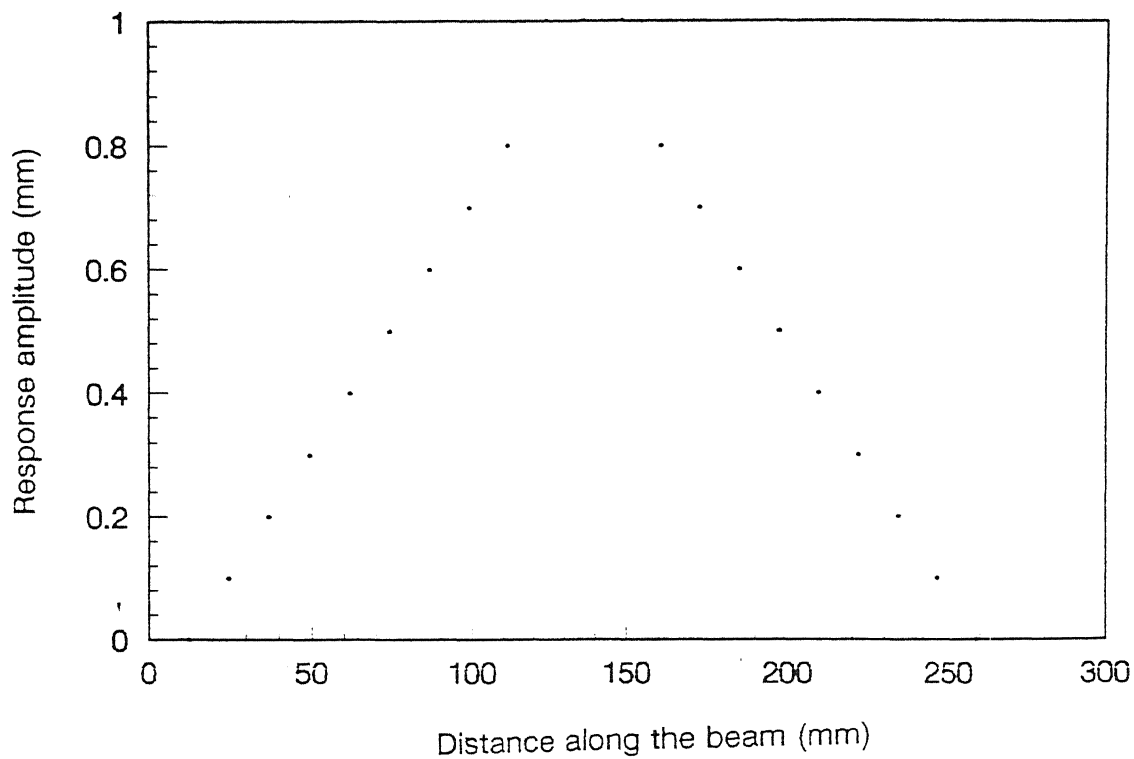


Fig. 4.16(a) Response amplitude of fixed-fixed beam with 20 number of stations ($\kappa=1.2769$)

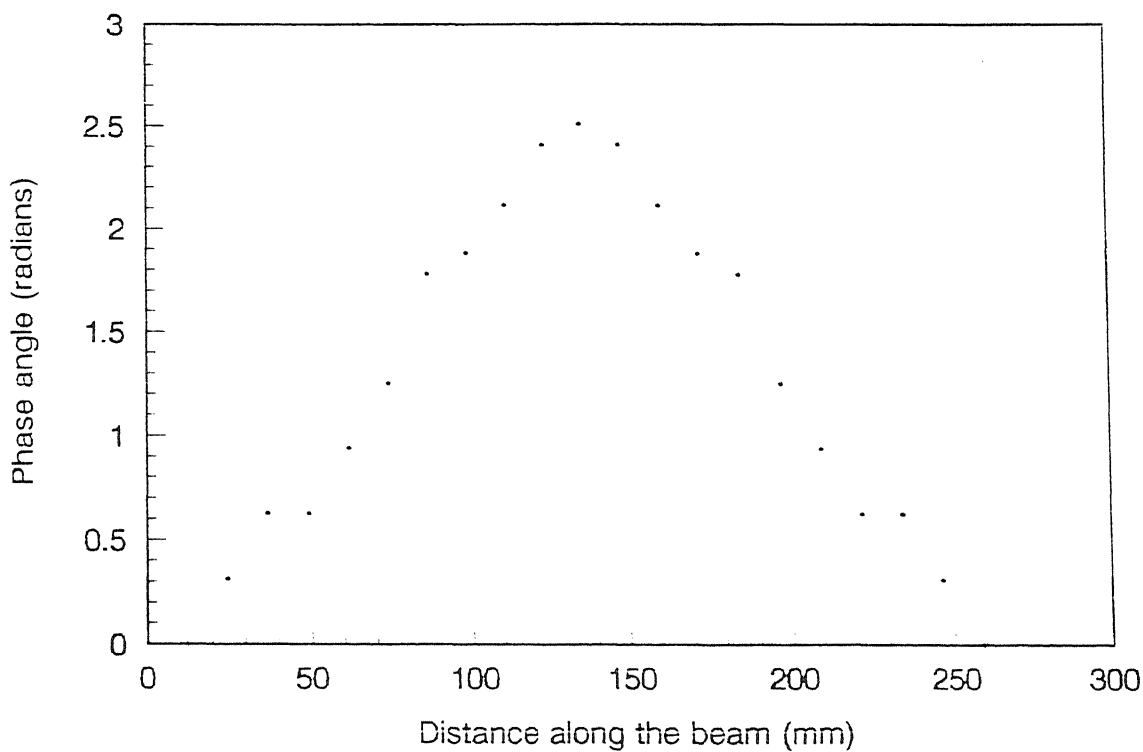


Fig. 4.16(b) Phase angle of fixed-fixed beam with 20 number of stations ($\kappa=1.2769$)

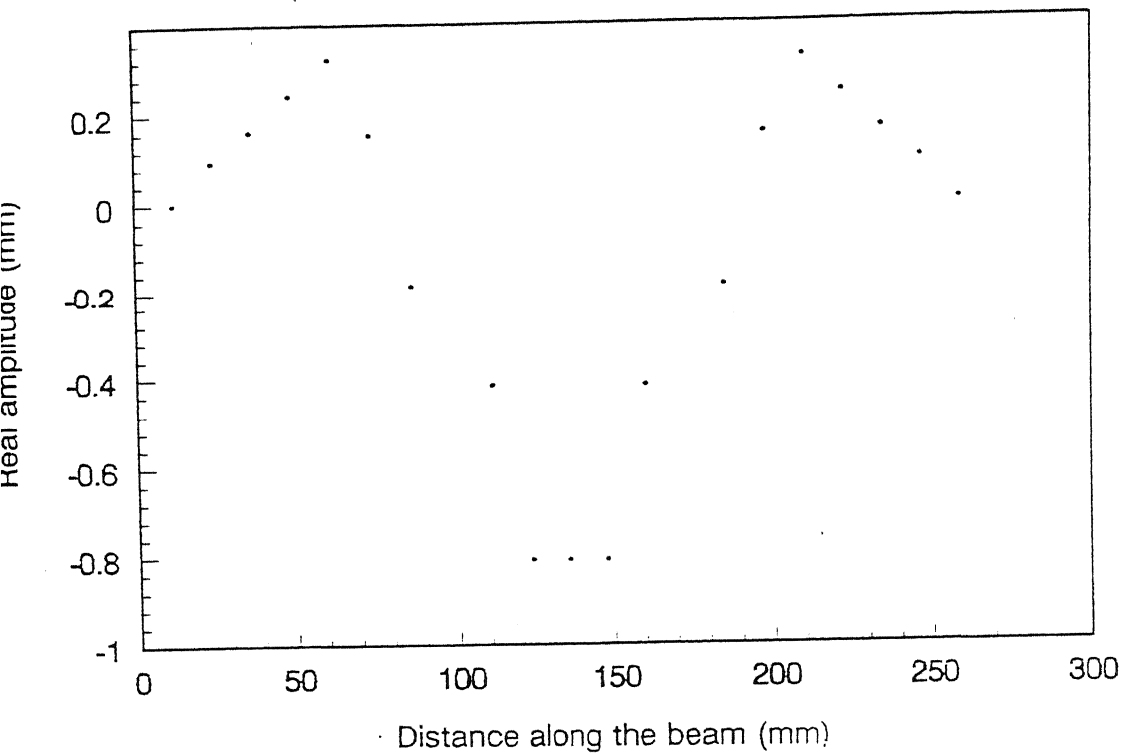


Fig. 4.17(a) In phase response amplitude of fixed-fixed beam with 20 number of stations ($\kappa=1.2769$)

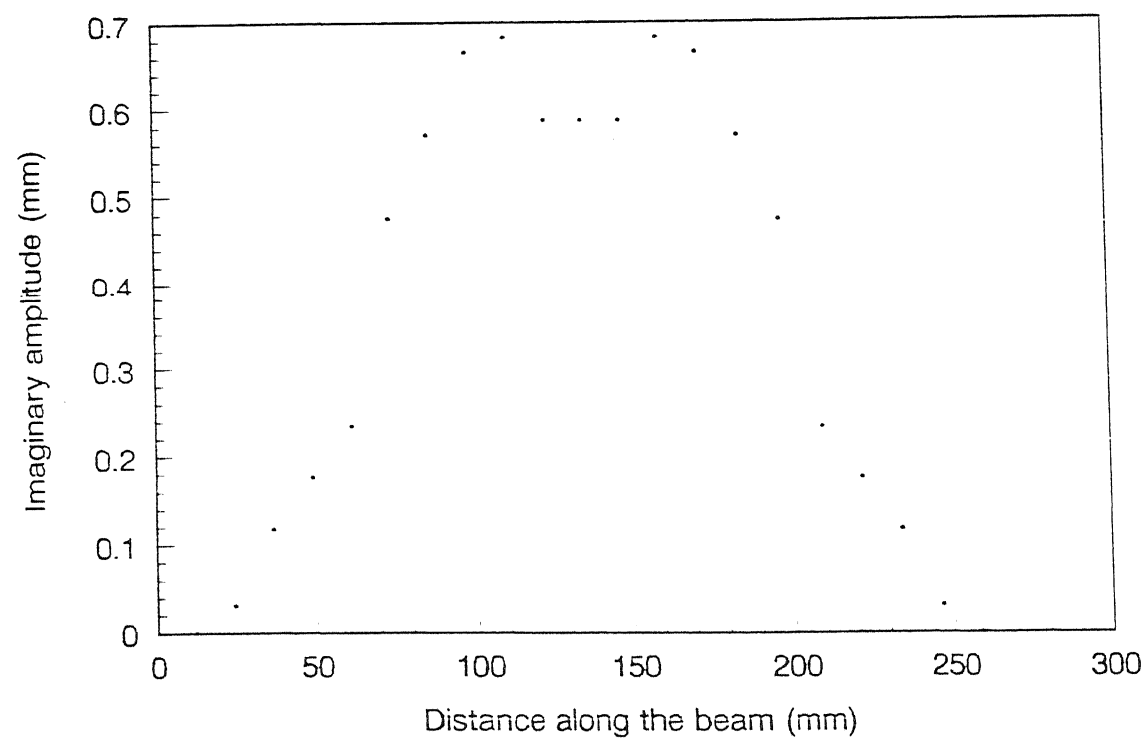
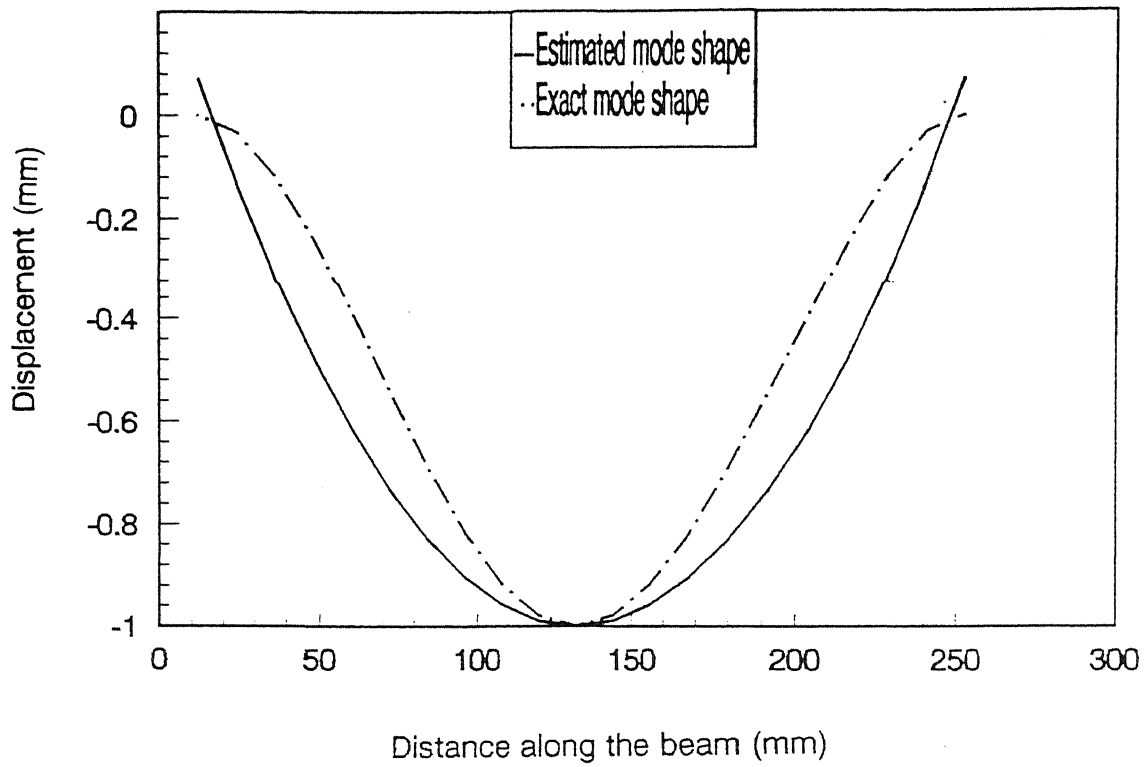
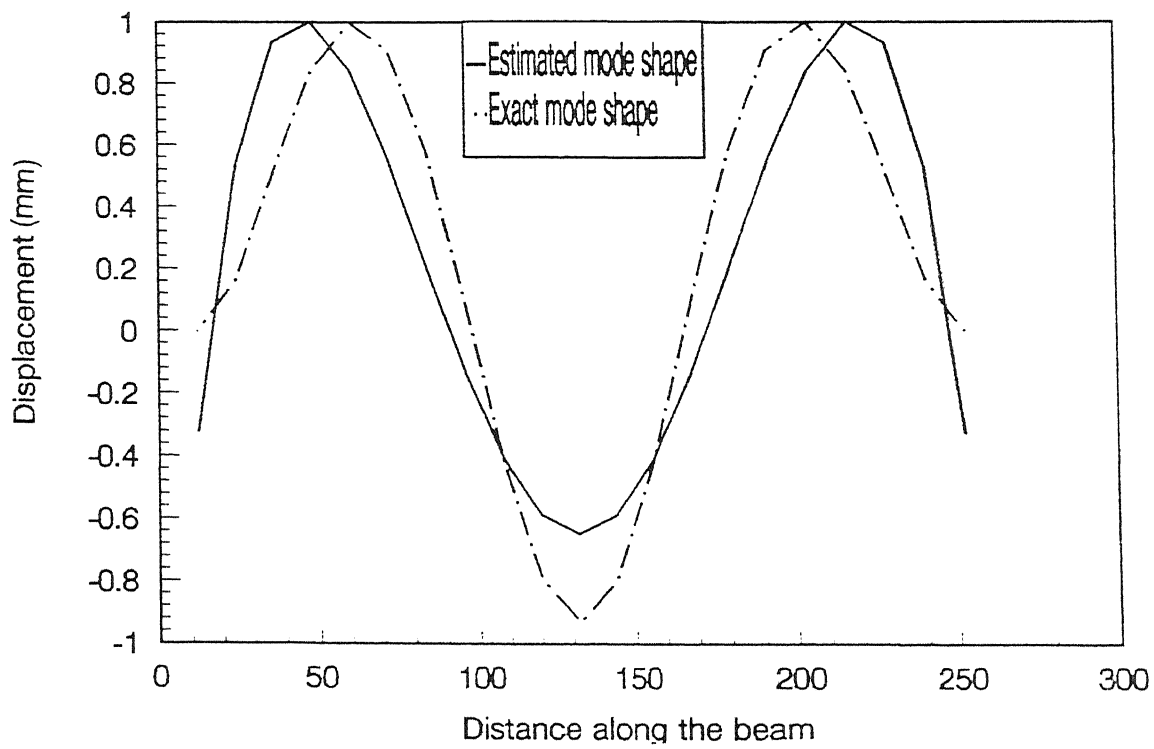


Fig. 4.17(b) Out of phase amplitude of fixed-fixed beam with 20 number of stations ($\kappa=1.2769$)

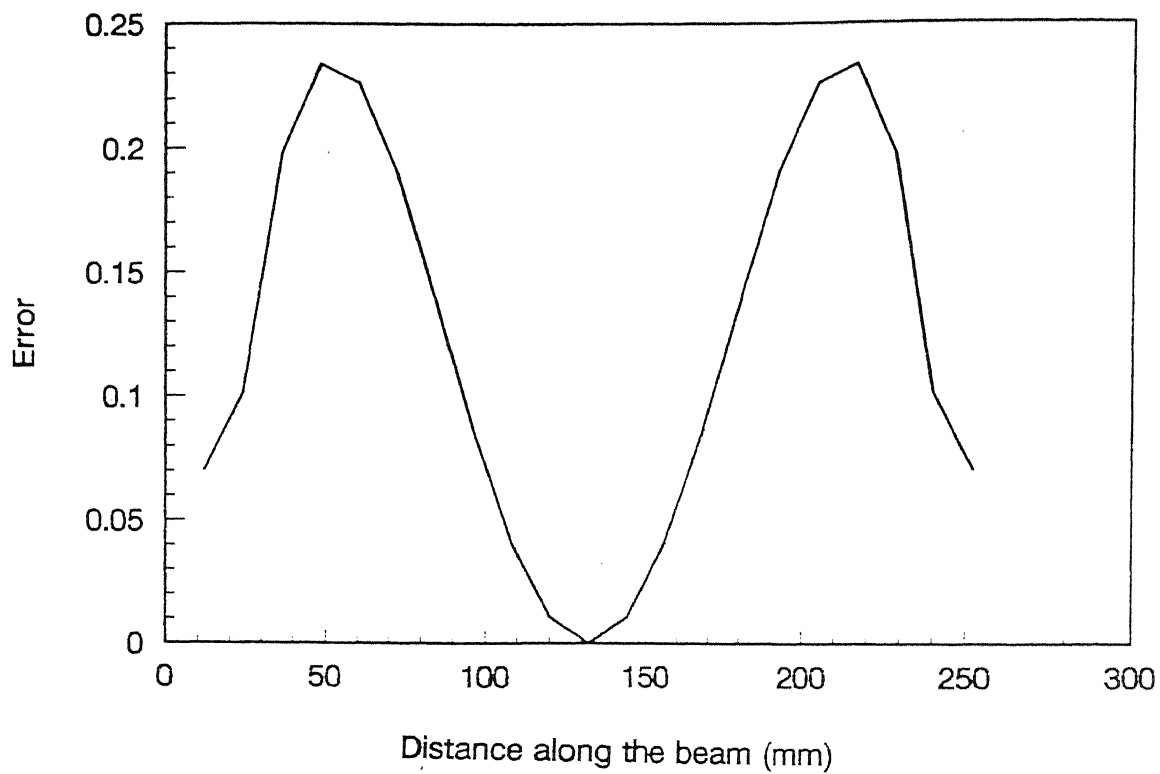


(a) Mode 1

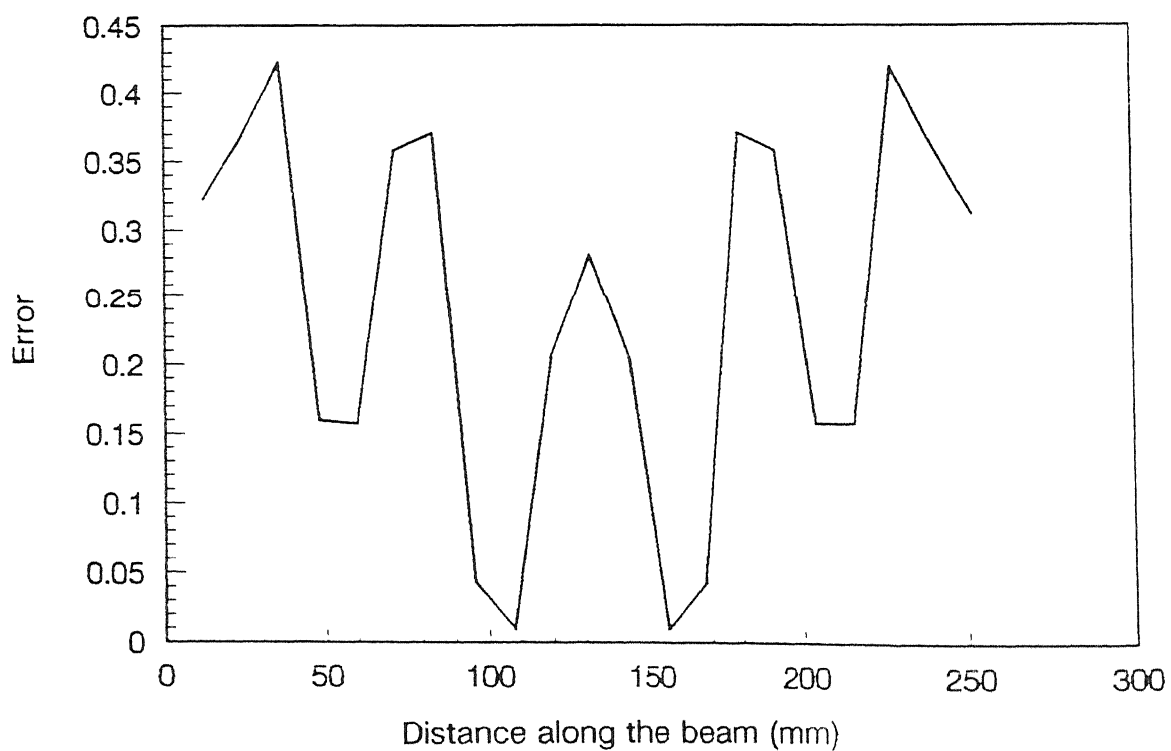


(b) Mode 2

Fig. 4.18 Estimated and exact mode shapes of fixed-fixed beam with 20 number of stations ($\kappa=1.2769$)



(a) Mode 1



(b) Mode 2

Fig. 4.19 Errors of fixed-fixed beam with 20 number of stations ($\kappa=1.2769$)

Table 4.2 Exact and estimated natural frequencies of fixed-fixed beam

No. of stations	Mode	Natural frequencies		
		Exact	Estimated	Error
10	1	8.750	8.112	7.29
	3	47.284	43.772	7.55
20	1	8.750	8.172	6.60
	3	47.284	43.910	7.13

Remarks

The experimental results, though not very accurate due to the reasons cited, do provide reasonable estimates. These estimates can be readily improved by employing more sophisticated non-contact type sensors. More accurate location of the applied force is also expected to yield better results. A major source of error is the assumption in calculation of the exact mode shapes and natural frequencies that the boundary conditions of the beam set-ups are ideally simply-supported and fixed-fixed. It is however, difficult to ensure ideal conditions, for such boundary configurations and it would be better to carry out investigations on a free-free beam configuration, as is conventionally done in most modal analysis investigations.

CHAPTER 5

CONCLUSIONS

The work presented in this thesis is an extension of the existing Spatial Modal Analysis Procedures which deal with estimation of a single natural mode, of a vibrating beam, which is close to the excitation frequency. An algorithm has been developed, during the present study, to estimate the modal properties of two modes of the beam, adjacent to a excitation. frequency. The general procedure constitutes of mode shape estimation, calculation of natural frequencies and damping ratios, from steady state spatial data of beam excited at a specified frequency and location. The deflected beam shape is approximated by employing recursive form of Forsythe polynomials and Least Square technique is used to curve fit the measured responses and obtain the coefficients of Forsythe polynomials. Orthogonality properties are further employed to decompose the Forsythe polynomial representation into the individual mode shapes of the beam contributing to the response. The individual mode shapes estimates are further processed to fit the governing fourth order spatial equation of beams to obtain the spatial modal frequency. The procedure has been illustrated through computer simulation as well as experiments on beams with some standard boundary configurations. The procedure is found to give accurate modal descriptions for sufficiently large number of measurement stations. It is also seen to be robust to the presence of measurement noise.

The procedure needs to be extended for estimation of more than the two adjacent modes, dealt with in this study. The influence of the number of Forsythe polynomials in the mode shape approximations, also need to be investigated. A more rigorous investigation is required to explore and account for the errors incurred due to inaccuracies in the force application point. It has been obvious through the present experimental work that conventional contact type sensors like the accelerometer can provide data at a limited number of spatial locations and a non-contact type of sensor like the Laser Vibrometer is essential to get the dynamic information at sufficient number of stations on the beam. The study also opens the possibility of developing similar procedures for plate vibration applications. Possibilities of application of multiple- point excitations can also be investigated.

REFERENCES

- Allemang, R. J., Experimental Modal Analysis Bibliography, Proac IMAC 2, 1984
- Archibald, C.M., An Analysis Of Sample Rate Considerations For Parametric Sinusoidal Estimation Methods, Proceedings 10th International Modal Analysis Conference, San Deigo, Ca, 1992
- Archibald, C.M., and Wicks, A. L., An Alternative time domain system identification algorithm, Proceedings 9th International Modal Analysis Conference, Florence, Italy, 1991
- Bishop, R. E. D. , Gladwell, G. M. L., An Investigation Into The Theory of Resonance Testing, Proc. Roy Soc. Phill Trans 255(a)241, 1963
- Bishop, R. E. D. , Johnson D. G., The Mechanics of Vibrations, Cambridge University Press, 1960
- Ewins D. J., Modal Testing Theory and Practice, John Wiley and Sons Inc., 1986
- Ewins D. J., Griffin J., A State of The Art Assessment of Mobility measurement Techniques , J. Sound And Vibration, Vol. 78, No. 2, , p.197-222, 1981
- Forsythe, G. E., Generation And Use Of Orthogonal Polynomials For Data-Fitting With A Digital Computer, J. Soc. Indust. Appl. Math. Vol. 5, No.2, June 1957, p. 75-88
- Kennedy, C. C., Pancu, C. D. P., Use of Vectors In Vibration Measurement And Analysis, J. Aero. Soc., Vol. 14, No. 11, 1947
- Mitchell, L. D., Modal Analysis Bibliography -An Update-1980-1983, Proc. IMAC 2, 1984
- Pisarenko, V. F., The Retrieval Of Harmonics From A Covariance Function, Geophysics J. R. Astr. Soc., Vol. 33,p.346-366,1973
- Rao S. S., Mechanical Vibrations Addison-Wesley, 1986
- West, R.I., Archibald, C.M., and Wicks, A. L. Spatial Modal Analysis Using Regressive and Autoregressive techniques, Proceedings 11th International Modal Analysis Conference, Orlando, Florida, 1993